



Single Molecule Electronics: from Chemical Design to Functional Devices

Journal:	<i>Chemical Society Reviews</i>
Manuscript ID:	CS-REV-04-2014-000143.R1
Article Type:	Review Article
Date Submitted by the Author:	29-Apr-2014
Complete List of Authors:	Sun, Lanlan; Chalmers University of Technology, Chemical and Biological Engineering Diaz Fernandez, Yuri; Chalmers University of Technology, Chemical and Biological Engineering Gschneidner, Tina; Chalmers University of Technology, Chemical and Biological Engineering Westerlund, Fredrik; Chalmers University of Technology, Chemical and Biological Engineering; University of Gothenburg, Physics Lara-Avila, Samuel; Chalmers University of Technology, Micro and Nanotechnology, MC2 Moth-Poulsen, Kasper; Chalmers University of Technology, Department of Chemical and Biological Engineering

1§211111Cite this: DOI: 10.1039/x0xx00000x
Received 00th January 2014,
Accepted 00th January 2014
DOI: 10.1039/x0xx00000x
www.rsc.org/

Single-Molecule Electronics: from Chemical Design to Functional Devices

Lanlan Sun,^a Yuri A. Diaz-Fernandez,^a Tina A. Gschneidner,^a Fredrik Westerlund,^a Samuel Lara-Avila,^b and Kasper Moth-Poulsen^{*a}

Abstract. The use of single molecules in electronics represents the next limit of miniaturisation of electronic devices, which would enable to continue the trend of aggressive downscaling of silicon-based electronic devices. More significantly, the fabrication, understanding and control of fully functional circuits at the single-molecule level could also open the possibility of using molecules as devices with novel, not-foreseen functionalities beyond complementary metal-oxide semiconductor technology (CMOS). This review aims at highlighting the chemical design and synthesis of single molecule devices as well as their electrical and structural characterization, including a historical overview and the developments during the last 5 years. We discuss experimental techniques for fabrication of single-molecule junctions, the potential application of single-molecule junctions as molecular switches, and general physical phenomena in single-molecule electronic devices.

ARTICLE

1 **1. Introduction and background** 57
 2 58
 3 The developments of micro-fabrication and field effect 59
 4 transistors are key enabling technologies for today's 60
 5 information society. It is hard to imagine superfast and 61
 6 omnipresent electronic devices, information technology, the 62
 7 internet and mobile communication technologies without access 63
 8 to continuously cheaper and smaller microprocessors. The giant 64
 9 leaps in performance from the first computing machines 65
 10 today's mobile devices are to a large extent realized via 66
 11 miniaturization of the active components. 67
 12 Further miniaturization of electronic devices remains 68
 13 enormous challenge. Conventional top-down lithography has 69
 14 reached the limit where reliable and reproducible fabrication 70
 15 sub-20 nm features is cumbersome and economically 71
 16 unfeasible. In this sense, it is remarkable that chemically 72
 17 identical molecules, with sizes on the order of 1 nm, can be 73
 18 synthesized in molar amounts and yet perform a variety 74
 19 of electronics tasks including current limiting, rectification and 75
 20 switching, reminiscent of their solid-state device counterparts. 76
 21 Experimental findings in electron transport through single 77
 22 molecules put forth the idea that beyond silicon CMOS 78
 23 technology, the next limit of miniaturization of electronic 79
 24 components is the realization of single-molecule electronics.¹ 80
 25 Since the first theoretical proposal by Aviram and Ratner 81
 26 in the 70's,² it took almost 20 years of technological development 82
 27 to realize the first experiment resembling transport through 83
 28 single molecules.³ Since then, 20 more years after, the 84
 29 techniques to investigate transport through single molecules 85
 30 appear to have stagnated and the experimental methods 86
 31 developed in the 90's are still in widespread use. Nonetheless, 87
 32 along this time several technical and theoretical developments 88
 33 have helped us to understand electron transport through single 89
 34 molecules. For example, fundamentally new concepts for 90
 35 device function beyond CMOS-like logics have emerged.⁴ 91
 36 Examples include spintronics, quantum interference, 92
 37 electromechanics and thermoelectronic devices studied at the 93
 38 single molecule level. Nonetheless, many challenges need to be 94
 39 overcome before single-molecule electronics can be a reality. 95
 40 One of the main challenges involves the realisation of 96
 41 technology for mass production of single molecule devices.⁵ 97
 42 Chemistry has been the key element in the design and synthesis 98
 43 of functional molecules, and it is one of the most promising 99
 44 ways to bridge the state-of-the-art lithography techniques 100
 45 (resolution ~20-50 nm) and molecular-scale dimensions (1-10 101
 46 nm) via *e.g.* chemically driven self-assembly techniques.⁶ 102
 47 Several recent review articles have focused on specific 103
 48 experimental aspects of molecule electronics.⁴⁻¹⁴ In this review 104
 49 we aim at giving broad overview of this field, with a focus on 105
 50 vital issues such as self-assembly of nanogaps, molecular 106
 51 systems, and physical phenomena. To narrow the scope of the 107
 52 paper, we focus our discussions on systems with a single or a 108
 53 few molecules in each functional device, however we have not 109
 54 been strict with this definition and have included some 110
 55 examples of devices with small ensembles of molecules as well. 111
 56 To put the recent research progress into historical perspective,

we include some historical references as well as introductions to the most commonly employed experimental methods. We discuss the most relevant physical phenomena observed in single molecule devices throughout the years and then we focus on single molecule switches that we consider the most promising way to materialize the implementation of single molecule devices.

2. Experimental methods to address single-molecule electron transport

One of the main challenges in single-molecule electronic devices is to fabricate electrodes with a single molecule in between them. Ideally, these electrodes would allow reliable and reproducible characterization of single molecule devices at room temperature. A variety of techniques have been developed to construct metal-molecule-metal junctions, including mechanical break junctions,¹⁵ electrochemical deposition,¹⁶ electromigration,¹⁷ electron beam lithography,¹⁸ shadow mask evaporation,¹⁹ scanning probe techniques,^{3, 20} on-wire lithography^{21, 22} and molecular rulers.^{23, 24} The focus here is a discussion of fabrication methods of single-molecule junctions, for example, scanning probe microscope (SPM), mechanical break junctions (MCBJ), electromigration break junctions (EBJ), and self-assembly of nanostructures. The first three methods have been widely used for experimental single-molecule electronics, while the self-assembly method is an emerging, yet very promising route towards (mass) production of single-molecule devices.

2.1 Scanning Probe Microscopy (SPM). The great advantage of SPM-based techniques is that they enable the direct observation of the system (molecule) under investigation, while simultaneously allowing realization of other types of studies such as electron transport.²⁵⁻³⁰ SPM includes a range of microscopy techniques that are considered as an evolution of scanning tunneling microscopy (STM). Two SPM techniques, STM and conducting probe atomic force microscopy (C-AFM), have been widely used to investigate single-molecule electronics systems by forming a metal-molecule-metal junction between the metallic tip and substrate (Fig. 1). In order to form the molecular junction, the tip/substrate can be either immersed in the target molecule solution during experiments or decorated with molecules before measurements. Using STM experiments, Weiss *et al.* probed the conductivity of molecular wires self-assembled monolayers on Au.³ The molecular wires acted as a conducting link from the gold substrate through a "non-conducting" layer to the top of the STM tip.

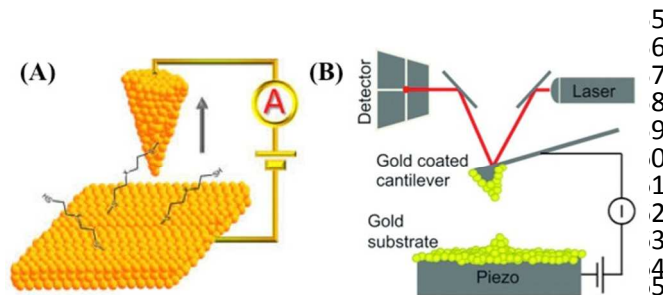


Fig. 1 (A) Schematic representation of the STM break junction. Reprinted with permission from E. Wierzbinski, X. Yin, K. Werling and D. H. Waldeck, *J. Phys. Chem. B*, 2012, **117**, 4431-4441. Copyright 2013 American Chemical Society.³¹ (B) A modified conductive atomic force microscope (C-AFM): the junction is formed between the Cr-Au coated cantilever and an Au-coated substrate, and the separation is controlled by a piezo. Reprinted with permission from M. Frei, S. V. Aradhya, M. Koentopp, M. S. Hybertsen and L. Venkataraman, *Nano Lett.*, 2011, **11**, 1518-1523. Copyright 2011 American Chemical Society.³²

The electron transport mechanisms of STM and C-AFM are somewhat different. In STM, the current is due to tunneling since the metallic tip and a conducting substrate are in very close proximity but not in actual physical contact. In C-AFM, on the other hand, an external circuit is used to apply current between the metallic tip and a conducting substrate, which are in direct contact. A detailed introduction to the use of STM and AFM into chemistry in single molecule electronics can be found in ref.^{33,34,35,36,37}

A further development is SPM-based break junctions, where the charge transport properties of a single molecule, or a small number of molecules, is studied by repeatedly crashing the SPM tip into and out of contact with the substrate electrode surface containing the target molecules.^{34,35} Many efforts have been made to develop the SPM break junction technique. Haiss *et al.* introduced a simple method to measure single alkanedithiol molecule conductivities, using the spontaneous formation of molecular wires between the STM tip and Au substrate.³⁶ In a recent review, Niu *et al.* presented recent SPM studies of phthalocyanine, a candidate for molecular electronics, highlighting the power of SPM techniques in the ability to both image and probe the properties of single molecule electronic systems.^{37,41}

^{29, 39, 42-4637, 47-5354-61566162, 63}

2.2 Mechanically controlled break junction (MCBJ). MCBJ is a powerful technique for characterizing conductance through single-molecular devices. MCBJ allows automated cycle formation/breaking of metal-single molecule-metal junctions which enables collecting statistics (conductance histograms) over an experimentally reasonable time for different geometries/realizations of a molecule/metal interface.⁸ This technique allowed understanding of, for example, why independent experiments, aiming at measuring the conductance of the same molecule, might yield different results. MCBJ was first introduced by Moreland *et al.*³⁸ and Muller *et al.*³⁹ and then further developed by Reed *et al.*^{15,40} to fabricate electrodes with a gap of a few nanometers. As shown in Fig. 2, a notched metal wire glued onto a bendable substrate is elongated and finally fractured, when the substrate is bent by moving a piezo controlled pushing rod. Two sharp electrodes are formed automatically after the wire is broken and then molecules and two terminal anchoring groups can be assembled to link the

electrodes. The molecules can be introduced both before and after the formation of the electrodes. In Reed's study, 1,4-benzenedithiol (BDT) in tetrahydrofuran (THF) was introduced before the breaking, and a monolayer of BDT was formed on the surface of the gold wire.¹⁵ The reproducibility of the minimum conductance at a consistent value implied that the number of active molecules in the junction could be as few as one. Experimental details and comparisons of the different experimental platforms used for MCBJ-break junctions for molecular electronics are discussed in ref.⁸

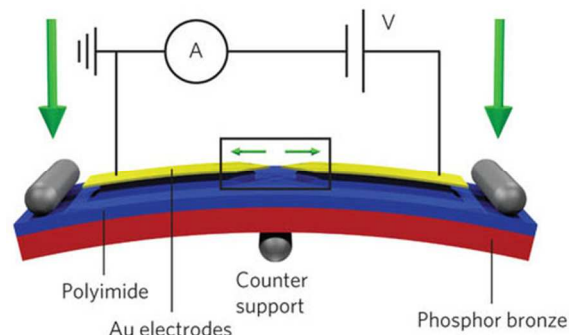
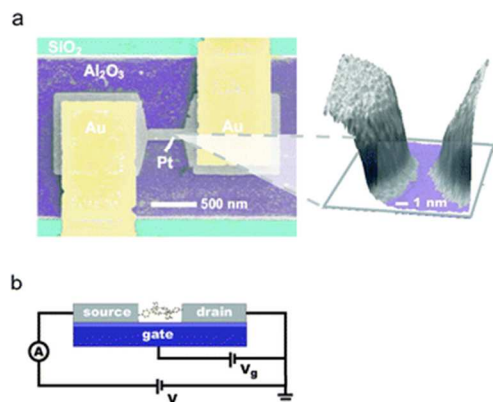


Fig. 2. Schematic illustrating a MCBJ, which shows the layout of the MCBJ set-up. Reprinted with permission from Nature Nanotechnology (M. L. Perrin, C. J. O. Verzijl, C. A. Martin, A. J. Shaikh, R. Eelkema, H. van EschJan, J. M. van Ruitenbeek, J. M. Thijsen, H. S. J. van der Zant and D. Dulic, *Nat. Nanotechnol.*, 2013, **8**, 282-287), Copyright (2013).⁴¹

The unambiguous identification of a single molecule contacted in the junction is still a challenge, but significant progress has been made to establish that a single molecule forms the contact.⁴²⁻⁴⁷ For these purposes, the MCBJ technique has been combined with other experimental methods, such as STM imaging,⁴⁸ Raman spectroscopy,⁴⁹ inelastic electron tunneling spectroscopy,^{50,51} and inelastic noise spectroscopy.⁵² Both inelastic electron tunneling spectroscopy and inelastic noise spectroscopy are useful molecular signature techniques. For inelastic noise spectroscopy, the molecular-vibration-induced current noise is useful for single-molecule identification. In particular, Ruitenbeek *et al.* studied the conductance of a single hydrogen molecule by using MCBJ to fabricate pure metallic Pt contacts of atomic size.⁴³ They demonstrated that a single hydrogen molecule could form a stable bridge between Pt electrodes. Ruitenbeek *et al.* then carried out shot noise measurements on the Pt-D₂-Pt junction formed by the MCBJ technique, and the observed quantum suppression indicated that the junction was indeed formed by just a single molecule.⁴⁵

2.3 Electromigration break junction (EBJ). EBJ incorporates the possibility of having an electrostatic gate to a single-molecule junction by forming nanoscale contacts for single molecules on top of an oxidized conducting substrate, which acts as a gate. The first report of fabricating metallic electrodes with nanoscale separation by electromigration was by Park *et al.* in 1999.¹⁷ When applying an electric field onto a metallic nanowire defined by electron-beam lithography, the metal atoms migrate, which results in the breakage of the nanowire. By carefully controlling the current, two stable metallic electrodes can be formed with 1-2 nm separation. This separation is a good match with the length scale of typical molecules employed in single-molecule nanodevices. The assembly of molecules into the junctions is similar to that in

1 STM junctions and MCBJs, where the molecules are deposited
 2 onto the electrode surface before or after the breaking. The
 3 breaking process can be controlled in real-time by monitoring
 4 the current-voltage curve until only a tunnelling signal
 5 is observed.^{17, 53}
 6 Above all, the EBJ is an advantageous method to fabricate
 7 three-electrode molecular device, as shown in Fig. 3.⁵³⁻⁵⁵ The
 8 third gate is already present under the wire before electro-
 9 breaking (or it can be the underlying conducting, oxidized
 10 silicon substrate).^{56, 57} When compared with the MCBJ method,
 11 the drawback of the EBJ technique lies in the difficulty
 12 obtaining a large number of metal/molecule geometries with
 13 same junction. Therefore, it is not simple to measure large
 14 numbers of single-molecule junctions, and many devices
 15 needed to study the statistical behaviour of the molecules.^{56, 58}
 16 To increase device yield, Johnson *et al.* used a feedback-
 17 controlled electromigration process to fabricate a large number
 18 of nanogaps simultaneously in a single-step process.⁵⁹ For
 19 detailed discussion on the feedback-EBJ we refer to recent reviews
 20 6, 10
 21 919293949596 A general challenge for MCBJ and EBJ is the lack
 22 of direct evidence (observation) of single-molecule junction
 23 formation. To circumvent this problem, and in order to improve
 24 the control the EBJ process, *in situ* STM, AFM imaging and
 25 transmission electron microscopy (TEM) have been employed
 26 during nanogap formation by electromigration.⁶⁰⁻⁶⁴ Although
 27 the electromigration-induced wire breaking approach can create
 28 a 1-2 nm gap to bridge the target molecules, identification
 29 the molecule in the gap is still a key issue for these single-
 30 molecule devices. In this context, Raman spectroscopy and
 31 inelastic electron tunneling spectroscopy (IETS) have been
 32 applied to complement the electronic transport of the single-
 33 molecule device.⁶⁵⁻⁶⁷ For example, Natelson *et al.* examined
 34 paramercaptoaniline (PMA) between electromigration-created
 35 nanogaps using Raman spectroscopy.⁶⁵ Before electromigration
 36 no Raman peak for PMA were observed; after electromigration
 37 surface enhanced Raman peaks for PMA were detected in the
 38 obtained gaps. IETS can also be used to identify molecules
 39 bridged in the electromigrated nanogap, which supplies a full
 40 spectrum and assigned vibrational spectra of the individual
 41 molecules.⁶⁸⁻⁷⁰ As described in the MCBJ section, Raman spectroscopy
 42 and inelastic electron tunneling spectroscopy can supply a large
 43 amount of information about the configuration of the molecule in
 44 EBJ produced gaps.⁷¹⁻⁷⁴
 45



46
 47 **Fig. 3** (a) Colorized SEM image of the single-molecule device based on
 48 the Pt nanogap. (b) Schematic representation of the EBJ device.⁷⁵
 49

50 **2.4 Self-assembly of nanostructures.** The methods mentioned
 51 above are all based on a top-down fabrication strategy, where

nanogaps are firstly constructed by using standard
 semiconductor nanofabrication technologies, and then in a
 second step the active molecules are introduced into the
 nanogaps. Another, much less explored, yet interesting
 approach is the bottom-up assembly of metallic electrodes from
 the molecule utilizing solution based self-assembly methods.⁷⁶
 77 The general idea is to pre-fabricate on a chip metallic contacts
 using photo- or e-beam lithography, with dimensions which will be
 limited by lithographic resolution (~250 nm for Deep UV and ~30-
 50 for e-beam) and then exploit self-assembly of chemically
 synthesized metal-molecule-metal structures to bridge
 lithographically pre-fabricated electrodes.⁷⁸

The first challenge is the synthesis of metal-molecule-metal
 nanostructures. In this context, Dadosh *et al.* have developed a
 method that can yield gold nanoparticle dimers linked by single
 molecules via self-assembly process.²⁴ Nanoparticle dimers
 (Au-molecule-Au) were fabricated by mixing a solution of
 dithiol molecules with a gold nanoparticle solution. In this
 method, it is possible to identify if a single molecule is in the
 nanogap, because trimers, tetramers, and aggregates will be
 formed when more than one molecule binds to a certain
 nanoparticle. In the method of Dadosh *et al.*, dimers of 30 nm-
 diameter gold nanoparticles were deposited onto electrodes
 with a 40-50 nm separation, and single-molecule conductance
 was measured. For a summary of synthesis of nanoparticle
 dimers we refer to our recent review.⁷⁷ With similar
 nanoparticle-molecule-nanoparticle bridge structures, Parsons
et al. investigated the conduction mechanisms and stability of
 single OPE (oligo(p-phenylene ethylenes)) molecules.⁷⁹

Furthermore, Jain *et al.* reported a strategy to fabricate 1-2 nm
 nanogaps via seed-mediated growth of end-to-end linked gold
 nanorods (AuNRs).⁸⁰ Mayor *et al.* demonstrated that the
 interparticle distance of gold nanoparticle dimers could be
 controllable by an atomic alteration in the structure of the linker
 molecule.⁸¹ Bar-Joseph *et al.* presented a single electron device
 by placing a self-assembled metallic nanoparticle dimer in
 between e-beam lithography defined electrodes.⁸² Maruccio *et al.*
 fabricated devices based on bisferrocene molecule-gold
 nanoparticles, and studied their transport properties.⁸³ The
 device was built on a solid support fabricated by a combination of
 optical lithography and chemical etching, and it showed similar
 behaviour as devices fabricated by conventional methods (Fig. 4).
 Firstly, the gold nanoparticles were assembled in the solution,
 linked by bisferrocene molecules. Secondly, the nanoparticle
 dimers were directed onto the electrodes by self-assembly. The
 bisferrocene molecules act not only as the linker molecule
 between the nanoparticles, but also as the functional molecular
 electronic component. This method demonstrates the potential
 of combining top down lithography with bottom self-assembly
 in fabrication of single-molecule device. Naaman *et al.*
 fabricated a hybrid device made from gold nanoparticles linked
 by alkyldithiol molecules with different lengths and
 investigated the dependence of conduction on the molecule
 length.⁸⁴ For further reviews on the use of self-assembly in
 single-molecule electronic devices, we refer to refs.^{7, 76}

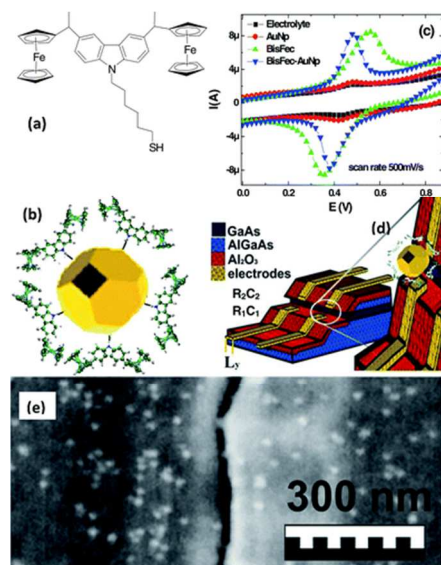


Fig. 4 Nanodevices based on bisferrocene-gold nanoparticle hybrids. (a) Structure of the bisferrocene molecules used in the device. (b) Schematic representation of the linkage of bisferrocene molecules on the surface of gold nanoparticles. (c) Cyclic voltammogram demonstrating the formation of bisferrocene-AuNPs hybrids. (d) Schematic view of the nanogap electrodes and (e) SEM image of the measured nanojunctions.⁸³

Chemical growth of metallic nanostructures can also be used as building blocks for the construction of nanogaps.^{85, 86} Bjørnholm *et al.* combined a top-down and bottom-up approach to construct the nanogaps by directed *in situ* growth of AuNRs based nanostructures inside PMMA nanochannels prefabricated by top-down e-beam lithography.⁸⁷ The PMMA nanochannels provide an additional handle for positioning the AuNRs, and nanoscale gaps between the electrode and the nanorods can be obtained. When the AuNRs are long enough to bridge the electrodes, 1–5 nm nanogaps are formed at the interface between *in situ* grown AuNRs and the pre-patterned gold electrode. Alivisatos *et al.* used a controlled assembly of gold nanoparticles into defined locations on a chip and within a circuit by utilizing capillary interactions.⁸⁸ Wolf *et al.* recently reported the oriented assembly of short gold nanorods (below 100 nm of length) from colloidal suspensions by a capillary assembly process on surfaces.⁸⁹ In their method, the gold nanorods can be aligned on the single particle level, and oriented nanorod dimers are obtained with narrow inter-particle gaps. Rey *et al.* reported a directed capillary method to assemble AuNRs into chains between two electrodes.⁹⁰ The gap between each AuNR is about 5–7 nm, which may be caused by the CTAB bilayer on the surface of the AuNRs. The thickness of one CTAB bilayer is about 3.2 nm,⁹¹ thus the interlayer between two AuNRs is about 6 nm. These AuNR based nanodevices.

In addition to AuNRs, carbon nanotubes (CNTs) have also attracted a lot of interest as building blocks for nanogaps because CNTs are one-dimensional conductors, semiconductors and have a diameter similar to the size of the target molecules.^{92–96} Typically, following metal deposition and a lift-off process, nanogaps of CNTs can be obtained. Besides CNTs, graphene and many nanowires, including nanowires made from organic and inorganic materials, can also be used to fabricate the nanogap.^{97–99}

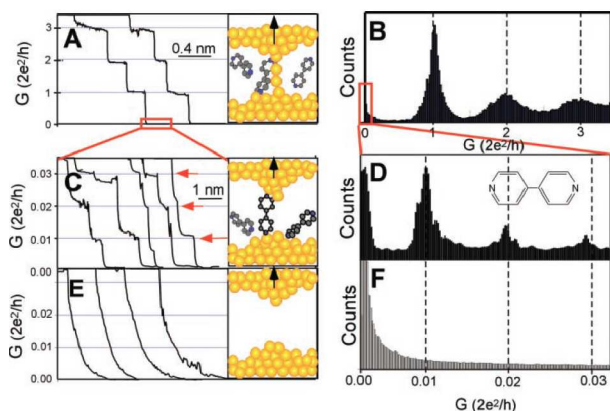
The on-wire lithography method has been widely used to fabricate nanogaps. Firstly, multisegmented Au-Ag nanowires are fabricated by electron beam evaporation. Secondly, the Ag segment can be removed using high temperature or chemical etching techniques, and the thickness of Ag determines the size of the nanogap.^{21, 22, 100, 101} Recently, Mirkin *et al.* developed the on-wire lithography technique to fabricate gold nanorod dimers with a 2 nm gap.^{102–105} One of the main advantages of the on-wire lithography method is that the gap size can be controllably tuned during the nanowire synthesis process.

In addition to bifunctional small organic molecules, biomolecules have also been used as single-molecule electronic components. Since thiolated DNA was used for the first time to link gold nanoparticle dimers in 1996, DNA has attracted substantial interests for self-assembly of nanoparticles.^{106, 107} Significant progress in DNA-directed assembly of nanoparticles have been reported in recent years,^{108–110} especially for DNA-linked nanoparticle dimers.^{111–116} In these studies, the gaps formed between two nanoparticles are tunable and depend on the length and number of linker DNA molecules.^{113–117} Another advantage of using DNA is that the assembly is reversible: by cycling the temperature of the DNA-nanoparticle solution above and below the melting temperature of the DNA, the nanoparticles can be linked or dissociated.^{106, 118} Bidault *et al.* reported reversible switching of inter-particle distances in DNA bridged gold nanoparticle dimers.¹¹⁹ The distance between gold nanoparticles could be switched from 5 nm to 15 nm, by hybridizing or removing a single DNA strand. A recent report revealed that a 1 nm gap can be generated by DNA-tailored nanoparticles.¹²⁰ The detailed electric properties of DNA molecules have raised some debate. Kasumov *et al.* reported that DNA between rhenium/carbon metallic contacts is possibly superconductive at low temperatures.¹²¹ Dekker *et al.* found that DNA with a length of about 10 nm is a semiconductor, while DNA with ~100 nm long strands is insulating.¹²² The measurements were carried out using conducting AFM and STM, in which collections of DNA molecules were measured. The conductivity of a single DNA strand was measured later by Guo *et al.*, where single DNA molecules terminated with amines were connected to electrodes.¹²³ The well-matched DNA in the gap exhibited a resistance on the order of 1 MΩ. A base mismatch in the DNA double helix decreased the conductivity about 300 fold compared with a well-matched one.

2.5 Data collection and analysis. The unequivocal identification of a single molecule between metallic electrodes is a challenge common to all experimental techniques employed to fabricate single-molecule devices. Measurements of current-voltage characteristics readily provide information about electrical resistance of the device under study, but the measured resistance is prone to large variations upon nanoscopic changes in the metal-molecule contact geometry. As a consequence, significant discrepancies in the measured electrical resistance of a single molecule can be found from experiment to experiment even when the same molecules and contacts are employed. The analysis of single molecule conductance simply from its current-voltage (IV) characteristic is therefore fundamentally incomplete.

A way to quantify the resistance of a metal-single molecule-metal junction in a meaningful way is by using the so-called conductance histogram method, a statistical analysis introduced by Krans *et al.*¹²⁴ for studying metallic quantum point contacts and first implemented for electrical measurements on molecules by Xu & Tao (Fig. 5).³⁴ This method consists on recording the

1 electrical conductance of a metal-molecule-metal junction 53
 2 (statistically) significant number of times (typically > 1000). 54
 3 practice, the large amount of molecular junctions realization 55
 4 needed to collect data is formed by repeatedly moving two 56
 5 metallic contacts into and out of contact, and thus the STM 57
 6 break junction technique and MCBJ techniques are better suited 58
 7 for recording conductance histograms. In an STM experiment 59
 8 finite bias voltage between the tip and the substrate, and the 60
 9 current is measured as the STM tip is pushed into/retracted 61
 10 from the substrate. The conductance of the molecule appears 62
 11 when the tip is pulled away from contact with the substrate. 63
 12 this low conductance regime (tunneling), a new sequence of 64
 13 peaks appears in conductance histograms that reveal the most 65
 14 likely conductance of the molecule under study. Since its 66
 15 introduction, the conductance histogram technique has been 67
 16 used to characterize the electric conductance of a variety of 68
 17 molecules.^{35, 125, 126} More importantly, it has served as powerful 69
 18 tool to understand electron transport mechanisms through 70
 19 single molecules,¹²⁵ and the role of the chemical anchoring 71
 20 group used to bind molecules to metal electrodes.¹²⁶ As an 72
 21 example, it has been shown that butane linked to gold 73
 22 electrodes via dimethyl phosphines (PMe₂) displays lower 74
 23 contact resistance compared to the same molecule linked to 75
 24 gold by amine groups (NH₂) or methyl sulfides.¹²⁶ 76
 25



26
 27 Fig. 5. Use of conductance histograms to investigate single-molecule 77
 28 electrical conductance. (A) The electrical conductance of a gold contact 78
 29 formed between the STM tip and substrate decreases in quantized units 79
 30 of $G_0 = 2e^2/h$ as the tip is retracted. (B) Corresponding conductance 80
 31 histogram shows peaks near 1, 2 and $3G_0$ due to conductance 81
 32 quantization. (C) The tip-substrate contact is broken, new conductance 82
 33 steps appear if molecules are present in the solution. These conductance 83
 34 steps arise from the formation of a molecular junction between the tip 84
 35 and the substrate electrodes. (D) Conductance histogram of the 85
 36 molecular junction depicted in (C), shows peaks near 0.01, 0.02, and 86
 37 $0.03 G_0$ that are ascribed to one, two, and three molecules, respectively 87
 38 (E and F) As a control experiment, no such steps or peaks are observed 88
 39 in the absence of molecules. Reprinted with permission from ref.⁵⁴. 89
 40

41 The potential of the conductance histogram method to study 90
 42 not only electronic transport through single-molecules but also 91
 43 fine details of metal/molecule contacts was immediately 92
 44 identified and the technique was further refined to extract 93
 45 information about molecule/metal mechanics. Building on 94
 46 previous studies from the same group, Nuckolls *et al.* performed 95
 47 a systematic STM-break junction study involving alkanedithiol 96
 48 molecules linked to gold electrodes via amine (NH₂), methyl 97
 49 sulfide (SMe), and dimethyl phosphine (PMe₂) groups, where 98
 50 conductance histograms were recorded as a function of junction 99
 51 elongation (Fig. 6).¹²⁷ It was found that the conductance versus 100
 52 displacement traces showed plateaux during elongation, which

provided a signature of junction formation; the plateau length 101
 102 probed the amount of elongation a junction can sustain without 103
 104 breaking. The modified conductance histogram method allowed 105
 106 to find that a) longer molecules have a higher probability of 107
 108 forming a single-molecule junction, b) under stress, anchoring 109
 110 groups can hop from one available Au site to another or even 111
 112 distort the Au structure by dragging Au atoms out of the 113
 113 surface and c) confirm that the stronger Au-PMe₂ bond - 114
 115 compared with the Au-NH₂- displays lower contact resistance 116
 117 and has higher probability of forming a molecular junction. 118

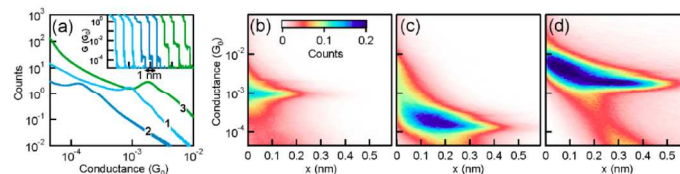


Fig. 6. (a) Conductance histograms in linear scale of 1,4-butanediamine 119
 120 (M1), 1,6-hexanediamine (M2) and 1,4-bis(dimethylphosphino) butane 121
 122 (M3). The inset displays conductance traces that show a molecular step 123
 124 for each molecule (offset horizontally for clarity). (b)–(d) 2D 125
 126 histograms for molecules M1, M2, and M3 showing that longer 127
 128 molecules with the same linking group (i.e. M1 and M2) have higher 129
 130 probabilities of forming a molecular junction (the stretching length for 131
 132 the conductance peak increases from 2.5 Å for M1 to 4.5 Å for M2) and 133
 134 that dimethyl phosphine anchoring groups have a higher probability of 134
 135 forming a junction than amino groups (i.e. M1 compared to M3) while 135
 136 displaying lower contact resistance. Reproduced with permission of 136
 137 Nuckolls *et al.* Formation and evolution of single-molecule junctions. 137
 138 Phys. Rev. Lett 102, 126803 (2009).¹²⁷ 138

139 Similar experiments aiming at understanding the effects of the 139
 140 anchoring group on transport and mechanics of single molecule 140
 141 junctions have been conducted in a comparison of amino and 141
 142 thiol terminated n-alkanes (n=2–6,8).¹²⁸ In this work, the effect 142
 143 of amino groups observed in ref.¹²⁷ was reproduced. 143
 144 Additionally, it was found that thiol groups provide lower 144
 145 contact resistance compared to amino groups in longer 145
 146 molecules (N>5), and also that these groups are more efficient 146
 147 in disturbing gold contacts (i.e. they lead to significantly higher 147
 148 Au atom re-arrangement). This latter observation was deduced 148
 149 from the fact that the maximum stretching length for molecular 149
 150 junctions of alkane-dithiols can reach values almost the double 150
 151 of the molecular length. In a recent work, the same group 151
 152 studied further the null impact of amino anchoring groups on 152
 153 re-arrangement of gold atoms in the contacts.¹²⁹ The binding 153
 154 stability of amino terminated oligo(phenylethyne) to gold 154
 155 electrodes was determined by recording conductance 155
 156 histograms as a function of junction elongation at different 156
 157 stretching speeds. Contrary to e.g. thiol terminated molecules in 157
 158 their previous report, it was found that the elongation of single- 158
 159 molecule junctions (amino-terminated) needed to break the 159
 160 junction is lower than molecular length irrespective of 160
 161 stretching speed, confirming that amino groups do not lead to 161
 162 rearrangement of gold atoms in the contacts. 162

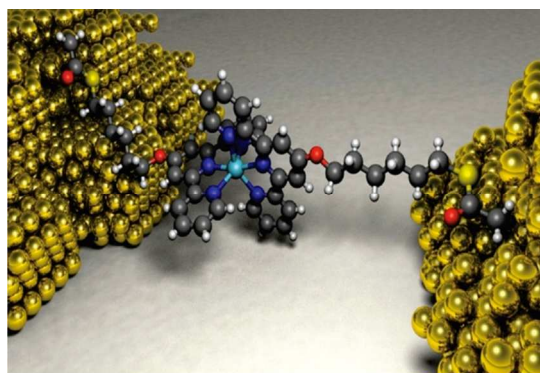
163 The electrical stability of a single molecule device is linked to 163
 164 the nanoscopic mechanical stability in a number of 164
 165 metal/molecule junctions. In this direction, Frei *et al.*³² have 165
 166 developed a technique to correlate conductance measurements 166
 167 and binding force in metal-single molecule junctions. Using a 167
 168 modified C-AFM setup, conductance and force histograms 168
 169 were studied for the case of Au point contacts, and gold linked 169
 170 to benzene, butane and hexamine via amine anchoring groups 170
 171 as well as the case of gold-bipyridine junctions. The Au point 171
 172 contact is used as a calibration measurement by comparing their 172
 173 measured value to literature reports. Authors show that 1,4-

1 benzenediamine binds most weakly to Au atoms, while the
 2 pyridine-gold bond exhibits the largest breaking force among
 3 all the molecules under study. Since all the anchoring groups
 4 contain a nitrogen atom, the stronger Au-N bond formed in Au-
 5 bipyridine was shown via DFT calculations to be
 6 consequence of the electronic structure of the molecule
 7 backbone altering the N-Au bond strengths in all molecules.
 8 Despite the enormous experimental challenges to fabricate
 9 identical single-molecule devices in a reproducible way, the
 10 development of clever techniques for data collection and
 11 analysis have enabled the study and understanding of electron
 12 transport through single molecules across different
 13 experimental realizations. A research line in single-molecule
 14 electronics is thus the development of techniques that allow
 15 unleashing the full potential of available fabrication techniques
 16 such as those described in this section.

18 3. Molecular systems for single-molecule electronics

20 The molecular unit in a single-molecule device can be divided
 21 into the anchoring groups, the link between the metallic
 22 contacts and the molecular kernel. The overall performance of a
 23 single-molecule electronic device is determined by the
 24 electrode/molecule interface (anchor) and the internal electronic
 25 structure of the molecular kernel. Thus, chemical design and
 26 synthesis are of paramount importance for single-molecule
 27 electronic devices. In this section we present some of the
 28 different designed motifs used to control the electronic
 29 properties and assembly of molecules into single-molecule
 30 electronic devices. Further, we discuss how chemical design
 31 the molecules influences the transport properties. This
 32 discussion is continued in further detail in section 4 (on
 33 physical phenomena in single-molecule junctions) and 5 (on
 34 molecular switches).

35 Electron transport through molecules in nanoscale junctions
 36 sensitive to very small changes in atomic configuration. One
 37 example is the possible arrangement of thiols on a gold surface,
 38 which is discussed by Häkkinen *et al.* in a recent review.
 39 Moreover, several studies have shown the influences
 40 different types of chemical anchoring groups on the molecule
 41 and metal surface in the junction.^{34, 131-136} Not only the specific
 42 anchoring group, but also variations in type of electrode
 43 material,¹³⁷⁻¹³⁹ different molecular geometries^{140, 141} and
 44 conformations¹⁴² heavily influence measurable properties of the
 45 metal-molecule-metal junction. Fig. 7 shows artist impression
 46 of a Mn(Terpy)₂ molecule bound in an asymmetric fashion to
 47 two electrodes. Structural differences in molecular wires
 48 including their anchoring groups, length, conformation and
 49 alignment with the Fermi level of the electrodes will
 50 discussed in this section.



52

Fig. 7 Schematic of a single-molecule device in which a [Mn(terpy-O-(CH₂)₆-SAC)₂]²⁺ molecule is bound in between two gold electrodes. The asymmetric geometry illustrates a likely realization of the device which gives rise to asymmetric coupling to the source and drain electrodes and the difference in gate-coupling to the two ligand moieties that is implied by the transport data.¹⁴³ Reprinted with permission from E. A. Osorio, K. Moth-Poulsen, H. S. J. van der Zant, J. Paaske, P. Hedegård, K. Flensberg, J. Bendix, and T. Bjørnholm, *Nano Lett.*, 2010, **10**, 105-110. Copyright 2010 American Chemical Society.³¹

3.1 Anchoring groups. The anchoring group, responsible for the direct contact between metal and the molecular kernel, needs to be considered in terms of its mechanical stability and also regarding its electronic transparency (weak or strong coupling).

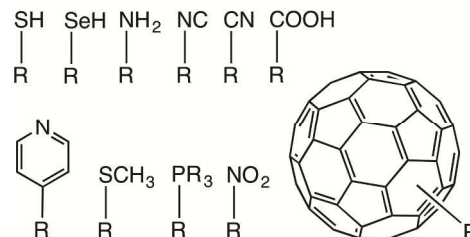


Fig. 8 Typical anchoring groups for single-molecule electronics.

The most explored example of anchoring groups is thiols on gold surfaces (Fig. 8). But in addition to thiol (-SH),¹⁴⁴⁻¹⁴⁸ some functional groups with good affinity for gold are selenium (-SeH),^{126, 149} amino (-NH₂),^{131, 132, 135} isocyano (-NC),^{131, 150} cyano (-CN),^{133, 134} pyridyl,^{34, 151} carboxy acid (-COOH),¹³⁵ nitro (-NO₂),¹³⁴ methylthioether (-SCH₃),¹²⁶ phosphino¹²⁶ and fullerenes (Fig. 8).¹⁵²⁻¹⁵⁴

Thiols were the first explored anchoring groups for charge transport experiments and are still the most widely used. They bind strongly to gold (as well as to silver and copper) and the bond is even stronger than the gold-gold bond itself.^{15, 155} Amines form a donor-acceptor bond to gold surfaces, preferably with under-coordinated gold,¹³¹ and carboxy acids are believed to bind by ionic and coordinating interactions.¹⁵⁶ Due to different electronic coupling by different types of anchoring groups, the contact resistance varies as Au-S > Au-NH₂ > Au-COOH.^{135, 157} Due to a weaker binding strength of amines and carboxyl groups, a higher bias on the electrode creates instability in the metal-molecule bond. The stability has also been examined for methylphosphines, methylsulfides and primary amines in the order: PMe₂ > SMe > NH₂.^{126, 127} The junction formation probability and stability of pyridyl, thiol, amine and cyano has been compared and resulted in this sequence: pyridyl > SH > NH₂ > CN.¹⁵⁸

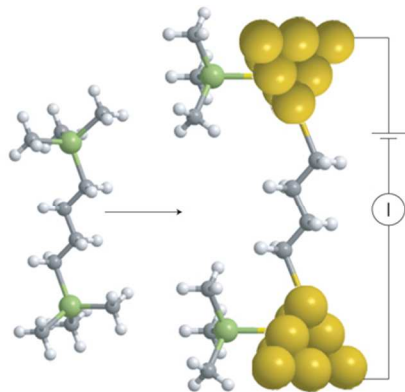
One challenge with assigning the contact resistance is that the detailed gold-ligand structure might differ significantly from device to device. As an example several different type of coordination geometries exists for the gold-thiol bond such as top-bridge and hollow sites. The relative stability of the different coordination sites might change due to minute changes in local chemistry and/or the forces employed to the system in e.g. a MCBJ setup. Small variations contact resistance been found to be the main reason for the discrepancies between of the reported results from different research groups for the measured conductivities of alkane thiols.¹⁵⁹

In addition to bond stability, different anchoring groups provide different charge transport mechanisms (transparency) due to their influence on the effective mixing of the HOMO-LUMO (HOMO: highest occupied molecular orbital, LUMO:

1 lowest unoccupied molecular orbital) levels of the molecule
 2 kernel and the Fermi energy (E_F) of the metal. Thiols show how
 3 transport through the HOMO, since the HOMO is the closest
 4 energy level to the E_F of the gold.^{160, 161} Amines,^{162, 165}
 5 nitriles¹³³ and pyridines¹⁶³, on the other hand, are expected
 6 use the LUMO as the transport channel. The position of the
 7 HOMO and LUMO relative to the Fermi levels of the
 8 electrodes can be measured experimentally in two terminal
 9 devices by a method known as transition voltage spectroscopy
 10 (TVS). One recent example of TVS employed in a study
 11 alkane thiols is found in ref.¹⁶⁴ Other recent examples of TVS
 12 studies on molecular systems can be found in ref.¹⁵⁹

13 Single-molecule electronics usually requires thousands
 14 measurements to describe the specific behaviour of a single
 15 molecule in a junction.^{140, 151} Increasing temperature or
 16 adjusted electronic potential at the electrodes to align the E_F
 17 the metal electrode with the HOMO or LUMO of the molecule
 18 might subsequently result in re-arrangement of the atoms at the
 19 electrode (e.g. Au) or a switching of the anchor between
 20 different bonding motifs.¹³⁰ To decrease geometric fluctuations
 21 of the anchor, multidentate binding motifs have been used by
 22 Lee *et al.*¹⁶⁵ They demonstrated that several functional groups
 23 bound to the surface could minimize the effect of individual
 24 bond fluctuations. Another possibility is to predefine and
 25 functionalize the electrodes *via* a selective organic chemistry
 26 such as click-chemistry¹⁶⁶ or wrap the electrodes with the
 27 molecular backbone of the molecular wire.¹⁶⁷ Conductance
 28 measurements with the gold-amine bond reveals quite good
 29 reproducibility, due to the defined electronic coupling of the
 30 lone pair electrons of the nitrogen to the gold and a high
 31 specificity in which NH_2 binds to under-coordinated gold
 32 sites.¹³¹ Also, the conductance in a junction keeps a constant
 33 value when changing the binding site from one under-
 34 coordinated Au to another.¹²⁷

35 Another system for ambient temperature conditions has been
 36 developed by Venkataraman *et al.*, in which a direct Au-C σ -
 37 bond is responsible for the contact between the electrode and
 38 the molecule.^{155, 168} The terminated trimethyltin ($Me_3Sn-CH_2-\pi$ -
 39 CH_2-SnMe_3) end groups cleave off *in situ* to form a direct C-Au
 40 bond. The development of new synthetic routes to promote the
 41 formation of covalent sulfur-free bonds between organic
 42 molecules and metal surfaces (Fig. 9) is opening new
 43 possibilities to control the charge-transport properties at metal
 44 molecule-metal junctions in a reproducible way.¹⁶⁸



46
 47 **Fig. 9** Junction formation and conductance measurements with
 48 bis(trimethylstannyl)butane molecules between gold electrodes.
 49 atoms, white; C atoms, grey; Sn, green). Reprinted by permission
 50 Nature Nanotechnology (Z. L. Cheng, R. Skouta, H. Vazquez, J. R.
 51 Widawsky, S. Schneebeli, W. Chen, M. S. Hybertsen, R. Breslow and

L. Venkataraman, *Nat. Nanotechnol.*, 2011, **6**, 353-357), Copyright
 (2011).¹⁶⁸

Strong electronic coupling is achieved by the direct covalent
 σ -bond connection *via* a methylene group and the π -conjugated
 wire. Compared with a traditional amine-Au contact, the direct
 covalent connection shows a 100-fold higher conductance. The
 Au-C bond couples well with the π -system of the molecule, in
 contrast to a Au-C bond which is connected directly to the
 molecular wire, without a methylene bond in between.¹⁶⁸ A
 near-resonant tunnelling is suggested to be responsible for the
 electron charge transfer. Compared to thiol anchors, Au-C
 shows a three-order-of-magnitude increase in efficiency for the
 charge transfer, meaning that devices could be run at lower
 voltages.¹⁶⁹ Wandlowski *et al.* showed the same approach for
 alkyne terminated OPE's to create Au-C bonds via an *in situ*
 deprotection of a trimethylsilyl group.⁴⁸ Anchoring groups are
 often covalently bound to the gold electrode, but another
 possibility is that molecules, such as fullerene (C_{60} , Fig. 8), are
 adsorbed to the electrode,^{51, 170, 171} where a strong hybridization
 results in a high conductance.¹⁷² Tao *et al.* reported coupling of
 single molecules with Au electrodes by electrochemical
 reduction of a diazonium terminal group which produced direct
 Au-C covalent bonds *in situ* between the molecule and the Au
 electrodes.¹⁷³

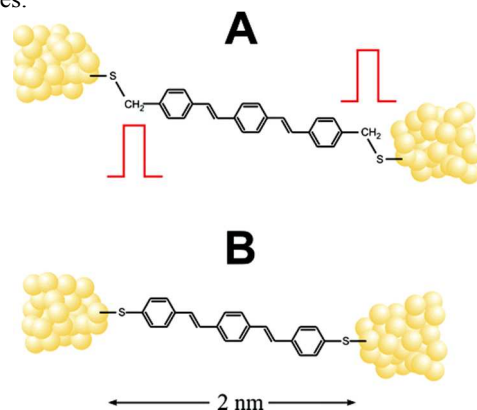


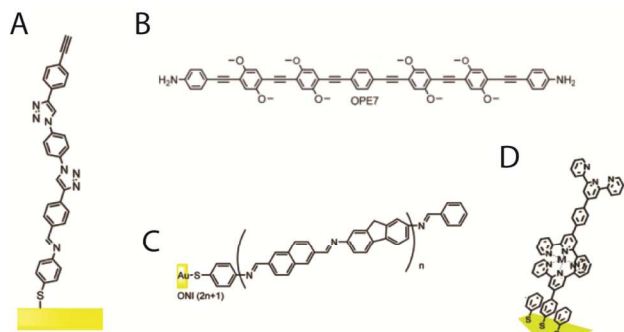
Fig. 10 Schematic representation of molecule A and B placed in
 electrode gaps. Derivative A has an extra methylene ($-CH_2-$) group
 inserted between sulfur and the π -conjugated moiety, providing a
 tunneling barrier (red). Reprinted with permission from A. Danilov, S.
 Kubatkin, S. Kafanov, P. Hedegård, N. Stühr-Hansen, K. Moth-Poulsen
 and T. Bjørnholm, *Nano Lett.*, 2007, **8**, 1-5. Copyright 2007 American
 Chemical Society.¹³⁷

Danilov *et al.* studied the influence of a single methylene
 groups inserted between the molecular π -systems and the metal
 electrodes.¹³⁷ Fig. 10 depicts the two different molecules
 incorporated in a junction. A change in the charge transport
 mechanism from coherent tunnelling to sequential tunnelling
 (decreased transparency) and Coulomb-blockade behaviour was
 observed. Due to the insertion of methylene groups, an increase
 in the resistance in the open state was observed. The directly
 connected wire shows higher conductance and no gate
 dependence, which resulted from a strong metal-molecular
 orbital coupling.¹³⁷

3.2 Molecular backbone. This is the part of the molecular
 system, which largely defines the electronic functionality of the
 single-molecule device. That is, for a given electronic structure
 of the molecular kernel, the single-molecule device function
 might turn out to be that of a resistor, a diode, a transistor, etc.
 Molecular switches, a thoroughly studied system, are reviewed

1 in section 4. For this part we limit the discussion to molecules
 2 wires, in which charge transfer occurs through the π -conjugated
 3 part of the molecule. Electrons can move freely in the
 4 delocalized orbitals over “long” distances. Typical molecules
 5 wires¹⁷⁴ (Fig. 11) are oligomers such as oligo(p-phenylene
 6 ethylenes) (OPE's),^{175, 176} oligo(p-phenylene vinylene)
 7 (OPV's),^{19, 177} oligophenyleneimine (OPI),¹⁷⁸ 211,
 8²¹² oligothiophenes,¹⁷⁹ oligofluoreneimine (ONI's),¹⁸⁰
 9 oligophenylenetriazole (OPT's),¹⁸¹ oligoanilines,¹⁸²
 10 oligoynes,¹⁸³ or oligoaryleneethylene (OAE).¹⁸⁴ Another class
 11 of molecules are short alkyls such as alkanedithiols,^{20, 185, 186}
 12 alkydiamines¹³¹ or phenyldithiols,³⁵ which have been widely
 13 studied as well. Other types of “molecular” systems include
 14 metal complexes such as terpyridines incorporating metal
 15 ions.^{187, 188}

16



17
 18 **Fig. 11** (A) Oligophenylenetriazole (OPT) synthesized by click
 19 chemistry, (B) oligo(p-phenylene ethylenes): OPE7, (C)
 20 oligofluoreneimine (ONI) and (D) a metal containing molecular wire as
 21 examples for typical molecules for single-molecule electronics.¹⁷⁴

22
 23 At the macroscopic length scale, the conductance of
 24 molecular wire decreases linearly with its length. A junction
 25 conductance for short molecules (<3 nm) decays exponentially
 26 with the length of the molecule.^{142, 189, 190} Conductance data can
 27 be measured using conducting probe AFM (C-AFM) on single
 28 molecules or in break junctions (via STM or MCBJ).¹⁹⁰
 29 Charge transfer in saturated and short conjugated molecules
 30 occurs due to non-resonant tunnelling,¹⁷⁴ meaning that the
 31 electron has no real retention time on the wire. The energy
 32 of the tunnelling electron does not have to match the molecular
 33 orbital energies well. One example is alkanes, which are poor
 34 conducting^{20, 34, 151} because of a large HOMO-LUMO gap. The
 35 conductance decreases with the length of the molecule and with
 36 an increasing HOMO-LUMO gap.¹³⁵
 37 Frisbie *et al.* explained a transition from a short range
 38 tunnelling charge transport mechanism to a long range
 39 “hopping” mechanism by measuring how the electrical
 40 resistance varies with temperature and with the length of the
 41 molecular wire (from 1 to 7 nm).^{178, 101, 212} This study revealed
 42 the theoretically predicted change in direct-current transport
 43 from coherent tunnelling to incoherent charge hopping in
 44 molecular junctions, as the oligophenyleneimine (OPI)
 45 molecular system extends more than 4 nm (Fig. 12).¹⁷⁸ Frisbie
 46 *et al.* further showed that a break in the conjugation
 47 introducing a non-conjugating molecule in the wire reduced the
 48 conductivity of the molecular wire dramatically. This effect was
 49 not observed in short wires, most probably due to the fact that
 50 tunnelling is the dominant transport mechanism.¹⁵¹ The change
 51 in the charge transfer mechanism from hopping to tunnelling has
 52 been shown in other molecular systems as well.^{180, 181, 187} Lu
 53 *et al.* observed a transition of the charge transport mechanism

from tunnelling to hopping at around 2.75 nm for amine
 terminated OPE's.¹⁹¹ The hopping conduction seems to be less
 length dependent, but more temperature dependent than
 transport in the tunnelling regime.^{180, 189}

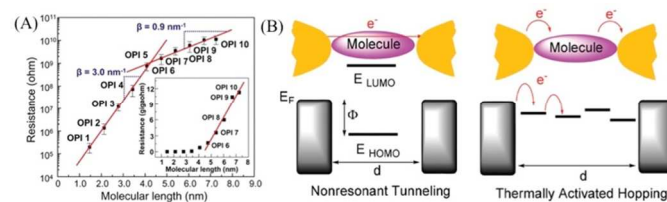


Fig. 12 (A) Electrical resistance of conjugated oligophenyleneimine (OPI) molecular wires.¹⁷⁸ From [S. H. Choi, B. Kim and C. D. Frisbie, *Science*, 2008, 320, 1482-1486]. Reprinted with permission from AAAS. (B) Schematic energy diagram for different transport mechanisms, nonresonant tunneling and multistep hopping through molecular wires between metal electrodes.¹⁸⁸

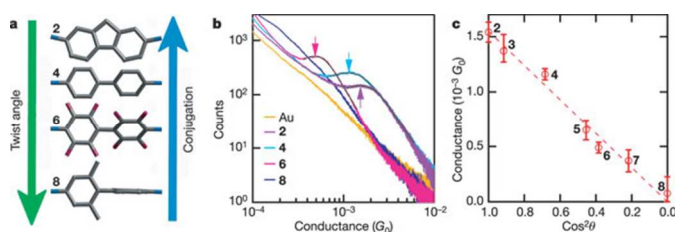
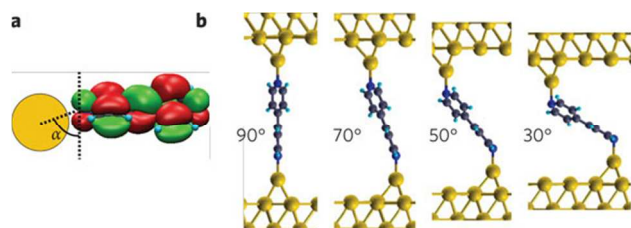


Fig. 13 Dependence of single-molecule junction conductance on molecular conformation. Reprinted by permission from Nature Nanotechnology (L. Venkataraman, J. E. Klare, C. Nuckolls, M. S. Hybertsen and M. L. Steigerwald, *Nature*, 2006, 442, 904-907), Copyright (2006).¹⁴²

The molecular conformation of molecular wires also plays an important role in conductance measurements of a metal-molecule-metal junction. Steigerwald *et al.* have shown that an increasing twist degree of freedom of the bonds in the wire results in a decrease in the degree of π -conjugation and therefore a decrease in the junction conductance.¹³¹ Fig. 13 shows schematically a change in the twist angle, and the resulting change of the conjugation path. The highest conductance is measured with molecule 2, which has the lowest twist angle. Another example of variations in the torsion angle in biphenyl was reported by Wandlowski *et al.*¹⁹² They changed the torsion angle of 4,4'-biphenyldithiol and monitored the Raman spectra *in situ*. The intensity of the C=C stretch in Raman spectra depends on the degree of conjugation between the two phenyl rings.

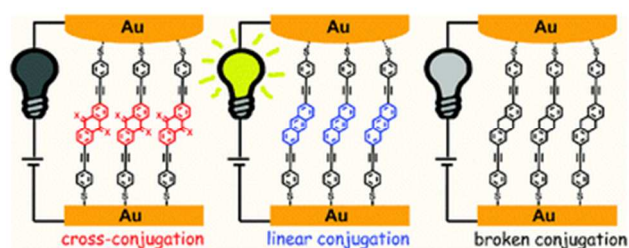
Venkataraman *et al.* showed that some molecules, like bipyridine, could assemble in a metal junction in different geometries, which have an effect on the junction conductance.¹⁶² Conductance histograms of bipyridine-based molecular wires show a double-peak feature, due to its two different binding geometries.^{140, 162} As a consequence, it is possible to mechanically switch between two defined conductance states by changing the distance in a mechanically controlled break junction. Fig. 14a shows a schematic coupling between the gold s-orbitals (orange) and the bipyridine LUMO (π^*), which is the orbital expected to be responsible for the charge transmission. The π^* is expected to be perpendicular to the nitrogen lone pair, therefore a high tilting angle α between the nitrogen-gold bond and the π -system allows strong coupling and high conductance. Fig. 14b shows schematically the case of high conductance. These pull-push break junctions have been

1 used to explore the influence of geometry in junction
2 conductance, proven with a library of pyridine-based molecules
3 wires.¹⁴⁰



5
6 **Fig. 14** Mechanically controlled binary conductance. Reprinted by
7 permission from Nature Nanotechnology (S. Y. Quek, M. Kamenetska,
8 M. L. Steigerwald, H. J. Choi, S. G. Louie, M. S. Hybertsen, J. B.
9 Neaton and L. Venkataraman, *Nat. Nanotechnol.*, 2009, 4, 230-234),
10 Copyright (2009).¹⁶²

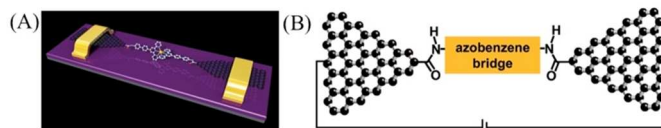
11 Hummelen *et al.* studied the difference in conductance
12 between linear conjugated, broken conjugated and cross-
13 conjugated wires.¹⁹⁰ In cross-conjugated wires, two subsequent
14 single bonds connect π -conjugated systems. These are linear
15 conjugated to a double bond, a sp^2 hybridized carbon, called
16 vinylidene double bond, as in *e.g.* anthraquinone. Hummelen
17 *et al.* found that cross-conjugated wires show a very low
18 conductivity,^{193,194} and even lower conductivity than molecular
19 wires with a broken conjugation, see Fig. 15.¹⁹⁰ This effect is
20 correlated with the destructive quantum interference effect
21 of cross-conjugated wires (Fig. 15, red molecules).^{194,197-199}



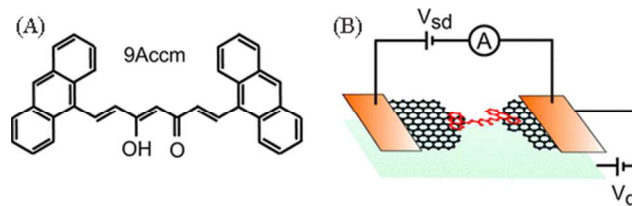
24
25 **Fig. 15** Schematic of OPEs in a conductive probe AFM junction. With
26 three different molecules: cross conjugated (red), linear (blue) and
27 broken (black) conjugated.¹⁹⁰

28
29 **3.3 Electrode material.** As discussed above, the formation of
30 efficient and reproducible molecule-metal electrodes coupled
31 is one key factor for the integration of molecules into circuits
32 the future.¹⁶⁹ To date, due to its noble metal character, gold has
33 been the electrode material of choice. Future developments
34 could be focused on other materials, such as silicon or carbon.
35 Nanoscale junctions of Si have been fabricated, but the Si-C
36 bond is not as mobile as the S-Au bond, which makes it more
37 difficult to make a well defined SAM.²⁰⁰ Another approach
38 using carbon-based electrodes. Graphene and other 2D
39 materials can be grown without defects at wafer scale, and
40 since graphene is a 2D material, this might pose some
41 advantages when considering the number of contact geometries
42 compared to electrodes made of 3D materials. Guo *et al.*^{97,98}
43 functionalized graphene with molecular wires *in situ* by
44 covalent bonds.¹³⁸ The junction was fabricated by dash-line
45 lithography, the nanogaps were then cut out by oxygen plasma
46 ion etching. This etching produced carboxyl acid-terminated
47 graphene, which was further functionalized with groups such as
48 amine terminated molecular wires (Fig. 16). Van der Zant *et al.*⁹⁶
49 created graphene electrodes by feedback-controlled electro-

burning. The molecular system was introduced in a second step,
and the coupling between molecule and graphene was
established by π - π stacking (Fig. 17).⁹⁶



54
55
56
57
58
59 **Fig. 16** (A) Depiction of a single-molecule device based on graphene.⁹⁷
(B) Schematic of a grapheme-azobenzene junction.¹³⁸ Reprinted by
permission from John Wiley and Sons, copyright (2012) and (2013).



60
61
62
63
64
65
66
67
68
69
70 **Fig. 17** Anthracene terminated curcuminoid wire (A) brought into a
graphene nanogap (B). Reprinted with permission from F. Prins, A.
Barreiro, J. W. Ruitenber, J. S. Seldenthuis, N. Aliaga-Alcalde, L. M.
K. Vandersypen and H. S. J. van der Zant, *Nano Lett.*, 2011, 11, 4607-
4611. Copyright 2011 American Chemical Society⁹⁶

71 Molecular electronics experiments have also been done with
72 other electrode materials in which similar anchoring groups and
73 the same molecular wires can be used. Zhou *et al.* used
74 electrochemical jump-to-contact scanning tunnelling
75 microscope break junction (ECSTM-BJ) to create gold and
76 copper clusters.¹³⁹ They used different bipyridyl molecules and
77 compared the conductance between Au and Cu electrodes,
78 where the Cu electrodes showed a lower conductance. The
79 different electronic coupling efficiencies between the metal and
80 the wire were suggested as the cause of this effect. In another
81 study, Danilov *et al.* compared devices with gold (Au) and lead
82 (Pb) electrode material and found that the low bias regime in
83 the Pb electrode case showed similar molecular charging
84 energies, but different open state gate voltages compared to the
85 gold electrode. For example, the -2.6V gate voltage separates
86 the same open state at +0.8V on the gold electrode.¹³⁷ This
87 effect was attributed to the differences in the Fermi level of Au
88 and Pb. In addition, Kaun *et al.* found that the conductance of
89 alkanedithiol junctions could be increased by changing the
90 electrode orientations [100] and [111] using first principle
91 calculations.²⁰¹ Their work indicates that Au(100) electrodes
92 provide the high conductance, while Au(111) provides the low
93 conductance in alkanedithiol single-molecule junctions, which
94 is an interesting observation when considering the spread of
95 different electrode metal facets one can envision observing in
96 the actual device. The effects of different electrode materials,
97 including Au, Ru, and carbon nanotubes, on electronic transport
98 of molecular electronic devices have been studied theoretically
99 by Kim *et al.*²⁰²

100 In all examples here, it can be concluded that the molecular
101 structure, including anchoring group, molecular wire
102 architecture, length, conformation, and alignment of the Fermi
103 level with the HOMO-LUMO gap, are key factors for the
104 junction conductance and opens for a wealth of opportunities
105 for chemical design of molecules with tailored properties for
106 single-molecule devices.

310311310

4. Physical phenomena in single-molecule electronics

Beyond their novelty as electronic devices, metal-molecule junctions are a unique test bed for performing electron transport studies at the nanoscale. These systems offer plethora of rich physics, ranging from electrical rectification to quantum mechanical interference at the molecular level. In this section we highlight the experimental work describing physical phenomena observed in single molecules, since the first proposal of unimolecular electronic devices.²

4.1. Rectification. A rectifier, also called a diode, is a two-terminal in which current flow is allowed for a given polarity of the voltage applied across its terminals (forward bias), but is blocked when the polarity is inverted (reverse bias). An ideal rectifier is thus a voltage-controlled switch.

Rectification is an almost ubiquitous phenomenon in semiconductor technology. A simple metal-semiconductor interface exhibits rectification as a consequence of the mismatch in the Fermi level of the metal and either the conduction or valence band of the semiconductor. When a metal and an n-type semiconductor are brought into contact and thermal equilibrium (i.e. equalization of Fermi levels) is reached, an energy barrier (so-called Schottky barrier) is formed. Rectification occurs because in order for electrons to go from the conduction band of the semiconductor into the metal, this barrier has to be overcome by, for example, applying an external voltage equal to the barrier height. Inversion of the polarity of the voltage (reverse bias) leads to an increase of the barrier, which in principle impedes electron flow, but in practice it leads to a very small saturation current. Large rectification (ON/OFF ratio) can be achieved by replacing the metal with a p-doped material; in this case the barrier height increases and the saturation current decreases orders of magnitude.

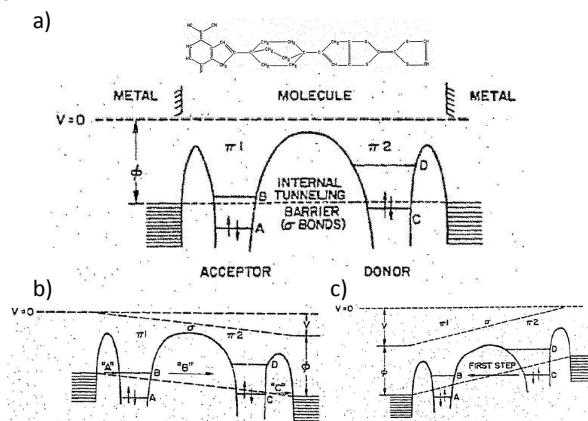


Fig. 18 Aviram-Ratner single-molecule rectifier based on acceptor tetracyanoquinodimethane (TCNQ) and donor tetrathiolfulvalene (TT) separated by a triple methylene bridge. (A) Structure and energy diagram of the molecule in contact with cathode and anode electrodes. (B) Energy diagram in forward bias (On state) and (C), reverse bias (OFF state). Reprinted from Aviram and M. A. Ratner, *Chem. Phys. Lett.*, 1974, **29**, 277-283, with permission from Elsevier.²

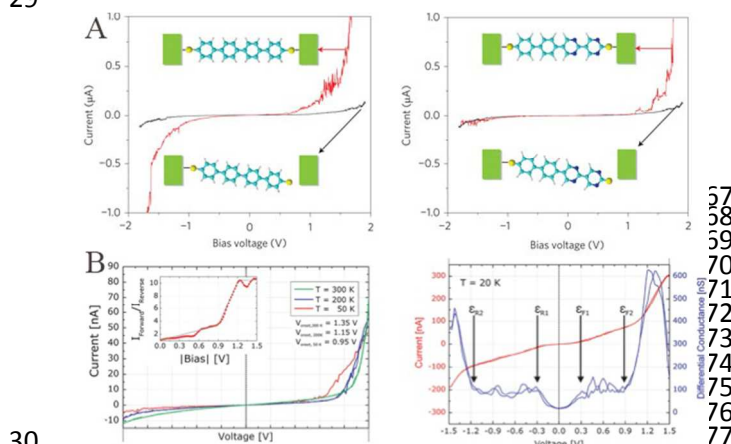
In analogy with a p-n diode, Aviram and Ratner proposed a single molecule consisting of electron rich/donor (n-type) and electron poor/acceptor (p-type) units, separated by a sigma bond that behaves as tunnelling barrier or (Fig. 18,a).² In these asymmetric molecules, rectification occurs if the acceptor/donor levels are carefully chosen. If this is the case, forward bias (on state) corresponds to a negative voltage applied to Metal 1 (cathode) respect to Metal 2 (anode).

forward bias (Fig. 18,b) electrons tunnel from the cathode to the anode in a three step process: 1) from the cathode (metal) to the LUMO of acceptor level, 2) from the LUMO of the acceptor level to the HOMO of donor level and 3) From the HOMO of the donor level out into anode (metal). For reverse polarity the downhill tunneling of electrons from cathode to anode is no longer possible (Fig. 18,c).

Experimentally, STM became the first technological platform capable of contacting single molecules adsorbed on metallic surfaces. Following the theoretical proposal, studies of rectification in single molecule were obscured by employing dissimilar contact metals (different workfunction), which in principle could by themselves display rectification due to asymmetric tunnelling current. The first experiment reported rectification in a monolayer of hemiquinone (acceptor-donor pair) attached to the surface of Au/Ag (anode) on mica using a Pt tip (cathode).²⁰³ A similar study reported rectification in phthalocyanines chemically bonded to the surface of highly-oriented pyrolytic graphite (HOPG) by wet chemistry.²⁰⁴ In both cases rectification was explained to be a consequence of the presence of molecules, although a simple mismatch in tip-substrate work functions was not ruled out. To address the case of molecular rectification with symmetric metallic contacts, gold substrate and STM tip were used to study SAMs in sterically hindered Donor- π -Acceptor (D- π -A) moieties (instead of D- σ -A).²⁰⁵ In the studied molecules (C₁₆H₃₃-Q3CNQ), the donor and acceptor are twisted out of the plane to avoid donor and acceptor overlap of molecular orbitals. Remarkably, the planarity of the molecule (dihedral angle between donor acceptor) could be controlled chemically, and this was achieved by sequential exposure of the molecule to HCl (to twist molecule) and NH₃ (to restore planarity). The gold substrate and tip were chemically functionalized with sulfur and a decanethiolate link chains to achieve symmetric contacts to the molecule. As a result, rectification in molecules with twisted moieties was observed, while those that are planar or have a weak donor-acceptor combination exhibited no rectification. Rectification (50-150 ON/OFF ratio) was thus attributed to the molecule asymmetry itself, since rectification disappears when the molecules are planar and molecule contact to anode/cathode is symmetric. Another example where rectification occurred in the absence of a sigma bond was the case of (asymmetric) dipyrimidinyl-diphenyl covalently attached to the gold electrodes with thiol groups (Fig. 19, a). As a control experiment, the symmetric version of the molecule (tetraphenyl) showed no rectification. At zero bias, the hole wave function is strongly localized at the biphenyl end of the molecule near the surface. This is the consequence of the original electronic structure, which reflects the underlying chemical differences between the dipyrimidinyl and diphenyl blocks. Upon application of bias, the lack of symmetry of the molecule wave function results in an enhanced probability of hole transfer from the anode to the molecule.²⁰⁶

Using a MCBJ set-up,^{15, 43, 44, 207, 208} rectification was reported for the first time in a variety of Aviram-Ratner type molecules consisting of two weakly coupled electronic π -systems,²⁰⁹ covalently attached to electrodes using sulfur-gold bonds. The authors observed asymmetric IV curves for asymmetric molecules and symmetric for symmetric molecules, emphasizing the effects of the molecular system. In addition to rectification, this work reported the observation of steps in the IV curve that were attributed to the internal electronic structure of the molecule. The origin of this is that, in the presence of an electric field, the energy levels of the π systems are shifted

1 relative to each other. Whenever an unoccupied level passes 52
 2 an occupied one, an additional transport channel opens up and 53
 3 the current increases in discrete amounts. In addition, it was 54
 4 found that the current through the junction was also affected 55
 5 the polarizability of the molecule, since the height of the 56
 6 steps depended on the bias magnitude and polarity. 57
 7 In general, since rectification is a property inherent to mater- 58
 8 interfaces, the current focus in single-molecule rectification 59
 9 to avoid experimental artefacts by controlling the 60
 10 molecule/metal contacts and comparing experimental data 61
 11 theoretical simulations. There are only a few cases where 62
 12 measurements on the same molecule using a different 63
 13 experimental realization agree, notably C₆₀ coupled to silver 64
 14 electrodes in a lithographically defined nanogap and STM, 2005 65
 15²¹³ and more recently diblock dipyrimidinyldiphenyl studied 66
 16 a MCBJ and STM setup (Fig. 19).^{46, 206} For C₆₀, though IV 67
 17 curves were not quantitatively reproduced (due to the different 68
 18 metal/molecule contacts), a great similarity was observed in the 69
 19 tunneling LDOS by looking at dI/dV(V) plot. For the case of 70
 20 diblock dipyrimidinyl diphenyl, the current-voltage 71
 21 characteristics in a MCBJ set-up exhibited a temperature- 72
 22 independent rectification of up to a factor of 10 in the 73
 23 temperature range between 300 and 50 K, greater to what was 74
 24 reported using STM. As an outlook, the challenges in single- 75
 25 molecule device are to demonstrate high rectification ratio (e.g. 76
 26 by molecular design) and to develop technologies to improve 77
 27 the reproducibility, room temperature stability and integration 78
 28 of single-molecule rectifiers. 79



32 **Fig. 19** Rectification in dipyrimidinyl and diphenyl blocks measured 79
 33 STM (A) configuration and MCBJ (B). In both (independent) 80
 34 experiments rectification was observed only for symmetric molecules 81
 35 (left in a,b). (A) Reprinted by permission from Nature Nanotechnology 82
 36 (I. Diez-Perez, J. Hihath, Y. Lee, L. Yu, L. Adamska, M. 83
 37 Kozhushner, I. I. Oleynik and N. Tao, *Nat. Chem.*, 2009, **1**, 635-640. 84
 38 Copyright (2009).²⁰⁶ (B) Reprinted with permission from E. Lörtscher, 85
 39 B. Gotsmann, Y. Lee, L. Yu, C. Rettner and H. Riel, *ACS Nano*, 2010, 86
 40 **6**, 4931-4939. Copyright 2013 American Chemical Society.⁴⁶ 87

42 **4.2. Vibrational Effects.** Molecules are flexible entities that 88
 43 undergo deformations when they exchange energy with the 89
 44 environment. For example, in optical spectroscopy 90
 45 experiments, molecules display sharp absorption for certain 91
 46 wavelengths. When the energy scale of the incoming light is 92
 47 the order of eV's (UV-visible), absorption lines correspond 93
 48 transitions between molecular electronic levels. Absorption at 94
 49 lower energy scales (~100 meV's, infrared) reveals vibrations 95
 50 in molecular bonds (e.g. stretching) and at even lower energy 96
 51 scales (~meV's, microwave), absorption correspond to motion 97

in molecular degrees of freedom such as translations and 98
 rotations. The total absorption spectrum from the UV-vis to the 99
 microwave can be thought of as the fingerprint of a molecule 100
 and this is used to identify molecular species in macroscopic 101
 samples.

In electron transport experiments, the typical energy scale is in 102
 the range of a few hundred milli-electronvolts, which means in 103
 principle electrons can excite motion, rotation and vibrations in 104
 molecules. For this to be possible, the time the electron spends in 105
 the molecule should be comparable to the time the electron 106
 needs to interact with a vibrational level. It turns out that 107
 features observed in IV due to molecular modes can be 108
 compared with optical spectroscopy (e.g. Raman or IR) and can 109
 be used to identify molecules present in between metallic 110
 electrodes.

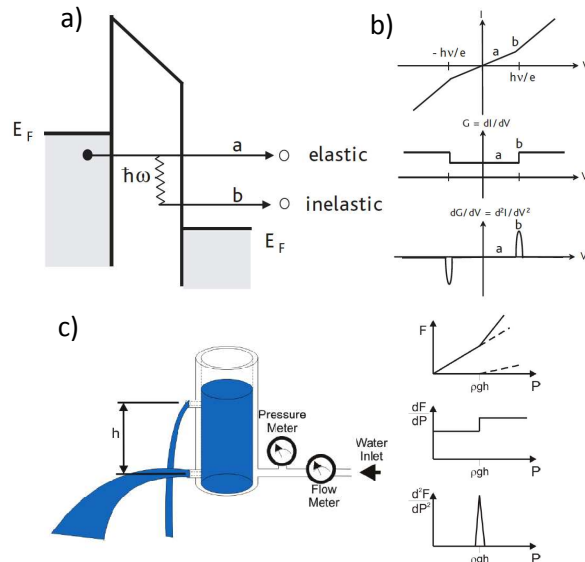


Fig. 20 Study of vibrational effects in molecules by inelastic electron 101
 tunnelling spectroscopy (IETS).³⁶² (A) In addition to elastic tunnelling 102
 current through a molecule, an additional inelastic current channel 103
 opens every time the applied voltage matches a characteristic 104
 vibrational mode with energy $h\nu$.²¹⁴ (B) The small current due to 105
 inelastic tunnelling is better observed as symmetric (antisymmetric) 106
 steps (peaks) around zero bias in the (dI/dV) $d^2I/dV^2(V)$ plot. (C) An 107
 analogy to IETS in a water tank with two openings separated by a 108
 height h . Water flow (current) has two components: 1) a flow in the 109
 bottom channel which increase with input pressure P (V) and 2) a flow 110
 through the top channel which has a threshold pressure ρgh . The total 111
 water flow F has a kink when the input pressure matches $P_i = \rho gh$. 112

The excitation of vibrations in molecules due to electrons, 113
 inelastic electron tunnelling spectroscopy (IETS), was 114
 investigated by Jacklevic and Lambe.²¹⁵ In their seminal 115
 experiment, IETS was used to identify OH groups contained in 116
 an insulating barrier between metallic electrodes. In IETS 117
 experiments the total current has two components (Fig. 20,a): 118
 1) due to elastic electron tunnelling, which increases steadily as 119
 a function of voltage and 2) due to inelastic electron tunnelling, 120
 which causes discrete steps in current every time the applied 121
 voltage matches a characteristic vibrational mode with energy 122
 $h\nu$ and increases steadily thereafter. The current due to inelastic 123
 tunnelling is only a minimal fraction of the total current and can 124
 thus be better observed as antisymmetric (around zero bias) 125
 peaks in the $d^2I/dV^2(V)$ plot (Fig. 20,b). An analogy to aid in 126
 the understanding of tunnelling spectroscopy is presented in 127
 Fig. 20,c.²¹⁶ A water tank has two openings separated by a 128
 height h and therefore two components of the water flow: 1) a 129
 flow through the bottom channel which increase with input pressure 130
 P (V) and 2) a flow through the top channel which has a threshold 131
 pressure ρgh . The total water flow F has a kink when the input 132
 pressure matches $P_i = \rho gh$.

1 steadily increasing flow in the bottom channel and 2) a flow 65
 2 through the top channel, which has a threshold pressure ρgh 66
 3 (with ρ the density of water and g the gravitational constant) 67
 4 and steadily increases thereafter. The total water flow F has 68
 5 kink when the input pressure matches $P_i = \rho gh$. This kink might 69
 6 be difficult to observe in an $F(P)$ plot, but it would be easier 70
 7 see it in $dF/dP(P)$ and even easier in $d^2F/dP^2(P)$: a flow 71
 8 opening at height h is revealed by a peak at pressure $P = \rho gh$. 72
 9 IETS, the pressure threshold corresponds to a voltage threshold 73
 10 every time the input voltage matches the energy scale of a 74
 11 vibrationally or rotationally excited molecular level. 75

12 Over the years, IETS has been developed and it is currently 76
 13 understood that the effect of vibrational effects in current 77
 14 depends on the electron-phonon coupling as well as electron 78
 15 coupling between the electrodes and molecule.^{134, 217} The latter 79
 16 can be tuned in different experimental realizations such as 80
 17 STM, MCBJ or three terminal devices. 81

18 STM was the first experimental platform to describe IETS 82
 19 the single-molecule level, by recording the C-H stretching 83
 20 mode of C_2H_2 adsorbed on copper.²¹⁸ In this report, authors 84
 21 replaced hydrogen by its heavier isotope, deuterium in order 85
 22 confirm the origin of peaks observed in d^2I/dV^2 in the energy 86
 23 scale corresponding to C-H stretching mode. In this seminal 87
 24 paper it was already acknowledged that certain expected 88
 25 vibrational modes were observed while others were hindered 89
 26 and it was suggested the molecule-substrate coupling as a 90
 27 possible cause. Further understanding in this direction was 91

28 achieved in an experiment in which copper phthalocyanine was 92
 29 electronically decoupled from the substrate, by using bare and 93
 30 oxidized NiAl (110).²¹⁹ In this work, vibronic features were 94
 31 only observed for molecules adsorbed on the oxidized substrate 95
 32 (ultra-thin Al_2O_3); the absence of vibrational signatures on the 96
 33 bare NiAl(110) surface was attributed to spectral broadening 97
 34 when the molecule is coupled to the metallic substrate. Another 98
 35 case of absence (appearance) of expected (unexpected) vibronic 99
 36 modes is nitrobenzene on Cu(111), which was expected to 100
 37 display 39 internal modes out of which only seven were 101
 38 observed in the IETS spectra.²²⁰ Both absent and additional 102
 39 modes in the spectra were attributed to molecular-metal 103
 40 coupling, which suggested that intimate details of the metal- 104
 41 molecule interface might be unveiled from this type of 105
 42 measurements. Along this line, IETS was recently used to 106
 43 understand the changes in a molecule-metal contact with 107
 44 benzenedithiol (BDT) attached to gold electrodes in a STJ 108
 45 break junction setup.²²¹ Two modes were identified: a 14 meV 109
 46 mode (due to either oscillation of BDT with respect to the gold 110
 47 electrodes or to gold-gold bonds in the contact) and mode 111
 48 between 0.1-0.2 eV (due to vibrations of the benzene ring). 112
 49 These modes changed with displacement of the STM tip and 113
 50 this was used to demonstrate that strain was applied at the 114
 51 molecule-electrode contact when stretching or compressing the 115
 52 junction. 116

53 In an attempt to perform both STM and optical spectroscopy 117
 54 on the same molecule, STM has been combined with 118
 55 enhanced Raman spectroscopy (TERS).²²²⁻²²⁴ These types of 119
 56 experiments allow not only chemical identification of 120
 57 molecules adsorbed on a surface, but also information about 121
 58 adsorption configuration and chemical bonding in or between 122
 59 molecules. In particular for copper phthalocyanine (CuPc) on 123
 60 Ag(111), up to eight vibrational modes were identified and 124
 61 assigned *via* DFT calculations.²²⁴ Further progress in STM 125
 62 IETS includes the observation of spin splitting of individual 126
 63 vibronic states in neutral and charged magnesium porphyrins 127
 64 a magnetic field up to 9 T.²²⁵ These types of studies may help

unveiling the nature of the electron charge and spin coupling to 128
 molecular vibrations. 129

As a remark, STM studies of vibrational modes in molecules 130
 correspond to off-resonant tunnelling where the electron- 131
 phonon interaction is weak and thus the signature of vibrational 132
 modes is a small increase in the differential conductance, better 133
 seen as antisymmetric peaks in $dI^2/dV^2(V)$. However, an 134
 interesting regime appears in the strong metal-molecule regime, 135
 where the electrical conductance of the junctions is of the order 136
 of $G_0 = 2e^2/h$ (with e the elementary charge and h the Planck 137
 constant). In this case, vibrations are observed as dips (instead 138
 of peaks) in the $dI^2/dV^2(V)$ spectrum. This has been observed 139
 on chains of gold atoms,^{226, 227} hydrogen,^{43, 228} and water 140
 molecules.²²⁹ The reader is referred to ref. (217, 230) for a 141
 comprehensive discussion. 142

Other techniques that offer a similar test bed as STM 143
 experiments for the study of vibrational effects in single 144
 molecules are the cross-wire tunnel junction,²³¹ the nanopore 145
 technique,²³² and MCBJ.^{43, 228} Albeit these experiments probe 146
 SAM's rather than single molecules, progress has been made in 147
 recent years to understand if metallic electrodes are bridged by 148
 a single molecule using conductance histograms.^{43, 50, 228, 233-235} 149
 Similar to STM studies, IETS has been used in these 150
 experimental set-ups to explain changes of molecular 151
 conformation, contact geometry, and metal-molecule bonding 152
 in *e.g.* alkanedithiol molecular junctions (Fig. 21).⁵⁰ 153

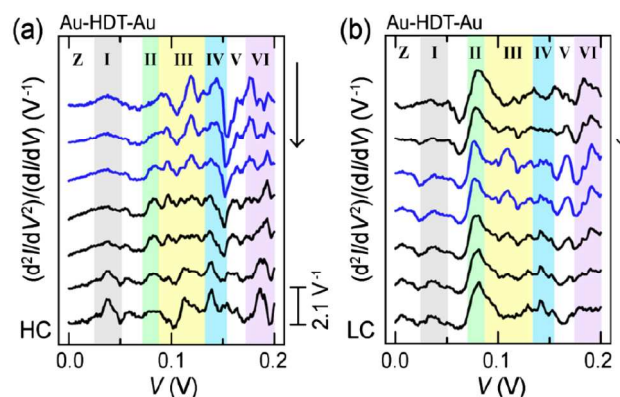


Fig. 21 IETS from a MCBJ experiment to identify hexanedithiol (HDT) 154
 conformation and geometry of contact to gold electrodes in a high 155
 conductance HC (A) and low conductance LC (B) molecular junction 156
 made.⁵⁰ The IETS spectra are measured as the metal-molecule-metal 157
 junction is stretched (arrow direction) from 0.5 Å (top) to 4.5 Å 158
 (bottom). The vibrational modes correspond to Z, longitudinal 159
 metal phonon; I, Au-S stretching; II, C-S stretching; III, C-H rocking; 160
 IV, C-C stretching; V, C-H wagging; VI, C-H scissoring. Reprinted by 161
 permission from (Y. Kim, H. Song, F. Strigl, H.-F. Pernau, T. Lee and 162
 E. Scheer, Phys. Rev. Lett., 2011, 106, 196804). Copyright (2011) by 163
 the American Physical Society 164

Altogether, state-of-the-art IETS in single-molecule junctions 165
 can be used to identify the presence of molecules as well as to 166
 infer the geometry at the molecule-metal interface. Similar to 167
 optical spectroscopy, where selection rules predict the 168
 observation of certain vibrational modes, intense theoretical 169
 work is being carried out to develop such selection rules in 170
 IETS.^{220, 236-238} 171

In comparison to two terminal devices, three-terminal devices 172
 offer a new regime in electron-phonon coupling in single 173
 molecules (weak coupling). Particularly, for this case, when a 174
 gate electrode is available, vibrational effects induce peculiar 175

1 features on the current transport through the junction. This 65
2 discussed in further detail in section 4.4. 66

3 67
4 **4.3. Switching.** A particularly attractive type of molecule 68
5 (electrical) functionality is that of a switch, where the transmoecule 69
6 conductance can be changed between two or more states. The reason 70
7 for this is that transistors, the core of modern computing, are 71
8 ultimately operated as switches where the conductance is efficiently 72
9 turned on and off by a gate electrode. Single molecule switches 73
10 might thus, in principle, be the prototypical device used to replace 74
11 silicon in logic and memory elements offering the *a priori* advantage 75
12 of ultra-large density integration, of the order of $\sim 1 \text{ TBcm}^{-2}$. 76

13 Molecules that display stable isomers are good candidates to 77
14 used as the kernel in molecular switches. Changes in molecular 78
15 conductance arise from changes in their geometry, since the spatial 79
16 arrangement of atoms lead to changes in several physical properties 80
17 including the electronic structure of the molecule and thus in 81
18 density of states. When a molecule is placed between electrodes 82
19 (Fig. 22a), the current I through it as a function of the voltage 83
20 across the device can be estimated using the Landauer formalism 84
21 The device conductance is $dI/dV \propto (2e^2/h) T(E_F - eV)$, where e is 85
22 elementary charge, h is Planck's constant, E_F is the 86
23 electrochemical potential of the contacts and $T(E_F - eV)$ is related 87
24 to the molecular transmission function through the density of states 88
25 in the molecule. The conductance of a molecule, directly 89
26 proportional to the density of states, reflects thus the interplay 90
27 electronic structure of the molecule and can be switched 91
28 triggering molecular rearrangements. From an engineering point 92
29 view, the challenge is to fabricate a single molecule switch where 93
30 changes in conductance are significant, ideally from zero (OFF state) 94
31 to infinite (ON state). 95

32 The conductance (bi-) multi-stability of a molecular switch requires 96
33 molecules with (two) several stable isomers, and the transition 97
34 between isomers to be controlled by external stimuli (e.g. light, heat, 98
35 current or electric field). Fig. 22b shows the potential landscape of a 99
36 bistable molecule for its ground and excited state. The reaction 100
37 coordinate axis is a physical parameter such as intramolecular bond 101
38 length or torsion angle. The two states of the switch (state 1 and state 102
39 2) correspond to the two minima in the ground state separated by an 103
40 activation barrier ΔE_{act} , much larger than the thermal energy $k_B T$. 104
41 Switching between states can be done by bringing the molecule from 105
42 state 2 to an excited state then let it relax to state 1, or by driving the 106
43 molecule over the potential barrier by stimuli such as heat or electric 107
44 field. 108

45 Early studies of single-molecule switches were performed in STM 109
46 setups. The first example of single molecule switch based on 110
47 conformation changes of molecules was carried out in phenylene 111
48 ethynylene oligomers isolated in matrices of self-assembled 112
49 monolayers (SAM) of alkanethiolate.²⁹ In this work, a special 113
50 protocol was used to assemble the functional molecules on an Au 114
51 surface. Once the SAM is present on the Au surface, ammonium 115
52 hydroxide was used to hydrolyse the acetyl group of the functional 116
53 molecule, generating the thiolate or thiol that adsorbed on the 117
54 surface at existing defect sites in the dodecane thiolate SAM. During 118
55 STM imaging, the stability of the SAM contrasted with that of the 119
56 phenylene ethynylene molecules, which reversibly changed 120
57 conductance state between high and low with persistence times 121
58 the range from seconds (poorly ordered SAM) to tens of hours (well 122
59 ordered SAM). The origin of conductance switching was attributed 123
60 to conformational changes in the molecules rather than electrostatic 124
61 effects of charge transfer. This latter observation was derived from 125
62 topographic profile of the molecule, since in the high conductance 126
63 state the active molecules protruded out of the SAM, while in the 127
64 low conductance state their height relative to the SAM is lower. 128

In Section 5 we present a thorough description of how to 129
implement molecular switches by chemical design of the molecular 130
systems, a variety of stimuli used to trigger molecular transition and 131
their applicability as devices. Here we highlight the importance for 132
molecular switches, and more generally for any single-molecule 133
device, of considering the environment for adequate modeling, 134
design and implementation. In practice, even if the existence of two 135
states is encoded in molecular design, the crucial operational 136
parameters, switching voltages and the mere existence of bistability 137
are environmentally sensitive. Strong coupling to metallic contacts 138
or electrostatic interaction with the substrate might be detrimental 139
for the operation of single molecule switches. An example of the 140
environment effect on the electronic structure of the molecule is the 141
case of bianthrone on aluminum oxide substrate connected to silver 142
electrodes.²⁴⁰ Bianthrone is a sterically hindered compound that 143
exists in the form of two nonplanar isomers, and the transition can be 144
triggered by light or heat (Fig. 22a). In ref.²⁴⁰, a single bianthrone 145
switch revealed persistent switching of the electric conductance at 146
low temperatures, which was associated with molecular 147
isomerization events from spectroscopic dI/dV measurements. Based 148
on the statistics of switching events, authors were able to measure 149
the activation energy of the process to be of the order of 35-90 meV. 150
This value was an order of magnitude lower to that measured for free 151
bianthrone ($\Delta E_{\text{act}} \sim 0.9 \text{ eV}$) and the explanation for this is that, when 152
placed in contact with silver and on high permittivity dielectric, one 153
of the bianthrone isomers acquires negative charge that shifts 154
molecular geometry (due to image forces in the substrate) which in 155
turns lowers the transition barrier. This result showed that the impact 156
of the environment on the performance of single molecules devices, 157
and in particular, the profound changes induced in the energy 158
landscape of the molecular kernel by highly polarizable substrates 159
and metallic electrodes. 160

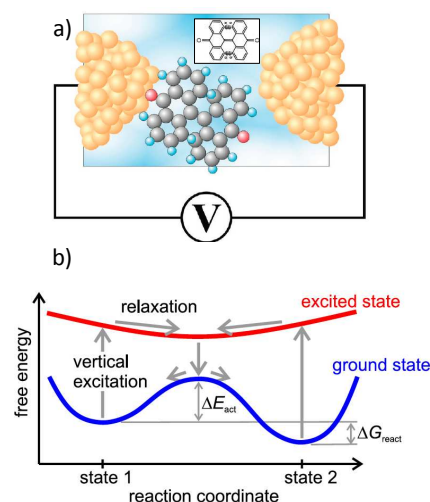
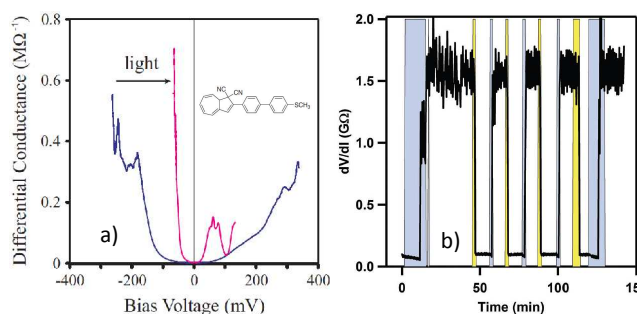


Fig. 22. Molecular switches. A) Schematic representation of a molecular switch based on bianthrone connected to metallic electrodes. Reprinted by permission from (S. Lara-Avila, A. Danilov, V. Geskin, S. Bouzakraoui, S. Kubatkin, J. Cornil, and T. Bjørnholm, *J. Phys. Chem. C*, 2010, 114, 20686–20695). Copyright (2010) by the American Physical Society. B) Potential energy landscape of a bistable molecular switch; bistability arises from the two local minima of molecular the ground state. On the x axis, a ‘reaction coordinate’ is physical parameter such as a distance between two atoms or a rotation angle between intramolecular bonds. Switching is realized by bringing the molecule to an excited state via external stimuli (e.g. light) or by exciting the molecule over the ground state barrier by means of heat, vibrations (i.e. electron phono coupling) or by electric-field induced barrier lowering.²³⁹ Reprinted by permission from (van der Molen and

1 Liljeroth. Charge transport through molecular switches. Journal of
 2 Physics: Condensed Matter (2010) vol. 22 (13) pp. 133001
 3
 4 Single-molecule photoswitches are another example where it has
 5 been shown that coupling to electrodes can modify or even suppress
 6 bistability. In this type of devices, if the molecule is strongly coupled
 7 to metallic contacts, the photo-excited electron and hole may escape
 8 the molecule before triggering the transition between isomers. One
 9 route to prevent this is to decouple the molecular switch from the
 10 metal as it was demonstrated in a single molecule photoswitch with
 11 the dihydroazulene (DHA) and vinylheptafulvene (VHF) isomers.^{241,}
 12 ²⁴² Despite the inherent bistability of this molecule, authors in ref.²⁴¹
 13 observed reversible light-triggered conductance switching for only
 14 three times when the molecule is strongly coupled to metallic
 15 electrodes. In a follow-up work by the same group, authors showed
 16 an enhanced performance of the DHA/VHF switch in which the
 17 weak coupling to electrodes was ensured by incorporating $-SCH_3$
 18 end groups into the molecule.²⁴² The result was that conductance
 19 through both DHA (high resistivity) and VHF (low resistivity) (Fig.
 20 23a) could be systematically reversed, achieving a high conductance
 21 state (ON) by light, and the reverse (OFF) by heat and electric field
 22 (Fig. 23b).



24
 25 **Fig. 23** Single molecule photo switch measurements. A) The effect
 26 shining light on molecular junction which incorporates dihydroazulene
 27 (DHA)/ vinylheptafulvene (VHF) (inset) weakly coupled to electrodes leads
 28 to a reduced transport gap (zero-current area) observed in the dI/dV (V)
 29 B) A series of ON-OFF switching events in the same device. The highlighted
 30 background indicates the time intervals when the sample was illuminated
 31 with light (yellow) or the bias voltage was increased to 80 mV (blue) to reset
 32 the switch. The differential resistance dV/dI was taken at the bias voltage
 33 = 25 mV for both ON (VHF) and OFF (DHA) states. Taken with permission
 34 of authors from REF.²⁴² Broman, S. L. et al. Dihydroazulene Photoswitch
 35 operating in Sequential Tunneling Regime: Synthesis and Single-Molecule
 36 Junction Studies. Adv. Funct. Mater. (2012).

37
 38 **4.4. Coulomb Blockade.** Compared to measurements
 39 transport in a two-terminal configuration, studies of transport
 40 molecules in a three terminal configuration offer significantly
 41 more information about the molecular system. In addition to
 42 source and drain electrodes, a third (gate) electrode
 43 capacitively coupled to the molecule, allowing tuning of the
 44 energy level spectrum of the molecule with respect to the
 45 probing source and drain electrodes (Fig. 24). That is, the gate
 46 can tune the internal energy levels of the molecule (redox
 47 charge states) to be in resonance with Fermi level in the leads.
 48 If the coupling between metallic electrodes and the molecules is
 49 weak, electrons tunnel one by one in and out of the molecule
 50 “island” (or quantum dot, QD) due to electrostatic repulsion
 51 when the molecule is occupied by one electron, that is, due to
 52 Coulomb blockade. These type of devices are called
 53 (molecular) single electron transistors (SET's), and
 54 sequential tunnelling of electrons on and off the island reveals
 55 itself as steps in the IV curve of the SET whenever the resonance
 56 condition is met.²⁴³ Solid-state SET's have been extensively

studied for decades and a classic review of single electron
 transistors can be found in ref.²⁴⁴

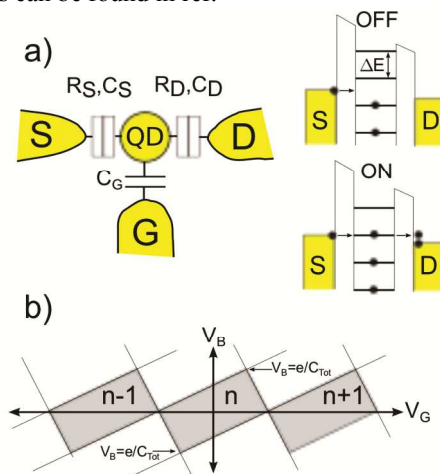


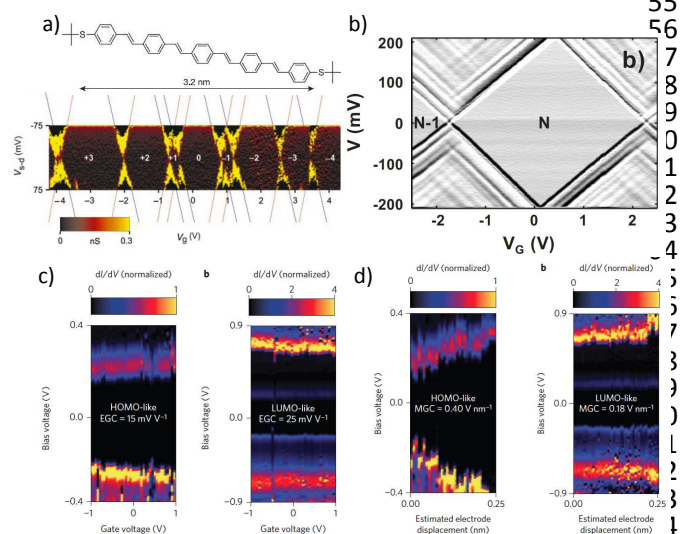
Fig. 24 Electron transport in quantum dots (QD) (three-terminal
 configuration). (a) In addition to source and drain electrodes, a three-
 terminal measurement incorporates a third electrode capacitively
 coupled to the quantum dot (molecule), allowing tuning of its energy
 level spectrum with respect to source and drain electrodes. (b) Stability
 diagram of a quantum dot in the coulomb blockade regime show the
 charge state of the dot n .

Conditions to observe single-electron tunnelling are 1) thermal
 energy must be below the charging energy $k_B T < e^2/C$ (with k_B
 the Boltzmann constant, T temperature and C the self-
 capacitance of the island) and 2) the (tunnelling) resistance
 between source/drain electrodes and island should be greater
 than the resistance quantum $R_T > h/2e^2$. Smaller islands (small
 self capacitance) lead to greater charging energies, potentially
 enabling observation of single electron tunnelling at room
 temperature. The conductivity of a single electron transistor
 (SET) as a function of source-drain bias as well as gate
 electrode potential is typically displayed in a so-called stability
 diagram (Fig. 24), where the differential conductance of the
 SET is colour coded and the greyed rhomboids (also called
 Coulomb diamonds) represent charging states of the dot.

Sufficiently small islands can be fabricated using state-of-the-
 art lithography (e.g. e-beam lithography).²⁴⁵ A practical
 disadvantage of these top-down fabricated devices is the
 challenge to make several of them with the exact same
 geometry. The lack of reproducibility on the island dimensions
 translates into substantial changes in the stability diagram,
 making large-scale integration very difficult. In this sense,
 SETs fabricated with semiconducting nanoparticles²⁴⁶ and
 carbon nanotubes²⁴⁷ offer better reproducibility. The use of
 molecules as QDs to make SETs offers several advantages. One
 of them is their QDs small size (a single to a few nm), which leads to
 a very small self-capacitance and therefore large charging
 energies, enabling potential room temperature operation.
 Furthermore, molar amounts of identical molecules can be
 chemically synthesized; in principle, intra molecular tunnel
 barriers can be defined during chemical synthesis in order to
 improve reproducibility even further.¹³⁷ The chemical aspect of
 molecular synthesis is well developed, but the fabrication of
 stable nano-contacts remains a large challenge. In practice,
 molecular SET's are studied at low temperatures to ensure
 stability of the molecule-metal junction.

The first demonstration of a molecular SET involved C_{60}
 coupled to gold electrodes created by electro migration.⁵⁴ The
 gate electrode is the underlying oxidized, degenerately doped,

1 silicon substrate. This study showed evidence for transport
2 through a single molecule by coulomb blockade with a 150 mV
3 gap. Additionally, two vibrational modes were observed: 33 mV
4 due to internal vibration of C₆₀ and a 5 mV mode corresponding
5 to motion of the entire C₆₀ molecule in the van der Waals
6 potential of the gold electrodes.



7
8
9 **Fig. 25** Renormalization of addition energies in molecules on solid-
10 state devices. (A, B) Stability diagram of OPV5 from two independent
11 experiments revealed a decrease of addition energies of the molecule
12 due to image charges (from $\Delta E_{\text{HOMO-LUMO}} \sim 2.5$ eV to $\Delta E_{\text{HOMO-LUMO}} \sim 0.73$
13 eV).^{19, 70} (B) shows (color coded) the numerically calculated second
14 derivative, which serves to highlight the fine structure of the excitations
15 showing as lines running parallel to coulomb diamonds. Reprinted by
16 permission from Nature, copyright (2003).¹⁹ Reprinted by permission
17 from John Wiley and Sons, copyright (2007).⁷⁰ The evolution of
18 HOMO-like and LUMO like levels in thiol terminated zinc porphyrin
19 gateable-MCMBJ experiment under electrostatic (C) and geometric
20 control (D) confirmed renormalization effects due to electrostatic
21 environment. Under geometric control the measured renormalization
22 the HOMO-like level was remarkably large (0.40 V nm⁻¹). Reprinted
23 permission from Nature Nanotechnology, copyright (2013).⁴¹

24
25 Kubatkin *et al.* reported a single electron transistor with a thiol-
26 end-capped oligophenylene vinylene, OPV5, and gold contacts
27 (Fig. 25,a).¹⁹ The device was fabricated using the angle-
28 evaporation technique in which the nanogap formation and
29 molecule deposition by sublimation are performed in the same
30 UHV cycle, ensuring a very clean and well-characterized
31 system. Though the precise geometry of the junction is not well
32 known in this experiment, weak metal molecule coupling
33 revealed by the observed coulomb blockade which displays
34 eight diamonds in the stability diagram corresponding to eight
35 different charging states of the molecule. A significant result
36 that the spectroscopic HOMO–LUMO gap of OPV5 has been
37 observed to be an order of magnitude lower than that in
38 vacuum. This renormalization was explained to be a
39 consequence of the electrostatic environment of the molecule
40 which substantially modifies its electronic structure. Image
41 charges generated by the charges in the molecule on metallic
42 contacts and dielectric effects are postulated to be the origin
43 of this effect.¹⁹ Importantly, the surprisingly large renormalization
44 of OPV5 was confirmed in an independent experiment where
45 contacts were prepared by electromigration^{248, 249}. Additionally,
46 vibronic effects were clearly observable and they manifested as
47 lines running parallel to coulomb diamonds (Fig. 25, b).
48 Following these experimental results, more complete

theoretical modelling of charging effects on the molecular
electronic spectrum has been made possible.^{70, 240, 249, 250} The
effect of solid-state environment on molecules is presented in a
thorough review.²⁵¹

Recently, the effect of image charges has been confirmed in a
porphyrin-type molecule using electrically gateable break
junctions (Fig 25, c and d).^{41, 252} In this set-up, the position of
the occupied and unoccupied molecular energy levels can be
followed *in situ* under simultaneous mechanical and
electrostatic control of the device. When increasing the
electrode separation (to reduce image charge effects) it was
observed an increase of the transport gap and level shifts as
high as several hundreds of meV (0.40 V nm⁻¹ for the HOMO-
like orbital). Analysis of this large gap renormalization based
on density functional theory confirms and clarifies the
important role of image-charge effects due to the electrostatic
environment in single-molecule junctions. The large changes in
electronic properties due to minute changes in geometry explain
the lack of reproducibility in numerous single-molecule
experiments, and suggest the need for both electrostatic and
geometric control of the molecular junction to achieve
reproducible IV characteristics of single-molecule junctions.

Coulomb blockade effects are thus not only a curious
phenomenon in single-molecule transistors, but also a very
powerful tool to unveil fine details of electron transport in these
nanoscopic systems.

4.5. Thermoelectric power in single-molecule junctions.

When two metals bridged by a molecule experience a gradient
of temperature across the molecular junction, a potential
difference ΔV between the cold and the hot electrodes can be
induced. Analogously to macroscopic thermoelectric effects,
this potential difference results from the thermal equilibration
of the free charge carriers. A fundamental difference in the
single-molecule thermoelectric effect is related to the large
mismatch between the discrete vibrational states of the
molecules and the metallic electrodes, which considerably
reduces the thermal conductivity across the molecular
junction.²⁴⁸ Furthermore, the discrete electronic-energy states of
the molecular systems allow transport across single energy
levels that cannot be easily achieved with continuous energy
bands present in bulk materials. In single-molecule junctions
the thermoelectric figure of merit, describing the efficiency of
the thermoelectric process, can be written as:

$$ZT = \frac{S^2 G_e T}{G_{th}}$$

where S is the thermoelectric power, T is the absolute
temperature, and G_e and G_{th} are the electronic and the thermal
conductance, respectively. G_e and G_{th} depend on the properties
of the molecules and of the materials constituting the
electrodes. The ideal junction for thermopower generation
would have a high electronic conductance and a low thermal
exchange between the hot and cold thermodynamic reservoirs,
leading to the maximum ZT value. In this sense, the relative
position of the Fermi level of the electrode with respect to the
HOMO and LUMO of the molecule determines the electronic
transport properties across the molecular junction,^{253, 254} while
the overlap of the vibrational states of the metal substrate and
the molecule is responsible for the thermal conductance through
phonons/molecular vibrations conversion. The combination of
these two opposite processes will determine the efficiency of
thermopower generation in the molecular junction. Murphy *et al.*
predicted that high ZT values can be achieved for weakly

1 coupled molecular orbitals if their energies were of the order 65
 2 $k_B T$ away from the Fermi energy of the electrodes.²⁵⁵ 66
 3 In recent years, there has been significant interest in both 67
 4 theoretical and experimental studies of single-molecule 68
 5 thermoelectric effects.²⁵⁶ The major reason for this interest 69
 6 the ability of molecular thermopower devices to generate work 70
 7 from heat without any moving parts. This feature gives a
 8 considerable advantage with respect to thermodynamic
 9 machines relying on the conversion of thermal energy into
 10 motion. Furthermore, the miniaturization level that can be
 11 achieved with single-molecule devices is beyond any power-
 12 generation technology available today. Therefore the
 13 development of thermopower devices based on molecular
 14 systems will represent a fundamental technological
 15 breakthrough for the future design of nanomachines and
 16 nanoactuators.

17 Experimentally, low-dimensional nanostructures, such as
 18 bidimensional arrays, have been investigated to improve ZT
 19 values with respect to bulk materials.²⁵⁷⁻²⁶⁵ Chen and Sootsman
 20 *et al.* have confirmed that quantum well superlattices are
 21 promising materials that allow independent control of the
 22 thermal conductivity through increased phonon scattering rates
 23 at the interfaces.^{257,266} Tsutsui *et al.* reported direct assessment
 24 of electrical heating in a metallic nanocontact, and found
 25 asymmetric electrical heating effects in symmetric single-atom
 26 contacts.²⁶⁷

27 In addition, the effect of molecular length on ZT has been
 28 investigated, leading to the fundamental understanding
 29 thermoelectric properties of single-molecule devices.²⁶⁸⁻²⁷⁹
 30 These studies indicate that an increase of molecular length
 31 results in an enhancement of the thermopower generation, but
 32 at the cost of a considerable decrease in electronic conductance.
 33 Therefore very long molecules may not be a good choice for
 34 the design of single-molecule thermoelectric devices. Ke *et al.*
 35 suggested a similar effect using density functional theory
 36 calculations.²⁷⁷ In this case the increase of molecular length
 37 induces an enhancement of thermopower generation, but the
 38 decay of conductance causes an overall decreasing contribution
 39 to ZT .

40 As an outlook, many efforts on single-molecule thermopower
 41 are focusing on improving the thermoelectric conversion
 42 efficiency by *e.g.* tuning of the Fermi level of the electrodes,
 43 chemical doping, and functional-groups substitution
 44 conductive organic molecules.^{265, 269, 278, 279} Examples in this
 45 direction include that by Yee *et al.*, who showed how n-type
 46 single fullerene molecules placed between metal electrodes
 47 could generate high thermopower values.²⁶⁵ and that of Bahar
 48 *et al.*, who reported that ZT could be increased by tuning the
 49 HOMO level of the molecules by modifying the molecular
 50 structure with donor or acceptor substituents.²⁷⁹

51 **4.6. Spintronics.** Using the spin degree of freedom
 52 information processing is in widespread use in consumer
 53 electronics, such as the use of the giant magnetoresistance
 54 (GMR) effect in magnetic hard-drives. The main component of
 55 a magnetic read head is a spin valve, a sandwich of magnetic
 56 nonmagnetic-magnetic materials, which displays a significant
 57 change in resistance depending on the polarization of the
 58 magnetic materials. The resistance value can go from high to
 59 low by changing from parallel to antiparallel magnetization
 60 (Fig. 26,a).

61 Molecular spin-based devices could lead to the ultimate
 62 integration level in magnetic memories or spin transistors with
 63 high speed and ultra low power consumption.^{280, 282}

Additionally, being of quantum mechanical nature,
 manipulation and read out of the spin degree-of-freedom can
 lead to hardware for quantum computing applications with long
 coherence times in organic molecules due to the low spin orbit
 coupling in such systems.

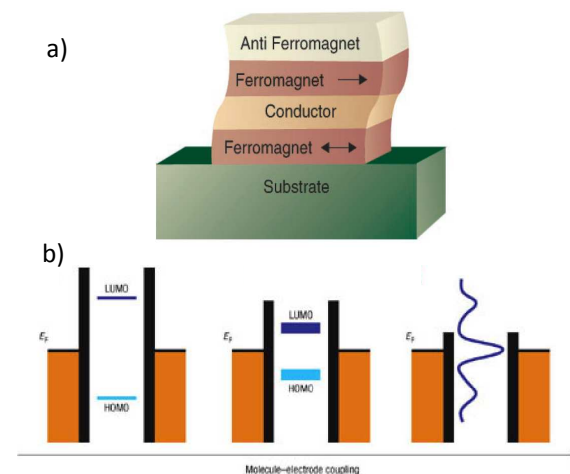


Fig. 26 Spin valve geometry (A)²⁸¹ (Reprinted by permission by Science, copyright (2001)) and formation of Kondo resonance in quantum dots in the intermediate coupling regime (B). Reprinted by permission from Nat. Mater., copyright (2008).²⁸²

Spin-electron coupling was manifested already in early studies of single-molecule transport,⁵³ such as the observation of Kondo resonances in single-molecule transistors. In metallic systems, the Kondo effect refers to the increase in resistance at low temperatures due to scattering of conduction electrons with magnetic impurities.²⁸³ In the context of transport through single molecules, intermediate coupling between a metal and magnetic molecule results in a multi-peaked transmission spectrum (Fig. 26,b). If the ground state of the molecule is spin 1/2 (unpaired electron), screening of the spin by conduction electrons occurs and manifests as an enhanced conductance at zero bias (Fig. 26). In seminal experiments by Park *et al.*⁵³ and Liang *et al.*⁵⁶ using devices fabricated by electromigration, it was observed that the Kondo resonance disappeared if the coupling to the magnetic molecule is decreased,⁵³ or by changing the charge in the molecule to an even number of electrons (*i.e.* $S=0$).

In recent years, single (magnetic) molecule devices have been used as “toy” models to understand quantum phase transition through Kondo resonances. Understanding electron correlations at the molecular scale could serve as a starting point for explaining behaviour of significantly more complex, strongly correlated materials (*e.g.* high temperature superconductors). In this direction, quantum phase transition between singlet and triplet states were studied in C_{60} -gold junctions fabricated by electromigration. By using the gate electrode it was possible to promote a transition from $S=0$ (even charge state) to $S=1/2$ (odd charge state).²⁸⁴ Kondo resonance was used as a way to read out the phase transition. In MCBJ experiments, it was found that phase transitions can also be observed by breaking the symmetry of the molecule upon stretching.²⁸⁵ In this experiment it was observed that the Kondo resonance splits into two peaks upon stretching individual cobalt complexes having spin $S=1$. The explanation is that the degeneracy of the $S=1$ triplet ground state is broken and the $S_z=0$ state will be lowered by a zero-field splitting energy D below the $S_z=+-T_1$ states. Inelastic tunnelling at energies $V = TD/e$ leads to double peak resonance.

1 In another experiment with MCBJ, the Kondo anomaly was
 2 used to detect a bias driven transition between a pseudo-singlet
 3 and a pseudo-triplet state in a cobalt complex.
 4 Experimentally, these states were assigned to the absence and
 5 occurrence of a Kondo-like resonance, respectively.

6 In practice, careful control experiments must be designed
 7 when interpreting these type of experiments, since Kondo
 8 effects can be observed in bare gold break junctions.²⁸⁷ Kondo
 9 resonances were found in 30% of the devices just after
 10 electromigration of gold, which was suggested to be caused by
 11 atomic-scale metallic grains formed during electromigration. In
 12 this sense, STM experiments have been crucial for providing
 13 insight into the nature of the Kondo effect at molecule/metal
 14 interfaces, since they allow the direct observation of the
 15 molecule and might, in principle, be less prone to artefacts.

16 STM experiments have shown that Kondo effects could be
 17 suppressed in a molecule by changing its conformation, since
 18 conformational changes lead to a different (enhanced or
 19 decreased) interaction of the molecule with electrons on the
 20 copper surface.²⁸⁸ This was the case for TBrPP-Co (TBrPP=
 21 5,10,15,20-tetrakis(4-bromophenyl)porphyrin). This molecule
 22 consists of a porphyrin unit with a cobalt (Co) atom caged at
 23 the center and four bromophenyl groups at the end parts. With
 24 TBrPP-Co deposited on a Cu(111) surface, a large voltage
 25 applied to the tip of the STM induced conformational changes
 26 in the molecule and switched the Kondo resonance on and off.
 27 It was also shown through Kondo resonances that the molecule
 28 metal coupling depends strongly on the adsorption site and
 29 configuration of the molecule on the metal.²⁸⁹ Another
 30 interesting finding of STM experiments is that magnetism and
 31 superconductivity can coexist within manganese
 32 phthalocyanine (MnPc) adsorbed on Pb(111) and compete to
 33 influence the ground state of a localized magnetic moment.²⁹⁰

34 Non-magnetic molecules are also relevant for molecular
 35 spintronics, especially when combined with ferromagnetic
 36 contacts into a spin-valve configuration. A 60% change in
 37 magnetoresistance has been reported in an STM experiment
 38 using (non-magnetic) hydrogen phthalocyanine contacted by a
 39 ferromagnetic tip of a scanning tunnelling microscope. This
 40 large magnetoresistance was explained to be the consequence
 41 of spin-dependent hybridization of molecular and electrode
 42 orbitals.²⁹⁰ A similar explanation was postulated in the large
 43 magnetoresistance (80%) observed in a single C₆₀ molecule
 44 transistor contacted with nickel using the electromigration
 45 technique.²⁹¹ An even larger value of magnetoresistance was
 46 reported for single-walled carbon nanotubes contacted with
 47 non-magnetic electrodes, coupled through supramolecular
 48 interactions to TbPc₂ single-molecule magnets.²⁹² In this
 49 molecule, a terbium atom is sandwiched between two
 50 phthalocyanine molecules, and the localized magnetic moment
 51 lead to magnetoresistance ratios up to 300% at temperatures
 52 less than 1 K.

53 An interesting direction in the field of molecular spintronics
 54 quantum informatics. In particular, the TbPc₂ system (Fig.
 55 a,b) has been widely investigated in recent years and it has been
 56 shown that it is possible to manipulate and read-out the
 57 quantum state of the Tb ion nuclear spin.²⁹³⁻²⁹⁵ For
 58 bis(phthalocyaninato) terbium(III) molecule, the Pc ligands
 59 form a molecular quantum dot and the anisotropic magnetic
 60 moment of the Tb³⁺ ion is coupled to the electron path
 61 indirectly (by ferromagnetic exchange interaction). In the
 62 presence of a magnetic field, the current through the Pc ligands
 63 was used to read-out the reversal of the electronic magnetic
 64 moment carried by the Tb³⁺ ion.²⁹⁵ Switching of the Tb³⁺

magnetic moment was observed as jumps in the differential
 conductance, which was used to extract spin relaxation times in
 the order of seconds (Fig. 27 c,d). This work has been extended
 recently and authors were able to detect up to four different
 nuclear spin states of the Tb³⁺ ion with high fidelity (better than
 69%). Another possibility to read the spin state of this molecule
 is to use high-Q nanomechanical resonators, which opens a
 route for enabling coherent spin manipulation and quantum
 entanglement.²⁹⁶

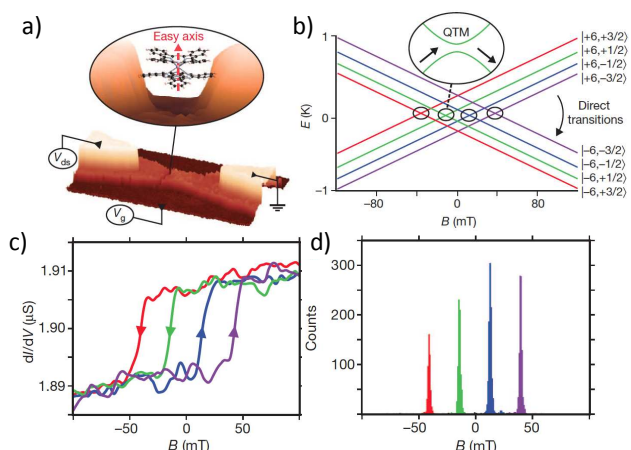


Fig. 27 (A) Geometry of the molecular spin transistor with bis(phthalocyaninato)terbium(III) (TbPc₂) made by the electromigration technique. (B) Zeeman diagram presenting the energy E of the two ground states as a function of the magnetic field. (C) Abrupt jumps in the differential conductance plot as function of the magnetic field (arrows indicate the field-sweep direction) are attributed to the switching of the Tb³⁺ magnetic moment. (D) Histogram of switching field obtained for 11,000 field sweeps showing four preferential field values that are assigned to Quantum Tunneling of Magnetization events. Reprinted by permission from Nature, copyright (2012).²⁹⁴

4.7. Quantum interference (QI). In view of electronic components and in analogy with semiconductor technology, one long-standing dream is to develop a single-molecule switch with a very high ON/OFF ratio operating at room temperature. One proposal to achieve this vision is to exploit quantum mechanical interference within the molecule so that the electron pathway from the source to the drain is effectively broken.²⁹⁷

Quantum interference effects have been studied in phase-coherent mesoscopic systems for decades. The classic example is an Aharonov-Bohm (AB) ring (Fig. 28, inset), where an electron wave coming from the left contact (source) splits, follows path A and B and can interfere on its way to the right contact (drain).²⁹⁸ The interference pattern can go from constructive to destructive by applying a magnetic field through the ring, because the electron waves travelling through A will accumulate a different phase than those travelling through B. Overall, interference leads to oscillations in the electrical resistance as a function of the externally applied magnetic field B , with period $\Delta B = h/(eA)$, h is Planck's constant, e is the elementary charge and A is the area of the ring. In these types of experiments, quantum interference is present as long as the phase-coherence length of the electron wave is comparable to the dimensions of the ring. Inelastic scattering leads to phase-randomization and thus to the suppression of quantum mechanical effects.

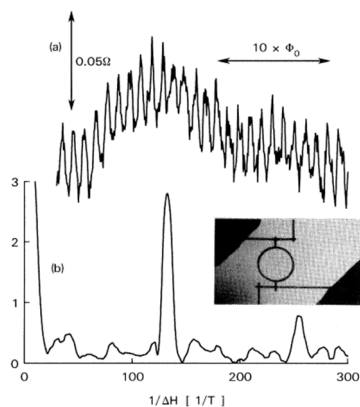


Fig. 28 (a) Magnetoresistance of an Aharonov-Bohm ring measured at $T=0.01$ K. (b) Fourier power spectrum in arbitrary units showing resistance peaks at (inverse) magnetic field $1/\Delta H$ corresponding to h/e ($1/\Delta H=131$ T $^{-1}$) and $h/2e$ ($1/\Delta H=260$ T $^{-1}$). The peak at $h/2e$ is a higher order mesoscopic effect. Inset showed a photograph of the larger ring. Reprinted by permission from Phys. Rev. Lett. Copyright (1985) by the American Physical Society.²⁹⁸

In the context of molecules, benzene can be thought as the ultimate miniaturization of an AB ring. However, in order to observe AB oscillations the magnetic field required is impractically high ($B=\Phi_0/A\sim 10$ kT). Nonetheless, interference effects can play a more subtle role in the electronic conduction through molecules by changing the intra-molecular current paths, which in turn affects profoundly the electron transmission through the molecule.

Quantum interference effects in intramolecular currents have been a matter of intense theoretical study for over a decade. Since the first proposal to use destructive interference within a molecular device to switch its conductance on and off, theoretical efforts have been devoted to understand how interference effects play a role as antiresonances (decrease of transmission) in the electron transmission spectrum.^{299, 300} Further studies have discussed the impact of electrical contacts in disturbing interference effects and it was anticipated that strong π - σ hybridization could suppress the effect of quantum interference in small molecules such as benzene, but play a less important role in larger molecules.³⁰¹

In general, from a theoretical point of view, there is consensus that quantum interference effects in molecules modify the transmission spectrum,³⁰² leading to a reduction in electron transmission. Transmission can be restored by breaking the translational symmetry of the molecule,³⁰³ and as a test-bed acyclic cross-conjugated molecules and linearly conjugated counterparts have been suggested.¹⁹⁹ Beyond modifications of the transmission spectrum, quantum interference has been found to affect intra-molecular electron transfer paths, and in some instances current can flow mainly through-space rather than through molecular bonds.³⁰⁴ These findings can have very important practical implications in the design of molecules suitable for single-electron devices, since they allow predicting if substituents will disrupt intramolecular current flows and overall transmission through the molecule.

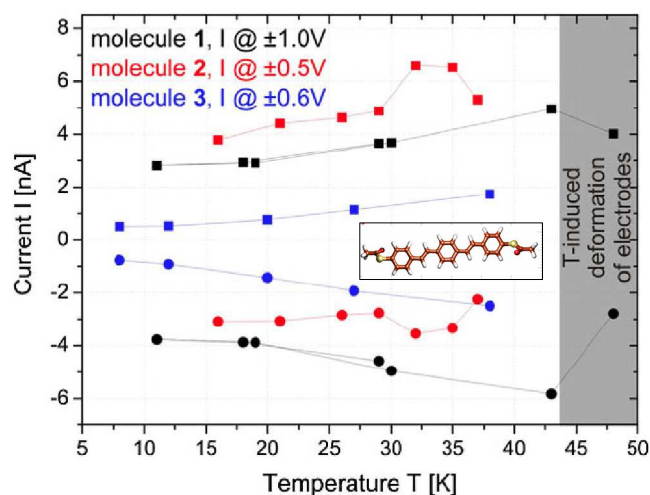


Fig. 29 A signature of decoherence due to molecular vibrations is signalled by the increase in molecular conductance as temperature is increased, in MCBJ experiments with cross conjugated molecular wires.³⁰⁵ Reprinted by permission from Phys. Rev. Lett. Copyright (2012) by the American Physical Society.

In analogy with mesoscopic experiments, where phase-breaking inelastic scattering leads to suppression of quantum interference, it was suggested that electron phonon coupling in molecules (vibrational effects) can quench quantum interference effects.³⁰⁶ For molecules where QI create antiresonances in the transmission spectrum, it was predicted that molecular vibrations (inelastic scattering) should destroy QI effects and thus cause an increase in molecular conductance. Stimulated by this theoretical prediction, Ballman *et al.* presented a study of interference effects in linear and cross conjugated molecules,³⁰⁵ and it was indeed demonstrated an enhancement of molecular conductance with increasing temperature (Fig. 29). The authors discussed that if current in the molecules is carried by energetically quasi-degenerate electronic states, then the current plateaus observed in the IV characteristics due to resonant tunnelling are sensitive only to vibrational excitation and no other effects, such as thermal broadening of electronic levels. Experimentally, it is complicated to perform temperature dependence measurements on nanogaps, because the small dimensions lead to thermal structural instabilities in the molecular junction. To rule out these effects, the authors presented an experiment using a pair of gold electrodes without molecules. The temperature range of measurements of the bare nanogap conductance was limited by instabilities at $T>22$ K, and it could be only monitored at low bias (0.2 V). In the presence of molecule, the junction becomes more stable, and the range of temperatures can be extended up to 40 K and 1.0 V.

Experiments to confirm the theoretical predictions that interference effects modify the transmission spectra (conductance) through single molecules have recently been performed.^{197, 307-310} These experiments involve conductance measurements on molecules that have been designed and synthesized with or without substituents to enable or avoid QI effects. In a room temperature AFM experiment,³⁰⁷ Aradhyia *et al.* showed that thiol end-capped para-stilbene and its meta- (symmetry-broken) counterpart display indeed significantly different conductance.³⁰⁷ Only para-stilbene showed a measurable current while the meta-stilbene, expected to display low transmission due to interference effects, showed a conductance two orders of magnitude smaller. Another

1 conducting AFM experiment by Guédon *et al.* showed evidence
2 for transmission anti-resonance in a multi-molecular junction
3 linear and cross conjugated molecules, in which a conductance
4 two orders of magnitude lower compared to that of the linear
5 conjugated molecule was measured.¹⁹⁷ As expected, the cross
6 conjugated molecule showed a dip in the differential
7 conductance close to zero-bias (anti-resonance). Quantum
8 interference effects were also suggested as the cause for
9 suppressed conductance in a single meta-coupled benzene ring
10 compared to para-coupled benzene.³⁰⁸ Similarly, low-bias
11 conductance through a single meta-OPV3 molecule is one order
12 of magnitude smaller than through a para-OPV3.³⁰⁹
13 In summary, the vision of demonstrating a high performance
14 quantum interference (QI) molecular switch is still to be materialized. Nonetheless,
15 studies of QI effects in molecules have contributed to our
16 understanding of electronic transmission through single
17 molecule devices. This knowledge can be eventually used to
18 assist the design and synthesis of molecules where substituents
19 added to the molecular structure enhance the operation of
20 single-molecule devices based on physical phenomena other than
21 QI.

23 5. Molecular Switches

24 In view of future applications, one of the most promising
25 functionalities of a single-molecule device is that of a bi- or
26 multi-stable element (i.e. switch). After all, the core of digital
27 electronics, the silicon-based transistor, is a switch in which its
28 electrical conductance can be turned on and off (with very high
29 ON/OFF ratio) by an additional electrode (i.e. gate). Molecular
30 switches might find application in ultra-low power, high-
31 density molecular memories and multi-valued logic processors.
32 Molecular switches have been widely studied in solution, but
33 the study of single molecules at surface increases the
34 complexity of the systems and the associated experimental
35 challenges, considering that the local environment of the
36 molecule at the surface is drastically different in bulk solution.

37 In the following section we review some of the molecular
38 switches that have been employed in molecular electronic
39 devices, including photochromic and electrochemical switches.

40 **5.1. Photochromic molecular switches: using light to trigger
41 electronic properties of molecules.** Molecular photoswitches are
42 molecular systems in which the excited state can undergo
43 reversible photoisomerization, leading to a new high-energy
44 isomer state that cannot decay spontaneously through electronic
45 transitions to the ground state.³¹¹⁻³¹⁴ For the high-energy
46 isomer, several characteristics, such as absorption
47 fluorescence properties, refractive index, crystal structure,
48 hydrophobicity, magnetic properties, and electric conductivity
49 may differ from that of the precursor in the ground state.³¹⁵⁻³⁴²

50 The increased interest in molecular photo-switches rises from
51 the complementary field of organic electronics. The impressive
52 improvement of electron mobility in organic conducting
53 materials has suggested the possibility to use photo-switches to
54 build single-molecule electronic transistors, able to perform
55 logical operations and data storage in very small volumes.³⁴³⁻³⁴⁶

56 During recent years, several examples of photochromic
57 molecular electronic switches have been demonstrated on the
58 single-molecule level.³⁴⁵⁻³⁵² Sensitive experimental techniques,
59 such as fluorescence spectroscopy and SERS, can provide
60 information on photochromic transitions at the single-molecule
61 level, and the potential of single-molecule electronic switches
62 in applications such as ultra-high density optical memory units
63 have been demonstrated.^{317, 353, 354} Also, photo-switching of

64 electrical transport properties based on photochromic
65 transitions has been proposed as a fundamental concept for
66 future design of molecular electronic circuits,³⁵⁵ organic light-
67 emitting devices,^{356, 357} and molecular machines.^{313, 358-360}

The first observation of this phenomenon can be attributed to
68 Yokoyama and Homma, who demonstrated switching of the
69 electrical current in solid film devices by photoisomerization of
70 diarylethene derivatives.³⁶¹ This pioneering work, originally
71 based on micrometer length scale measurements of multiple
72 molecules, established the basis for the subsequent
73 development of single-molecule photo-switches based on
74 photochromic transitions. Specifically for this molecular
75 system, since the ionization potentials of the two states of
76 diarylethene are similar, the difference in electrical conductivity
77 between different isomers can be attributed to the change in
78 mobility of charge carriers across the molecule.³⁶² He *et al.*
79 studied the electronic changes caused by light-induced
80 isomerization of a photochromic molecule between an open
81 state (that absorbs in the UV to become closed) and a closed
82 state (that absorbs in the visible to become open).³⁶³

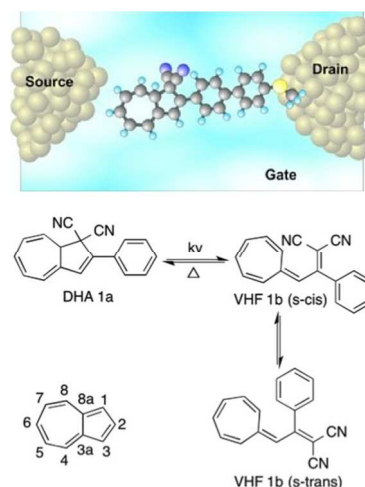


Fig. 30 Dihydroazulene (DHA 1a)/vinylheptafulvene (VHF 1b) photo-
/thermoswitch. A schematic representation of the sample geometry of a
molecule anchored to one electrode in a silver nanogap. Reprinted by
permission from John Wiley and Sons, copyright (2012).²⁴²

The switching of diarylethene conductivity upon photo-
isomerization has also been probed at the single-molecule
level.³⁶⁴ The change in conductivity between the two photo-
isomers is dependent on the molecular structure, and can reach
more than two orders of magnitude. In the case of diarylethene
molecules, the huge difference can be attributed to the
considerable change in molecular geometry between the two
isomers. This change is accompanied by the rearrangement of
covalent bonds. The reproducibility in the switching molecules,
promoting or disrupting the conjugation of π -electrons across
the molecule, bridging the probing electrodes. Exploiting these
particular properties, the electric conductivity of different
photo-isomers of single diarylethene molecules has been
studied, and experimental results were comparable to
theoretical calculations.^{363, 365-370} In these experiments, when
the high-energy isomer is deactivated by irradiation with a
specific wavelength, the molecules lose their π -conjugation and
become isolators (OFF state). In the OFF state, the resistance is
three orders of magnitude higher, and therefore the photo-
isomerization of the molecule induces a jump in resistance that
can be directly attributed to the change in the conformation of
the switching molecule. Following this concept, the current

switching in different diarylethene molecules has been demonstrated to be reversible.³⁶⁵ Recently, single-molecule switches, based on the photo-isomerization of dihydroazulene (DHA) to vinylheptafulvene (VHF), have been developed (Fig. 30).^{241, 242} The reproducibility and robustness of this molecule in single molecule transport measurements has been demonstrated by more than 20 "ON-OFF" cycles. By analysing the experimental conductance data, the authors of this report concluded that electric transport through both DHA (high resistivity) and VHF (low resistivity) isomers occurs sequentially.

In addition to the experimental study of molecular switches, theoretical simulations are very useful for the interpretation and design of single-molecule electronic switches. The electrical transport properties across diarylperfluorocyclopentene nanowire have been theoretically investigated using density functional theory and Green's function method.^{367, 369}

The affinity of thiol-groups for noble metal surfaces has been exploited to build photo-switchable devices incorporating metal nanoparticles.³⁷¹ The conductance of the two photo-isomers of diarylethene bridging Au nanoparticle networks has been studied using sulfur-based anchoring groups. The diarylethene derivatives hold thiophenol units at each end, allowing the interaction with the surface of metal nanoparticles.³⁷¹ These thiophenol moieties act as the junction, creating a conducting pathway between two metal electrodes, and hence allowing the charge carriers transport between two electrodes connected to a macroscopic power source. By measuring the conductance with alternate UV and visible light irradiation, the photoisomerization process can be triggered and the conductivity altered by a factor of 5.³⁷¹ The integration of the device with electrodes was facilitated by the use of metal nanoparticles as the probing units. A similar approach has been used to investigate the transport properties in two-dimensional lattices of gold nanoparticles connected with dithiol-diarylethene molecules.³⁷² The gold nanoparticles were self-assembled hexagonally ordered monolayers, and considering geometrical constraints, each interparticle junction could only hold a single or at most a few molecular bridges. This device showed reversible photo-induced switching of the transport properties that was reproducible up to eight ON/OFF cycles.

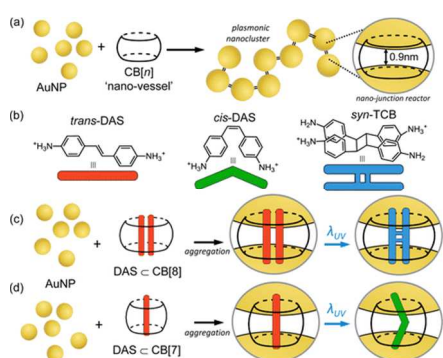


Fig. 31 (a) AuNPs ($d = 60$ nm) self-assemble into dendritic nanoclusters with fixed 0.9 nm interparticle separations by the action of the rigid sub-nm CB[n] linker. (b) Following UV irradiation in solution, trans-DAS predominantly undergoes photoisomerization into cis-DAS with photodimerization a minor pathway of which syn-TCB is a particular product. (c) When complexed within CB[8], the photoreaction of DAS is templated to yield almost exclusively syn-TCB, which can be measured *in situ* within the interparticle junction of the plasmonic cluster. (d) The complexation of a single DAS within narrower CB[7] results in a templated photoisomerization reaction to cis-DAS. Reprinted with permission from R. W. Taylor, R. J.

Coulston, F. Biedermann, S. Mahajan, J. J. Baumberg and O. A. Scherman, *Nano Lett.*, 2013, **13**, 5985-5990. Copyright 2013 American Chemical Society.³⁷³

Other types of self-assembly strategies to combine the components of single-molecule electronic devices have also been explored. Hydrophobic complexes of conjugated molecules with cyclodextrins have been used to assemble water-soluble molecular wires, able to build single-molecule junctions between metal nanoparticles.³⁷⁴ Scherman *et al.* have proposed an approach that combines supramolecular chemistry with nanoparticle self-assembly to develop a photoinduced molecular switch.³⁷³ The selective photoisomerism or photodimerization of diaminostilbene molecules can be monitored *in situ* within gold nanoparticle gaps, confined by a cucurbit[n]uril molecular cavity, and the size of this cavity can be tuned by choosing appropriate molecules (Fig. 31). This conceptual framework might be extended to several molecular systems and applications, and constitute a considerable advancement in the field, since it might be a way to control the local environment of the single molecules and thereby improve reproducibility in the performance of devices. Another interesting example of single-molecule electroluminescence measurements has been reported by Mayor *et al.*, using carbon nanotube tips bridged by a rod-like molecule.³⁷⁵

5.2. Electrochemically driven molecular switches.

Electrochemical switching is another way to modify single-molecule systems.³⁷⁶⁻³⁷⁹ The integration of organic molecules containing redox centres into complex assemblies remains challenging,^{380, 381} but the functional behaviour of these systems^{208, 382} and the ability to display resonant electron tunneling that can be reversibly controlled by the redox state of the molecule,^{383, 384} offers exciting opportunities. The principle behind this kind of devices is based on the change in transport properties of different oxidation states of conjugated molecules.³⁸⁰ When aromaticity is compromised by the incorporation or release of an electron during a redox process, the electric conductivity of the molecules changes considerably, allowing the control of the tunnelling current through the electrochemical potentials. Furthermore, some molecular systems are able to display more than one oxidation state that can be selectively reached by tuning the environmental conditions of the device. Electrochemical control of single-molecule electronic devices has been developed in the solid state *via* so-called three-terminal devices. In the liquid state, it is also possible to control the electrochemical environment, by using source and drain electrodes immersed into the solution and connected to a bipotentiostat.^{173, 385-388} The ability to combine electrochemistry with scanning tunnelling spectroscopy (STS) allows the investigation of electron transport through individual molecules.

Cryogenic STM has been used to control the formation of covalent bonds between conductive molecules and metal surfaces.³⁸⁹ The switching between the bonded and the nonbonded state has been associated with different electric charges, and it is accompanied by a considerable change in the tunnelling current, allowing the use of these kinds of devices as molecular switches. Tao *et al.* recently reported electrochemical gating of single anthraquinone-based switches bridging two Au electrodes by using the STM break-junction technique.³⁹⁰

M. Venturi studied a photoinduced memory effect in a redox controllable bistable mechanical molecular switch in the form of a bistable [2]rotaxane.³⁹¹ The [2]rotaxane-based device can be operated as a bistable memory element under kinetic control

(Fig. 32). The data can be written on the rotaxane by oxidation stimulus, and locked by UV light irradiation. After the writing process, the oxidized species can be reduced back to the original form without losing the written data for remarkably long time, compared to most thermodynamically controlled molecular switches. The data remains stored for hours at room temperature until the thermally activated opening of the azobenzene gate occurs spontaneously. Light irradiation not only locks the data previously recorded by oxidation, but also protects the nonoxidized rotaxanes from accidental writing. These characteristics confirm that these kinds of molecular switches could find technological applications in the future. However, in order to compete with established data storage devices, longer lifetime of the written information should be achieved.^{391,392}

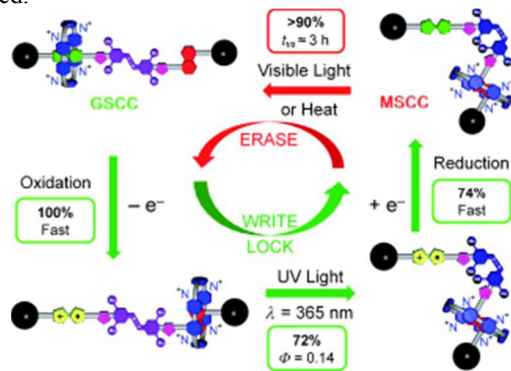


Fig. 32 Chemically and photochemically triggered memory switching cycle of the [2]rotaxane 14^+ . The lifetime of the MSCC can be controlled by isomerization of the TMeAB unit from its trans to cis configuration. Reprinted by permission from John Wiley and Sons copyright (2012).³⁹¹

Rigaut *et al.* have developed molecular transport junctions that are orthogonally modulated by optical and electrochemical stimuli.³⁹³ The molecules are placed on chemically fabricated nanogaps and display a reversible switching behaviour. These systems are able to perform basic logic operations associated with a modification of the transport properties across the electrodes. The electrochemically induced reciprocal transformations of DNA molecules adsorbed onto gold electrodes in the presence of Pb^{2+} have been used to develop molecular logic gates.³⁹⁴ This work opens new perspectives for the design of electrochemical logic devices that might be integrated into microprocessors or electronic chips.

Single molecule transport experiments have been combined with transient electrochemistry ensemble methods to investigate the correlation between molecular conductance and electron transfer rate-constants from coordinated metal centers to electrodes.³⁹⁵ This kind of multi-technique approach revealed that the evaluation of electronic coupling could lead different results, depending on the experimental set up used. Therefore, the understanding of intrinsic properties at the single molecule level requires the combination of complementary experimental and theoretical approaches. Non-conjugated redox-active molecules have been also used as switches for molecular-junction conductance experiments. Liao *et al.* have inserted dithiolated tetrathiafulvalene derivatives (TTFdT) in two-dimensional nanoparticle arrays, building interlinked networks of molecular junctions.³⁹⁶ Upon oxidation of the TTFdT unit the conductance of the networks increased by one order of magnitude. The system was proven to be redox-reversible, demonstrating switching of the transport properties across the linker molecules. This specific example was based on ensemble measurement, but one can foresee the use of this kind of redox switches in single molecule

experiments. Other redox active switching units, such as pyrrolo-tetrathiafulvalene, viologen, and anthraquinone have been successfully used to switch the transport properties across non-conjugated single-molecule junctions.^{379,388} In some of the examples described above, the electrochemical switching of the single-molecule junctions is achieved by STM break-junction methods, demonstrating the versatility of this technique.^{379,388,395}

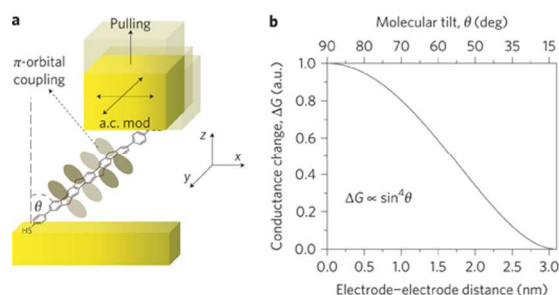
5.3. Nanomechanical molecular switches. Mechanical forces can be also used to control the conductance switching of single-molecule junctions. The possibility to build artificial single-molecule mechanical devices has been theoretically explored.³⁹⁷ However, the implementation of these systems in lab conditions still faces several challenges, which could be a major research interest in the coming years. One of the first experimental examples of a single-molecule mechanical device was introduced in 2002 by Gaub *et al.*³⁶⁰ They investigated polymeric azobenzenes, which have two photo-isomers, *cis* and *trans*, with bond angles changing by 120 degrees upon isomerization. This system was able to optically lengthen and contract across the polymer backbone against an external force applied with an AFM tip, delivering measurable mechanical work.

The integration of single-molecule pulling techniques with molecular electronics has contributed to develop applications for mechanically controlled electronic devices and to improve the set of tools for studying the states of single molecules, highlighting the relevance between conformation and properties of molecules.³⁹⁸⁻⁴⁰⁵ Tao *et al.* recently found that the conductance of individual 1,4'-benzenedithiol molecules bridging two gold electrodes could be increased by more than one order of magnitude when the molecules are stretched.²²¹ Intramolecular reversible translocations have also been used as a proof of principle for the cyclic action of molecular machines.⁴⁰⁶ Hihath *et al.* reported mechanically controlled molecular orbital alignment in single-molecule junctions.²²¹ The electromechanical properties of a 1,4'-benzenedithiol molecular junction change as the junction is stretched and compressed. It was also found that the conductance increases by more than one order of magnitude during stretching, decreasing again as the junction is compressed.

Martin *et al.* developed a gate based on tunable single-atom switches.⁴⁰⁷ The electrostatic attraction of the source-drain electrodes leads to a deflection and rotation of the electrode tips and a change in electrode separation, which results in the reversible break and formation of a single-atom contact. Their work indicated that the details of switching depend sensitively on the nanoscale morphology and geometry of the electrode tips. The work of Kawai *et al.* further demonstrated the geometrical dependence of mechanically controlled single-molecule switches.⁴⁰⁸

Additionally, theoretical studies suggested a novel type of electronic switching effect, driven by the geometrical reconstruction of nanoscale graphene-based junctions.⁴⁰⁹ The results suggested that it is possible to design modern logical switching devices or mechanophore sensors, monitored by mechanical strain and structural rearrangements. Bokes *et al.* investigated the conductance of dithioazobenzene-based optomechanical switches theoretically.⁴¹⁰ They demonstrated that the transport properties of different conformers were broadly similar. Venkataraman *et al.* also reported the reversible binary switching in a single-molecule contact geometry.¹⁶² The single-molecule junction 4, 4'-bipyridine-gold can be controllably switched between two conductance states by mechanical manipulation of the electrode separation. Ralph

1 *et al.* reported a single-molecule switch with pyridine-
 2 terminated dithiethylene with conducting closed
 3 configuration and nonconducting open configuration.⁴¹¹ The
 4 pyridine groups were used to link the molecules to gold
 5 electrodes to achieve relatively well-defined molecular contacts
 6 and stable conductance.
 7 Ratner *et al.* analysed the relationship between force-extension
 8 and molecular switch behaviour, by pulling the molecules with
 9 an AFM tip.⁴¹² Using molecular dynamics to simulate
 10 conducting AFM tip manipulating a molecule bound to
 11 surface, they were able to illustrate some of the fundamental
 12 structure-function relationships in this molecular switch
 13 mapping the dominant interactions in the molecule, mediating
 14 charge transport throughout the pulling simulation. Using a
 15 similar technique, Chi *et al.* directly measured the coordinative
 16 bonding strength of single molecules.³⁰
 17 The geometry of electrode-molecule bonds can influence
 18 transport properties at the single-molecule level, especially
 19 conjugated systems with lateral coupling of π orbitals (Fig.
 20 33).⁴¹³



22
 23 **Fig. 33** (a) Schematic of lateral coupling experiment. As the two
 24 electrodes are separated or modulated within the horizontal plane, the
 25 angle θ decreases and the conductance G falls; (b) Change in
 26 conductance, ΔG , versus electrode-electrode distance (bottom x-axis)
 27 and θ (top x-axis). Reprinted by permission from Nature
 28 Nanotechnology (I. Diez-Perez, J. Hihath, T. Hines, Z.-S. Wang, X.
 29 Zhou, K. Mullen and N. Tao, *Nat. Nanotechnol.*, 2011, **6**, 226-233).
 30 Copyright (2011).⁴¹³

32 6. Conclusions and outlook

33
 34 Single-molecule electronics seeks to incorporate single
 35 molecule components as functional elements in electronic
 36 devices. In recent years, we have seen an improved
 37 understanding in many aspects of single molecule electronics,
 38 including molecular design, molecule/contact interface
 39 engineering and the integration of this knowledge into more
 40 reproducible measurements. In combination with the evolution
 41 of experimental techniques to address single molecules,
 42 techniques for data collection and analysis have enabled
 43 study and further understanding of electron transport through
 44 single molecules across different experimental realizations.
 45 As a result, discrepancies among several single-molecule
 46 experiments have been clarified and fundamentally new
 47 molecular devices with not-foreseen functionality have
 48 emerged.⁴¹³
 49 In particular for the molecule/electrode interface, one of the
 50 long-standing challenges in single-molecule electronics is
 51 controlling the precise geometry at the molecule/metal contact
 52 which can dominate the performance of single-molecule
 53 devices. In this direction, a variety of systematic studies, with
 54 variations in both electrode materials and in functional groups
 55 in the molecular system, have been reported. These studies
 56 have lead to a more detailed understanding of a number of

anchoring systems, among others: sulfur-gold bond, amine- and
 phosphine-based anchors, as well as the development of new
 systems with multiple surface attachment sites, such as C_{60} , that
 are expected to be less prone to small variations in local
 microstructure at the interface and therefore should lead to
 more robust and reproducible systems.^{51, 170, 171} Another
 direction is the use of 2D materials as the electrode material for
 contacting single molecules. The impressive evolution of 2D
 materials, and the recent demonstration that it is possible to
 contact these electrodes with molecules,^{96, 138} is an area of
 research where we foresee new breakthroughs to occur.

While the experimental methods and setups developed to
 probe single molecule conductivity have improved during
 recent years, especially in terms of faster throughput, as well as
 the introduction of more complex devices (*e.g.* gateable break
 junctions^{41, 252}), experimental techniques to fabricate identical
 single-molecule devices in a reproducible way are still sought.
 Furthermore, a remaining challenge is to develop ways to
 fabricate multiple single molecule devices in a parallel way.
 One way to achieve this could be by improved resolution and
 smaller feature sizes offered by today's state of the art
 nanofabrication techniques.^{414, 415} Another approach might be to
 bridge the length scale between the single molecules and the
 nanofabricated systems by the use of combinations of advanced
 self-assembly techniques with nanofabricated templates.⁷ The
 versatility offered by the extensive repertoire of chemical
 synthesis might be the key to materializing large-scale single-
 molecule electronics.

In view of applications, our view is that two-terminal devices
 such as wires, rectifiers and multivalued logic single-molecule
 devices can be expected to emerge as the most feasible route
 towards molecular devices. In comparison, three-terminal
 molecular devices offer a complete experimental platform to
 perform studies of electronics at the single molecular level that
 could pave the road for improved understanding and increased
 complexity in future single-molecule devices. With the
 combined ingenuity and creativity possessed by researchers in
 this field worldwide, we are at this stage optimistic towards the
 future development of single molecule electronics from the
 research laboratory to real applications.

Acknowledgements

We would like to acknowledge S. Kubatkin, A. Roffey, J. Eklöf and M.B. Ergette for careful reading of this manuscript.

Financial support from the Knut and Alice Wallenberg Foundation, Chalmers Area of Advance in Materials Science and in Nanoscience and Nanotechnology, Wallenberg foundation, as well as the ERC Starting grant project SIMONE (Grant Agreement N° 337221) is acknowledged.

Notes and References

^a Department of Chemical and Biological Engineering, Chalmers University of Technology. E-mail: kasper.moth-poulsen@chalmers.se

^b Department of Micro and Nanotechnology, MC2, Chalmers University of Technology.

1. M. Ratner, *Nat. Nanotechnol.*, 2013, **8**, 378-381.
2. A. Aviram and M. A. Ratner, *Chem. Phys. Lett.*, 1974, **29**, 277-283.
3. L. A. Bumm, J. J. Arnold, M. T. Cygan, T. D. Dunbar, T. P. Burgin, L. Jones, D. L. Allara, J. M. Tour and P. S. Weiss, *Science*, 1996, **271**, 1705-1707.
4. H. Song, M. A. Reed and T. Lee, *Adv. Mater. (Weinheim, Ger.)*, 2011, **23**, 1583-1608.

- 1 5. R. L. McCreery and A. J. Bergren, *Adv. Mater. (Weinheim, Ger.)*, 2009, **21**, 4303-4322. **73**
 2 21, 4303-4322. **74**
 3 6. T. Li, W. Hu and D. Zhu, *Adv. Mater.*, 2010, **22**, 286-300. **75**
 4 7. T. A. Gschneidner, Y. A. Diaz Fernandez and K. Moth-Poulsen, *Mater. Chem. C*, 2013, **1**, 7127-7133. **76**
 5 Mater. Chem. C, 2013, **1**, 7127-7133. **77**
 6 8. D. Xiang, H. Jeong, T. Lee and D. Mayer, *Adv. Mater.*, 2013, **25**, 4847-4867. **78**
 7 4867. **79**
 8 9. N. Darwish, M. N. Paddon-Row and J. J. Gooding, *Acc. Chem. Res.*, 2014, **47**, 385-395. **80**
 9 2014, **47**, 385-395. **81**
 10 10. S. Guo, J. M. Artes and I. Diez-Perez, *Electrochim. Acta*, 2013, **111**, 741-753. **82**
 11 741-753. **83**
 12 11. M. Kiguchi and S. Kaneko, *Phys. Chem. Chem. Phys.*, 2013, **15**, 2267-2267. **84**
 13 2267. **85**
 14 12. M. Tsutsui and M. Taniguchi, *Sensors*, 2012, **12**, 7259-7298. **86**
 15 13. X. Guo and C. Nuckolls, *J. Mater. Chem.*, 2009, **19**, 5470-5473. **87**
 16 14. H. B. Akkerman and B. de Boer, *J. Phys.: Condens. Matter*, 2008, **20**, 013001. **88**
 17 013001. **89**
 18 15. M. A. Reed, C. Zhou, C. J. Muller, T. P. Burgin and J. M. Tour, *Science*, 1997, **278**, 252-254. **90**
 19 1997, **278**, 252-254. **91**
 20 16. A. F. Morpurgo, C. M. Marcus and D. B. Robinson, *Appl. Phys. Lett.*, 1999, **74**, 2084-2086. **92**
 21 1999, **74**, 2084-2086. **93**
 22 17. H. Park, A. K. L. Lim, A. P. Alivisatos, J. Park and P. L. McEuen, *Appl. Phys. Lett.*, 1999, **75**, 301-303. **94**
 23 1999, **75**, 301-303. **95**
 24 18. A. Bezryadin, C. Dekker and G. Schmid, *Appl. Phys. Lett.*, 1997, **71**, 1273-1275. **96**
 25 1273-1275. **97**
 26 19. S. Kubatkin, A. Danilov, M. Hjort, J. Cornil, J.-L. Bredas, N. Stubbgen, P. Hansen, P. Hedegard and T. Bjornholm, *Nature*, 2003, **425**, 698-701. **98**
 27 2003, **425**, 698-701. **99**
 28 20. X. D. Cui, A. Primak, X. Zaraté, J. Tomfohr, O. F. Sankey, A. L. Moore, T. A. Moore, D. Gust, G. Harris and S. M. Lindsay, *Science*, 2001, **291**, 571-574. **100**
 29 2001, **291**, 571-574. **101**
 30 21. S. R. Nicewarner-Peña, R. G. Freeman, B. D. Reiss, L. He, D. J. Peña, D. Walton, R. Cromer, C. D. Keating and M. J. Natan, *Science*, 2004, **294**, 137-141. **102**
 31 2004, **294**, 137-141. **103**
 32 22. L. Qin, S. Park, L. Huang and C. A. Mirkin, *Science*, 2005, **309**, 115. **104**
 33 2005, **309**, 115. **105**
 34 23. A. Hatzor and P. S. Weiss, *Science*, 2001, **291**, 1019-1020. **106**
 35 2001, **291**, 1019-1020. **107**
 36 24. T. Dadosh, Y. Gordin, R. Krahné, I. Khivrich, D. Mahalu, V. Frydman, J. Sperling, A. Yacoby and I. Bar-Joseph, *Nature*, 2005, **436**, 677-680. **108**
 37 2005, **436**, 677-680. **109**
 38 25. C. Joachim, J. K. Gimzewski, R. R. Schlittler and C. Chavy, *Phys. Rev. Lett.*, 1995, **74**, 2102-2105. **110**
 39 1995, **74**, 2102-2105. **111**
 40 26. J. K. Gimzewski and C. Joachim, *Science*, 1999, **283**, 1683-1688. **112**
 41 1999, **283**, 1683-1688. **113**
 42 27. L. E. Scullion, E. Leary, S. J. Higgins and R. J. Nichols, *J. Phys.: Condens. Matter*, 2012, **24**, 164211. **114**
 43 2012, **24**, 164211. **115**
 44 28. F.-R. F. Fan, J. Yang, L. Cai, D. W. Price, S. M. Dirk, D. V. Kosynkin, Y. Yao, A. M. Rawlett, J. M. Tour and A. J. Bard, *J. Am. Chem. Soc.*, 2002, **124**, 5550-5560. **116**
 45 2002, **124**, 5550-5560. **117**
 46 29. Z. J. Donhauser, B. A. Mantooth, K. F. Kelly, L. A. Bumm, J. Monnell, J. J. Stapleton, D. W. Price, A. M. Rawlett, D. L. Allara, J. Tour and P. S. Weiss, *Science*, 2001, **292**, 2303-2307. **118**
 47 2001, **292**, 2303-2307. **119**
 48 30. X. Hao, N. Zhu, T. Gschneidner, E. Ö. Jonsson, J. Zhang, K. Moth-Poulsen, H. Wang, K. S. Thygesen, K. W. Jacobsen, J. Ulstrup and J. Chi, *Nat. Commun.*, 2013, **4**, 2121. **120**
 49 2013, **4**, 2121. **121**
 50 31. E. Wierzbinski, X. Yin, K. Werling and D. H. Waldeck, *J. Phys. Chem. B*, 2012, **117**, 4431-4441. **122**
 51 2012, **117**, 4431-4441. **123**
 52 32. M. Frei, S. V. Aradhya, M. Koentopp, M. S. Hybertsen and Venkataraman, *Nano Lett.*, 2011, **11**, 1518-1523. **124**
 53 2011, **11**, 1518-1523. **125**
 54 33. J. Frommer, *Angew. Chem.*, 1992, **104**, 1325-1357. **126**
 55 1992, **104**, 1325-1357. **127**
 56 34. B. Xu and N. J. Tao, *Science*, 2003, **301**, 1221-1223. **128**
 57 2003, **301**, 1221-1223. **129**
 58 35. Xiao, Xu and N. J. Tao, *Nano Lett.*, 2004, **4**, 267-271. **130**
 59 2004, **4**, 267-271. **131**
 60 36. W. Haiss, H. van Zalinge, D. Bethell, J. Ulstrup, D. J. Schiffrin and R. J. Nichols, *Faraday Discuss.*, 2006, **131**, 253-264. **132**
 61 2006, **131**, 253-264. **133**
 62 37. T. Niu and A. Li, *J. Phys. Chem. Lett.*, 2013, **4**, 4095-4102. **134**
 63 2013, **4**, 4095-4102. **135**
 64 38. J. Moreland, J. W. Ekin, L. F. Goodrich, T. E. Capobianco, A. F. Chao, J. Kwo, M. Hong and S. H. Liou, *Phys. Rev. B: Condens. Matter*, 1986, **35**, 8856-8857. **136**
 65 1986, **35**, 8856-8857. **137**
 66 39. C. J. Muller, J. M. van Ruitenbeek and L. J. de Jongh, *Physical Superconductivity*, 1992, **191**, 485-504. **138**
 67 1992, **191**, 485-504. **139**
 68 40. C. J. Muller, B. J. Vleeming, M. A. Reed, J. J. S. Lamba, R. Hara, L. J. de Jongh and J. M. Tour, *Nanotechnology*, 1996, **7**, 409. **140**
 69 1996, **7**, 409. **141**
 70 41. M. L. Perrin, C. J. O. Verzijl, C. A. Martin, A. J. Shaikh, R. Elkema, J. van Esch, J. M. van Ruitenbeek, J. M. Thijssen, H. S. J. van der Zant and D. Dulic, *Nat. Nanotechnol.*, 2013, **8**, 282-287. **142**
 71 2013, **8**, 282-287. **143**
 72 42. C. Kergueris, J. P. Bourgoin, S. Palacin, D. Esteve, C. Urbina, M. Magoga and C. Joachim, *Phys. Rev. B*, 1999, **59**, 12505-12513. **144**
 43. R. H. M. Smit, Y. Noat, C. Untiedt, N. D. Lang, M. C. van Hemert and J. M. van Ruitenbeek, *Nature*, 2002, **419**, 906-909.
 44. J. Reichert, R. Ochs, D. Beckmann, H. B. Weber, M. Mayor and H. v. Löhneysen, *Phys. Rev. Lett.*, 2002, **88**, 176804.
 45. D. Djukic and J. M. van Ruitenbeek, *Nano Lett.*, 2006, **6**, 789-793.
 46. E. Lortscher, B. Gotsmann, Y. Lee, L. Yu, C. Rettner and H. Riel, *ACS Nano*, 2012, **6**, 4931-4939.
 47. M. Ruben, A. Landa, E. Loertscher, H. Riel, M. Mayor, H. Goerls, H. B. Weber, A. Arnold and F. Evers, *Small*, 2008, **4**, 2229-2235.
 48. W. Hong, H. Li, S.-X. Liu, Y. Fu, J. Li, V. Kaliginedi, S. Decurtins and T. Wandlowski, *J. Am. Chem. Soc.*, 2012, **134**, 19425-19431.
 49. J.-H. Tian, B. Liu, X. Li, Z.-L. Yang, B. Ren, S.-T. Wu, N. Tao and Z.-Q. Tian, *J. Am. Chem. Soc.*, 2006, **128**, 14748-14749.
 50. Y. Kim, H. Song, F. Strigl, H.-F. Pernau, T. Lee and E. Scheer, *Phys. Rev. Lett.*, 2011, **106**, 196804.
 51. J. Fock, J. K. Sorensen, E. Lortscher, T. Vosch, C. A. Martin, H. Riel, K. Kilsa, T. Bjornholm and H. van der Zant, *Phys. Chem. Chem. Phys.*, 2011, **13**, 14325-14332.
 52. M. Galperin, A. Nitzan and M. A. Ratner, *Phys. Rev. B*, 2006, **74**, 075326.
 53. J. Park, A. N. Pasupathy, J. I. Goldsmith, C. Chang, Y. Yaish, J. R. Petta, M. Rinkoski, J. P. Sethna, H. D. Abruna, P. L. McEuen and D. C. Ralph, *Nature*, 2002, **417**, 722-725.
 54. H. Park, J. Park, A. K. L. Lim, E. H. Anderson, A. P. Alivisatos and P. L. McEuen, *Nature*, 2000, **407**, 57-60.
 55. L. H. Yu and D. Natelson, *Nano Lett.*, 2003, **4**, 79-83.
 56. W. Liang, M. P. Shores, M. Bockrath, J. R. Long and H. Park, *Nature*, 2002, **417**, 725-729.
 57. H. Yu, Y. Luo, K. Beverly, J. F. Stoddart, H.-R. Tseng and J. R. Heath, *Angew. Chem. Int. Ed.*, 2003, **42**, 5706-5711.
 58. H. S. J. van der Zant, Y.-V. Kervennic, M. Poot, K. O'Neill, Z. de Groot, J. M. Thijssen, H. B. Heersche, N. Stuhr-Hansen, T. Bjornholm, D. Vanmaekelbergh, C. A. van Walree and L. W. Jenneskens, *Faraday Discuss.*, 2006, **131**, 347-356.
 59. D. E. Johnston, D. R. Strachan and A. T. C. Johnson, *Nano Lett.*, 2007, **7**, 2774-2777.
 60. C. Tao, W. G. Cullen and E. D. Williams, *Science*, 2010, **328**, 736-740.
 61. D. Stöffler, S. Fostner, P. Grütter and R. Hoffmann-Vogel, *Phys. Rev. B*, 2012, **85**, 033404.
 62. S. Girod, J.-L. Bubendorff, F. Montaigne, L. Simon, D. Lacour and M. Hehn, *Nanotechnology*, 2012, **23**, 365302.
 63. B. Gao, E. A. Osorio, K. B. Gaven and H. S. J. v. d. Zant, *Nanotechnology*, 2009, **20**, 415207.
 64. T. Kizuka, S. Kodama and T. Matsuda, *Nanotechnology*, 2010, **21**, 495706.
 65. D. R. Ward, N. K. Grady, C. S. Levin, N. J. Halas, Y. Wu, P. Nordlander and D. Natelson, *Nano Lett.*, 2007, **7**, 1396-1400.
 66. D. R. Ward, N. J. Halas, J. W. Ciszek, J. M. Tour, Y. Wu, P. Nordlander and D. Natelson, *Nano Lett.*, 2008, **8**, 919-924.
 67. D. R. Ward, F. Huser, F. Pauly, J. C. Cuevas and D. Natelson, *Nat. Nanotechnol.*, 2010, **5**, 732-736.
 68. H. Song, Y. Kim, J. Ku, Y. H. Jang, H. Jeong and T. Lee, *Appl. Phys. Lett.*, 2009, **94**, 103110.
 69. A. S. Zyazin, J. W. G. van den Berg, E. A. Osorio, H. S. J. van der Zant, N. P. Konstantinidis, M. Leijnse, M. R. Wegewijs, F. May, W. Hofstetter, C. Danieli and A. Cornia, *Nano Lett.*, 2010, **10**, 3307-3311.
 70. E. A. Osorio, K. O'Neill, N. Stuhr-Hansen, O. F. Nielsen, T. Bjornholm and H. S. J. van der Zant, *Adv. Mater.*, 2007, **19**, 281-285.
 71. Y. Naitoh, T. Ohata, R. Matsushita, E. Okawa, M. Horikawa, M. Oyama, M. Mukaida, D. F. Wang, M. Kiguchi, K. Tsukagoshi and T. Ishida, *ACS Appl. Mater. Interfaces*, 2013, **5**, 12869-12875.
 72. D. Natelson, Y. Li and J. B. Herzog, *Phys. Chem. Chem. Phys.*, 2013, **15**, 5262-5275.
 73. M. Rahimi and A. Troisi, *Phys. Rev. B*, 2009, **79**, 113413.
 74. H. Song, Y. Kim, H. Jeong, M. A. Reed and T. Lee, *J. Phys. Chem. C*, 2010, **114**, 20431-20435.
 75. F. Prins, A. J. Shaikh, J. H. van Esch, R. Elkema and H. S. J. van der Zant, *Phys. Chem. Chem. Phys.*, 2011, **13**, 14297-14301.
 76. T. Jain, Q. Tang, T. Bjornholm and K. Nørsgaard, *Acc. Chem. Res.*, 2013, **47**, 2-11.

- 1 77. Y. D. Fernandez, L. Sun, T. Gschneidtnr and K. Moth-Poulsen, *Adv. Mater.*, 2014, 2, 010702. 73
2 Mat., 2014, 2, 010702. 74
3 78. I. Amlani, A. M. Rawlett, L. A. Nagahara and R. K. Tsui, *Appl. Phys. Lett.*, 2002, 80, 2761-2763. 75
4 Lett., 2002, 80, 2761-2763. 76
5 79. J.-S. Na, J. Ayres, K. L. Chandra, C. Chu, C. B. Gorman and G. Parsons, *Nanotechnology*, 2007, 18, 035203. 77
6 Parsons, *Nanotechnology*, 2007, 18, 035203. 78
7 80. T. Jain, F. Westerlund, E. Johnson, K. Moth-Poulsen and T. Bjørnholm, *ACS Nano*, 2009, 3, 828-834. 79
8 ACS Nano, 2009, 3, 828-834. 80
9 81. J. P. Hermes, F. Sander, T. Peterle, C. Cioffi, P. Ringler, T. Pfohl and Mayor, *Small*, 2011, 7, 920-929. 81
10 Mayor, *Small*, 2011, 7, 920-929. 82
11 82. A. Guttman, D. Mahalu, J. Sperling, E. Cohen-Hoshen and I. B. Joseph, *Appl. Phys. Lett.*, 2011, 99, 063113. 83
12 Joseph, *Appl. Phys. Lett.*, 2011, 99, 063113. 84
13 83. S. Karmakar, S. Kumar, P. Marzo, E. Primiceri, R. Di Corato, R. Rinaldi, P. G. Cozzi, A. P. Bramanti and G. Maruccio, *Nanoscale*, 2012, 4, 232316. 85
14 P. G. Cozzi, A. P. Bramanti and G. Maruccio, *Nanoscale*, 2012, 4, 232316. 86
15 2316. 87
16 84. S. Kober, G. Gotesman and R. Naaman, *J. Phys. Chem. Lett.*, 2013, 2041-2045. 88
17 2041-2045. 89
18 85. K. Du, C. R. Knutson, E. Glogowski, K. D. McCarthy, R. Shenhar, M. Rotello, M. T. Tuominen, T. Emrick, T. P. Russell and A. Dinsmore, *Small*, 2009, 5, 1974-1977. 90
19 M. Rotello, M. T. Tuominen, T. Emrick, T. P. Russell and A. Dinsmore, *Small*, 2009, 5, 1974-1977. 91
20 Dinsmore, *Small*, 2009, 5, 1974-1977. 92
21 86. F. Yaghmaie, J. Fleck, A. Gusman and R. Prohaska, *Microelectron. Eng.*, 2010, 87, 2629-2632. 93
22 2010, 87, 2629-2632. 94
23 87. T. Jain, S. Lara-Avila, Y.-V. Kervennic, K. Moth-Poulsen, K. Nørgaard, S. Kubatkin and T. Bjørnholm, *ACS Nano*, 2012, 6, 3861-3867. 95
24 S. Kubatkin and T. Bjørnholm, *ACS Nano*, 2012, 6, 3861-3867. 96
25 88. Y. Cui, M. T. Björk, J. A. Liddle, C. Sönnichsen, B. Boussert and A. Alivisatos, *Nano Lett.*, 2004, 4, 1093-1098. 97
26 Alivisatos, *Nano Lett.*, 2004, 4, 1093-1098. 98
27 89. C. Kuemin, L. Nowack, L. Bozano, N. D. Spencer and H. Wolf, *Adv. Funct. Mater.*, 2012, 22, 702-708. 99
28 Funct. Mater., 2012, 22, 702-708. 100
29 90. A. Rey, G. Billardon, E. Lortscher, K. Moth-Poulsen, N. Stuhr-Hansen, H. Wolf, T. Bjørnholm, A. Stemmer and H. Riel, *Nanoscale*, 2011, 3, 8680-8688. 101
30 H. Wolf, T. Bjørnholm, A. Stemmer and H. Riel, *Nanoscale*, 2011, 3, 8680-8688. 102
31 8680-8688. 103
32 91. S. Gómez-Graña, F. Hubert, F. Testard, A. Guerrero-Martínez, I. García-L. M. Liz-Marzán and O. Spalla, *Langmuir*, 2011, 28, 1453-1459. 104
33 L. M. Liz-Marzán and O. Spalla, *Langmuir*, 2011, 28, 1453-1459. 105
34 92. X. Guo, J. P. Small, J. E. Klare, Y. Wang, M. S. Purewal, I. W. Tam, H. Hong, R. Caldwell, L. Huang, S. O'Brien, J. Yan, R. Breslow, J. Wind, J. Hone, P. Kim and C. Nuckolls, *Science*, 2006, 311, 356-359. 106
35 H. Hong, R. Caldwell, L. Huang, S. O'Brien, J. Yan, R. Breslow, J. Wind, J. Hone, P. Kim and C. Nuckolls, *Science*, 2006, 311, 356-359. 107
36 356-359. 108
37 93. J. Lefebvre, M. Radosavljević and A. T. Johnson, *Appl. Phys. Lett.*, 2000, 76, 3828-3830. 109
38 2000, 76, 3828-3830. 110
39 94. E. P. De Poortere, H. L. Stormer, L. M. Huang, S. J. Wind, S. O'Brien, M. Huang and J. Hone, *Appl. Phys. Lett.*, 2006, 88, 143124. 111
40 M. Huang and J. Hone, *Appl. Phys. Lett.*, 2006, 88, 143124. 112
41 95. D. Wei, Y. Liu, L. Cao, Y. Wang, H. Zhang and G. Yu, *Nano Lett.*, 2008, 8, 1625-1630. 113
42 2008, 8, 1625-1630. 114
43 96. F. Prins, A. Barreiro, J. W. Ruitenber, J. S. Seldenthuis, N. Aliaga-Alcalde, L. M. K. Vandersypen and H. S. J. van der Zant, *Nano Lett.*, 2011, 11, 4607-4611. 115
44 Alcalde, L. M. K. Vandersypen and H. S. J. van der Zant, *Nano Lett.*, 2011, 11, 4607-4611. 116
45 4607-4611. 117
46 97. Y. Cao, S. Dong, S. Liu, L. He, L. Gan, X. Yu, M. L. Steigerwald, W. Yu, Z. Liu and X. Guo, *Angew. Chem. Int. Ed.*, 2012, 51, 12228-12231. 118
47 W. Yu, Z. Liu and X. Guo, *Angew. Chem. Int. Ed.*, 2012, 51, 12228-12231. 119
48 98. L. Jiang, J. Gao, E. Wang, H. Li, Z. Wang, W. Hu and L. Jiang, *Adv. Mater.*, 2008, 20, 2735-2740. 120
49 Mater., 2008, 20, 2735-2740. 121
50 99. A. Ongaro, F. Griffin, L. Nagle, D. Iacopino, R. Eritja and F. Fitzmaurice, *Adv. Mater.*, 2004, 16, 1799-1803. 122
51 Fitzmaurice, *Adv. Mater.*, 2004, 16, 1799-1803. 123
52 100. C. R. Martin and L. A. Baker, *Science*, 2005, 309, 67-68. 124
53 101. S. Liu, J. B. H. Tok and Z. Bao, *Nano Lett.*, 2005, 5, 1071-1076. 125
54 102. X. Chen, S. Yeganeh, L. Qin, S. Li, C. Xue, A. B. Braunschweig, M. Schatz, M. A. Ratner and C. A. Mirkin, *Nano Lett.*, 2009, 9, 3974-3977. 126
55 Schatz, M. A. Ratner and C. A. Mirkin, *Nano Lett.*, 2009, 9, 3974-3977. 127
56 103. M. J. Banholzer, L. Qin, J. E. Millstone, K. D. Osberg and C. A. Mirkin, *Nat. Protocols*, 2009, 4, 838-848. 128
57 Nat. Protocols, 2009, 4, 838-848. 129
58 104. K. D. Osberg, A. L. Schmucker, A. J. Senesi and C. A. Mirkin, *Nano Lett.*, 2011, 11, 820-824. 130
59 Lett., 2011, 11, 820-824. 131
60 105. K. D. Osberg, M. Rycenga, N. Harris, A. L. Schmucker, M. R. Langford, G. C. Schatz and C. A. Mirkin, *Nano Lett.*, 2012, 12, 3828-3832. 132
61 G. C. Schatz and C. A. Mirkin, *Nano Lett.*, 2012, 12, 3828-3832. 133
62 106. C. A. Mirkin, R. L. Letsinger, R. C. Mucic and J. J. Storhoff, *Nano Lett.*, 1996, 382, 607-609. 134
63 1996, 382, 607-609. 135
64 107. J. Zheng, P. E. Constantinou, C. Micheel, A. P. Alivisatos, R. A. Kiehl and N. C. Seeman, *Nano Lett.*, 2006, 6, 1502-1504. 136
65 and N. C. Seeman, *Nano Lett.*, 2006, 6, 1502-1504. 137
66 108. J. J. Storhoff and C. A. Mirkin, *Chem. Rev.*, 1999, 99, 1849-1862. 138
67 109. E. Dujardin, L.-B. Hsin, C. R. C. Wang and S. Mann, *Chem. Commun.*, 2001, DOI: 10.1039/B102319P, 1264-1265. 139
68 2001, DOI: 10.1039/B102319P, 1264-1265. 140
69 110. S. Y. Park, A. K. R. Lytton-Jean, B. Lee, S. Weigand, G. C. Schatz and C. A. Mirkin, *Nature*, 2008, 451, 553-556. 141
70 C. A. Mirkin, *Nature*, 2008, 451, 553-556. 142
71 111. H. Yao, C. Yi, C.-H. Tzang, J. Zhu and M. Yang, *Nanotechnology*, 2007, 18, 015102. 143
72 18, 015102. 144
145
112. M. M. Maye, M. T. Kumara, D. Nykypanchuk, W. B. Sherman and O. Gang, *Nat. Nanotechnol.*, 2010, 5, 116-120.
113. M. P. Bussón, B. Rolly, B. Stout, N. Bonod, E. Larquet, A. Polman and S. Bidault, *Nano Lett.*, 2011, 11, 5060-5065.
114. G. P. Acuna, M. Bucher, I. H. Stein, C. Steinhauer, A. Kuzyk, P. Holzmeister, R. Schreiber, A. Moroz, F. D. Stefani, T. Liedl, F. C. Simmel and P. Tinnefeld, *ACS Nano*, 2012, 6, 3189-3195.
115. C. Chi, F. Vargas-Lara, A. V. Tkachenko, F. W. Starr and O. Gang, *ACS Nano*, 2012, 6, 6793-6802.
116. X. Lan, Z. Chen, B.-J. Liu, B. Ren, J. Henzie and Q. Wang, *Small*, 2013, 9, 2308-2315.
117. F. Vargas Lara and F. W. Starr, *Soft Matter*, 2011, 7, 2085-2093.
118. M.-P. Valignat, O. Theodoly, J. C. Crocker, W. B. Russel and P. M. Chaikin, *Proc. Natl. Acad. Sci. U. S. A.*, 2005, 102, 4225-4229.
119. L. Lermusiaux, A. Sereda, B. Portier, E. Larquet and S. Bidault, *ACS Nano*, 2012, 6, 10992-10998.
120. D.-K. Lim, K.-S. Jeon, J.-H. Hwang, H. Kim, S. Kwon, Y. D. Suh and J.-M. Nam, *Nat. Nanotechnol.*, 2011, 6, 452-460.
121. A. Y. Kasumov, M. Kociak, S. Guéron, B. Reulet, V. T. Volkov, D. V. Klinov and H. Bouchiat, *Science*, 2001, 291, 280-282.
122. D. Porath, A. Bezryadin, S. de Vries and C. Dekker, *Nature*, 2000, 403, 635-638.
123. X. Guo, A. A. Gorodetsky, J. Hone, J. K. Barton and C. Nuckolls, *Nat. Nanotechnol.*, 2008, 3, 163-167.
124. J. M. Krans, C. J. Muller, I. K. Yanson, T. C. M. Govaert, R. Hesper and J. M. van Ruitenbeek, *Phys. Rev. B: Condens. Matter*, 1993, 48, 14721-14724.
125. X. Li, J. He, J. Hihath, B. Xu, S. M. Lindsay and N. Tao, *J. Am. Chem. Soc.*, 2006, 128, 2135-2141.
126. Y. S. Park, A. C. Whalley, M. Kamenetska, M. L. Steigerwald, M. S. Hybertsen, C. Nuckolls and L. Venkataraman, *J. Am. Chem. Soc.*, 2007, 129, 15768-15769.
127. M. Kamenetska, M. Koentopp, A. C. Whalley, Y. S. Park, M. L. Steigerwald, C. Nuckolls, M. S. Hybertsen and L. Venkataraman, *Phys. Rev. Lett.*, 2009, 102, 126803.
128. C. R. Arroyo, E. Leary, A. Castellanos-Gomez, G. Rubio-Bollinger, M. T. Gonzalez and N. Agrait, *J. Am. Chem. Soc.*, 2011, 133, 14313-14319.
129. M. T. Gonzalez, A. Diaz, E. Leary, R. Garcia, M. A. Herranz, G. Rubio-Bollinger, N. Martin and N. Agrait, *J. Am. Chem. Soc.*, 2013, 135, 5420-5426.
130. H. Hakkinen, *Nat. Chem.*, 2012, 4, 443-455.
131. L. Venkataraman, J. E. Klare, I. W. Tam, C. Nuckolls, M. S. Hybertsen and M. L. Steigerwald, *Nano Lett.*, 2006, 6, 458-462.
132. M. S. Hybertsen, L. Venkataraman, J. E. Klare, A. C. Whalley, M. L. Steigerwald and C. Nuckolls, *J. Phys.: Condens. Matter*, 2008, 20, 374115.
133. A. Mishchenko, L. A. Zotti, D. Vonlanthen, M. Bürkle, F. Pauly, J. C. Cuevas, M. Mayor and T. Wandlowski, *J. Am. Chem. Soc.*, 2010, 133, 184-187.
134. L. A. Zotti, T. Kirchner, J.-C. Cuevas, F. Pauly, T. Huhn, E. Scheer and A. Erbe, *Small*, 2010, 6, 1529-1535.
135. F. Chen, X. Li, J. Hihath, Z. Huang and N. Tao, *J. Am. Chem. Soc.*, 2006, 128, 15874-15881.
136. C. Jia and X. Guo, *Chem. Soc. Rev.*, 2013, 42, 5642-5660.
137. A. Danilov, S. Kubatkin, S. Kafanov, P. Hedegard, N. Stuhr-Hansen, K. Moth-Poulsen and T. Bjørnholm, *Nano Lett.*, 2008, 8, 1-5.
138. Y. Cao, S. Dong, S. Liu, Z. Liu and X. Guo, *Angew. Chem. Int. Ed.*, 2013, 52, 3906-3910.
139. X.-Y. Zhou, Z.-L. Peng, Y.-Y. Sun, L.-N. Wang, Z.-J. Niu and X.-S. Zhou, *Nanotechnology*, 2013, 24, 465204.
140. M. Kamenetska, S. Y. Quek, A. C. Whalley, M. L. Steigerwald, H. J. Choi, S. G. Louie, C. Nuckolls, M. S. Hybertsen, J. B. Neaton and L. Venkataraman, *J. Am. Chem. Soc.*, 2010, 132, 6817-6821.
141. S. V. Aradhya and L. Venkataraman, *Nat. Nanotechnol.*, 2013, 8, 399-410.
142. L. Venkataraman, J. E. Klare, C. Nuckolls, M. S. Hybertsen and M. L. Steigerwald, *Nature*, 2006, 442, 904-907.
143. E. A. Osorio, K. Moth-Poulsen, H. S. J. van der Zant, J. Paaske, P. Hedegard, K. Flensberg, J. Bendix and T. Bjoernholm, *Nano Lett.*, 2010, 10, 105-110.
144. J. C. Love, L. A. Estroff, J. K. Kriebel, R. G. Nuzzo and G. M. Whitesides, *Chem. Rev.*, 2005, 105, 1103-1170.
145. A. Ulman, *Chem. Rev.*, 1996, 96, 1533-1554.

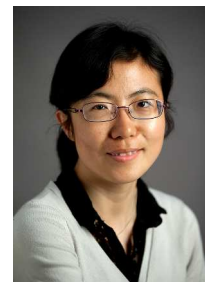
- 1 146.C. Li, I. Pobelov, T. Wandlowski, A. Bagrets, A. Arnold and F. Evers, *Am. Chem. Soc.*, 2007, 130, 318-326. 74
- 2 147.S. K. Yee, J. Sun, P. Darancet, T. D. Tilley, A. Majumdar, J. B. Neaton and R. A. Segalman, *ACS Nano*, 2011, 5, 9256-9263. 75
- 3 148.R. S. Klausen, J. R. Widawsky, T. A. Su, H. Li, Q. Chen, M. Steigerwald, L. Venkataraman and C. Nuckolls, *Chem. Sci.*, 2014, 5, 1561-1564. 76
- 4 149.S. Yasuda, S. Yoshida, J. Sasaki, Y. Okutsu, T. Nakamura, A. Taniguchi, O. Takeuchi and H. Shigekawa, *J. Am. Chem. Soc.*, 2006, 128, 7742-7747. 77
- 5 150.Kim, J. M. Beebe, Y. Jun, X. Y. Zhu and C. D. Frisbie, *J. Am. Chem. Soc.*, 2006, 128, 4970-4971. 78
- 6 151.B. Xu, X. Xiao and N. J. Tao, *J. Am. Chem. Soc.*, 2003, 125, 16165-16165. 79
- 7 152.C. A. Martin, D. Ding, J. K. Sørensen, T. Bjørnholm, J. M. Ruitenbeek and H. S. J. van der Zant, *J. Am. Chem. Soc.*, 2008, 130, 13198-13199. 80
- 8 153.E. Leary, M. T. González, C. van der Pol, M. R. Bryce, S. Filippone, G. Martín, G. Rubio-Bollinger and N. s. Agraft, *Nano Lett.*, 2011, 11, 2241-2241. 81
- 9 154.E. Lörtscher, V. Geskin, B. Gotsmann, J. Fock, J. K. Sørensen, Bjørnholm, J. Cornil, H. S. J. van der Zant and H. Riel, *Small*, 2013, 9, 332-332. 82
- 10 155.W. Chen, J. R. Widawsky, H. Vázquez, S. T. Schneebeli, M. Hybertsen, R. Breslow and L. Venkataraman, *J. Am. Chem. Soc.*, 2013, 135, 17160-17163. 83
- 11 156.W.-k. Paik, S. Han, W. Shin and Y. Kim, *Langmuir*, 2003, 19, 4216-4216. 84
- 12 157.E. Lörtscher, C. J. Cho, M. Mayor, M. Tschudy, C. Rettner and H. ChemPhysChem, 2011, 12, 1677-1682. 85
- 13 158.W. Hong, D. Z. Manrique, P. Moreno-García, M. Gulcur, Mishchenko, C. J. Lambert, M. R. Bryce and T. Wandlowski, *J. Chem. Soc.*, 2011, 134, 2292-2304. 86
- 14 159.J. Hihath and N. Tao, *Semiconductor Science and Technology*, 2014, 29, 054007. 87
- 15 160.F. Pauly, J. K. Viljas, J. C. Cuevas and G. Schön, *Phys. Rev. B*, 2009, 79, 155312. 88
- 16 161.D. R. Jones and A. Troisi, *J. Phys. Chem. C*, 2007, 111, 14567-14573. 89
- 17 162.S. Y. Quek, M. Kamenetska, M. L. Steigerwald, H. J. Choi, S. G. Louie, M. S. Hybertsen, J. B. Neaton and Venkataraman, *Nanotechnology*, 2009, 20, 230-234. 90
- 18 163.A. Bagrets, A. Arnold and F. Evers, *J. Am. Chem. Soc.*, 2008, 130, 9013-9018. 91
- 19 164.S. Guo, J. Hihath, I. Díez-Pérez and N. Tao, *J. Am. Chem. Soc.*, 2011, 133, 19189-19197. 92
- 20 165.P. Chinwangso, A. C. Jamison and T. R. Lee, *Acc. Chem. Res.*, 2011, 44, 511-519. 93
- 21 166.X. Chen, A. B. Braunschweig, M. J. Wiester, S. Yeganeh, M. A. Rabe and C. A. Mirkin, *Angew. Chem. Int. Ed.*, 2009, 48, 5178-5181. 94
- 22 167.J. P. Hermes, F. Sander, U. Fluch, T. Peterle, D. Thompson, R. Urbani, T. Pfohl and M. Mayor, *J. Am. Chem. Soc.*, 2012, 134, 14674-14677. 95
- 23 168.Z. L. Cheng, R. Skouta, H. Vazquez, J. R. Widawsky, S. Schneebeli, Chen, M. S. Hybertsen, R. Breslow and L. Venkataraman, *Nanotechnology*, 2011, 22, 353-357. 96
- 24 169.E. Lörtscher, *Nat. Nanotechnol.*, 2013, 8, 381-384. 97
- 25 170.C. Rogero, J. I. Pascual, J. Gómez-Herrero and A. M. Baró, *J. Chem. Phys.*, 2002, 116, 832-836. 98
- 26 171.E. Lörtscher, V. Geskin, B. Gotsmann, J. Fock, J. K. Sørensen, Bjørnholm, J. Cornil, H. S. J. van der Zant and H. Riel, *Small*, 2013, 9, 209-214. 99
- 27 172.T. Böhrer, A. Edtbauer and E. Scheer, *Phys. Rev. B*, 2007, 76, 12543-12543. 100
- 28 173.T. Hines, I. Díez-Pérez, H. Nakamura, T. Shimazaki, Y. Asai and Tao, *J. Am. Chem. Soc.*, 2013, 135, 3319-3322. 101
- 29 174.L. Luo, S. H. Choi and C. D. Frisbie, *Chem. Mater.*, 2011, 23, 631-637. 102
- 30 175.W. Hu, J. Jiang, H. Nakashima, Y. Luo, Y. Kashimura, K.-Q. Chen, Shuai, K. Furukawa, W. Lu, Y. Liu, D. Zhu and K. Torimitsu, *Phys. Rev. Lett.*, 2006, 96, 027801. 103
- 31 176.V. Kaliginedi, P. Moreno-García, H. Valkenier, W. Hong, V. M. García-Suárez, P. Buitter, J. L. H. Otten, J. C. Hummelen, C. J. Lambert and Wandlowski, *J. Am. Chem. Soc.*, 2012, 134, 5262-5275. 104
- 32 177.R. Huber, M. T. González, S. Wu, M. Langer, S. Grunder, V. Hornik, M. Mayor, M. R. Bryce, C. Wang, R. Jitchati, C. Schönenberger and Calame, *J. Am. Chem. Soc.*, 2007, 130, 1080-1084. 105
- 33 178.S. H. Choi, B. Kim and C. D. Frisbie, *Science*, 2008, 320, 1482-1486. 106
- 34 179.A. E. Nel, L. Madler, D. Velegol, T. Xia, E. M. V. Hoek, P. Somasundaran, F. Klaessig, V. Castranova and M. Thompson, *Nat. Mater.*, 2009, 8, 543-557. 107
- 35 180.S. H. Choi, C. Risko, M. C. R. Delgado, B. Kim, J.-L. Brédas and C. D. Frisbie, *J. Am. Chem. Soc.*, 2010, 132, 4358-4368. 108
- 36 181.L. Luo and C. D. Frisbie, *J. Am. Chem. Soc.*, 2010, 132, 8854-8855. 109
- 37 182.B. Q. Xu, X. L. Li, X. Y. Xiao, H. Sakaguchi and N. J. Tao, *Nano Lett.*, 2005, 5, 1491-1495. 110
- 38 183.P. Moreno-García, M. Gulcur, D. Z. Manrique, T. Pope, W. Hong, V. Kaliginedi, C. Huang, A. S. Batsanov, M. R. Bryce, C. Lambert and T. Wandlowski, *J. Am. Chem. Soc.*, 2013, 135, 12228-12240. 111
- 39 184.X. Zhao, C. Huang, M. Gulcur, A. S. Batsanov, M. Baghernejad, W. Hong, M. R. Bryce and T. Wandlowski, *Chem. Mater.*, 2013, 25, 4340-4347. 112
- 40 185.S.-Y. Jang, P. Reddy, A. Majumdar and R. A. Segalman, *Nano Lett.*, 2006, 6, 2362-2367. 113
- 41 186.Z. Li, I. Pobelov, B. Han, T. Wandlowski, A. Błaszczuk and M. Mayor, *Nanotechnology*, 2007, 18, 044018. 114
- 42 187.N. Tuccitto, V. Ferri, M. Cavazzini, S. Quici, G. Zhavnerko, A. Licciardello and M. A. Rampi, *Nat. Mater.*, 2009, 8, 41-46. 115
- 43 188.S. Rigaut, *Dalton Trans.*, 2013, 42, 15859-15863. 116
- 44 189.S. Ho Choi, B. Kim and C. D. Frisbie, *Science*, 2008, 320, 1482-1486. 117
- 45 190.H. Valkenier, C. M. Guedon, T. Markussen, K. S. Thygesen, S. J. van der Molen and J. C. Hummelen, *Phys. Chem. Chem. Phys.*, 2014, 16, 653-662. 118
- 46 191.Q. Lu, K. Liu, H. Zhang, Z. Du, X. Wang and F. Wang, *ACS Nano*, 2009, 3, 3861-3868. 119
- 47 192.L. Cui, B. Liu, D. Vonlanthen, M. Mayor, Y. Fu, J.-F. Li and T. Wandlowski, *J. Am. Chem. Soc.*, 2011, 133, 7332-7335. 120
- 48 193.Cornelis A. van Walree, Veronica E. M. Kaats-Richters, Sandra J. Veen, B. Wiczorek, Johanna H. van der Wiel and Bas C. van der Wiel, *Eur. J. Org. Chem.*, 2004, 2004, 3046-3056. 121
- 49 194.A. B. Ricks, G. C. Solomon, M. T. Colvin, A. M. Scott, K. Chen, M. A. Ratner and M. R. Wasielewski, *J. Am. Chem. Soc.*, 2010, 132, 15427-15434. 122
- 50 195.M. Zarea, D. Powell, N. Renaud, M. R. Wasielewski and M. A. Ratner, *J. Phys. Chem. B*, 2013, 117, 1010-1020. 123
- 51 196.J. P. Bergfield, G. C. Solomon, C. A. Stafford and M. A. Ratner, *Nano Lett.*, 2011, 11, 2759-2764. 124
- 52 197.C. M. Guedon, H. Valkenier, T. Markussen, K. S. Thygesen, J. C. Hummelen and S. J. van der Molen, *Nat. Nanotechnol.*, 2012, 7, 305-309. 125
- 53 198.D. Fracasso, H. Valkenier, J. C. Hummelen, G. C. Solomon and R. C. Chiechi, *J. Am. Chem. Soc.*, 2011, 133, 9556-9563. 126
- 54 199.G. C. Solomon, D. Q. Andrews, R. H. Goldsmith, T. Hansen, M. R. Wasielewski, R. P. Van Duyne and M. A. Ratner, *J. Am. Chem. Soc.*, 2008, 130, 17301-17308. 127
- 55 200.N. P. Guisinger, M. E. Greene, R. Basu, A. S. Baluch and M. C. Hersam, *Nano Lett.*, 2003, 4, 55-59. 128
- 56 201.A. Sen and C.-C. Kaun, *ACS Nano*, 2010, 4, 6404-6408. 129
- 57 202.Y. Cho, W. Y. Kim and K. S. Kim, *J. Phys. Chem. A*, 2009, 113, 4100-4104. 130
- 58 203.A. Aviram, C. Joachim and M. Pomerantz, *Chem. Phys. Lett.*, 1988, 146, 490-495. 131
- 59 204.M. Pomerantz, A. Aviram, R. A. McCorkle, L. Li and A. G. Schrott, *Science*, 1992, 255, 1115-1118. 132
- 60 205.G. J. Ashwell, W. D. Tyrrell and A. J. Whittam, *J. Am. Chem. Soc.*, 2004, 126, 7102-7110. 133
- 61 206.I. Díez-Pérez, J. Hihath, Y. Lee, L. Yu, L. Adamska, M. A. Kozhushner, I. I. Oleynik and N. Tao, *Nat. Chem.*, 2009, 1, 635-641. 134
- 62 207.J. M. van Ruitenbeek, A. Alvarez, I. Pineyro, C. Grahmann, P. Joyez, M. H. Devoret, D. Esteve and C. Urbina, *Rev. Sci. Instrum.*, 1996, 67, 108-111. 135
- 63 208.J. Chen, M. A. Reed, A. M. Rawlett and J. M. Tour, *Science*, 1999, 286, 1550-1552. 136
- 64 209.M. Elbing, R. Ochs, M. Koentopp, M. Fischer, C. von Hänisch, F. Weigend, F. Evers, H. B. Weber and M. Mayor, *Proc. Natl. Acad. Sci. U. S. A.*, 2005, 102, 8815-8820. 137
- 65 210.S. E. Kubatkin, A. V. Danilov, A. L. Bogdanov, H. Olin and T. Claeson, *Appl. Phys. Lett.*, 1998, 73, 3604-3606. 138
- 66 211.A. V. Danilov, P. Hedegård, D. S. Golubev, T. Bjørnholm and S. E. Kubatkin, *Nano Lett.*, 2008, 8, 2393-2398. 139

- 1 212.X. Lu, M. Grobis, K. H. Khoo, S. G. Louie and M. F. Crommie, *Phys. Rev. Lett.*, 2003, 90, 096802. 73
2 Rev. Lett., 2003, 90, 096802. 74
3 213.X. Lu, M. Grobis, K. H. Khoo, S. G. Louie and M. F. Crommie, *Phys. Rev. B*, 2004, 70, 115418. 75
4 Rev. B, 2004, 70, 115418. 76
5 214.M. A. Reed, *Mater. Today*, 2008, 11, 46-50. 77
6 215.R. C. Jaklevic and J. Lambe, *Phys. Rev. Lett.*, 1966, 17, 1139-1140. 78
7 216.P. K. Hansma and Editor, *Tunneling Spectroscopy: Capabilities Applications, and New Techniques*, Plenum Press, 1982. 79
8 Applications, and New Techniques, Plenum Press, 1982. 80
9 217.C. Schirm, M. Matt, F. Pauly, J. C. Cuevas, P. Nielaba and E. Scheer, *Nat. Nanotechnol.*, 2013, 8, 645-648. 81
10 Nat. Nanotechnol., 2013, 8, 645-648. 82
11 218.B. C. Stipe, M. A. Rezaei and W. Ho, *Phys. Rev. Lett.*, 1998, 81, 1266. 83
12 1266. 84
13 219.X. H. Qiu, G. V. Nazin and W. Ho, *Phys. Rev. Lett.*, 2004, 92, 206102. 85
14 220.K. Morgenstern, *J. Phys.: Condens. Matter*, 2011, 23, 484007. 86
15 221.C. Bruot, J. Hihath and N. Tao, *Nat. Nanotechnol.*, 2012, 7, 35-40. 87
16 222.J. Steidtner and B. Pettinger, *Rev. Sci. Instrum.*, 2007, 78, 103104. 88
17 223.J. Steidtner and B. Pettinger, *Phys. Rev. Lett.*, 2008, 100, 236101. 89
18 224.N. Jiang, E. T. Foley, J. M. Klingsporn, M. D. Sonntag, N. A. Valley, A. Dieringer, T. Seideman, G. C. Schatz, M. C. Hersam and R. P. Dwyne, *Nano Lett.*, 2012, 12, 5061-5067. 90
19 A. Dieringer, T. Seideman, G. C. Schatz, M. C. Hersam and R. P. Dwyne, *Nano Lett.*, 2012, 12, 5061-5067. 91
20 Dwyne, *Nano Lett.*, 2012, 12, 5061-5067. 92
21 225.U. Ham and W. Ho, *Phys. Rev. Lett.*, 2012, 108, 106803. 93
22 226.N. Agrait, C. Untiedt, G. Rubio-Bollinger and S. Vieira, *Phys. Rev. Lett.*, 2002, 88, 216803. 94
23 2002, 88, 216803. 95
24 227.C. Untiedt, G. Rubio Bollinger, S. Vieira and N. Agrait, *Phys. Rev. B*, 2000, 62, 9962-9965. 96
25 2000, 62, 9962-9965. 97
26 228.D. Djukic, K. S. Thygesen, C. Untiedt, R. H. M. Smit, K. W. Jacobsen and J. M. van Ruitenbeek, *Phys. Rev. B*, 2005, 71, 161402. 98
27 and J. M. van Ruitenbeek, *Phys. Rev. B*, 2005, 71, 161402. 99
28 229.O. Tal, M. Krieger, B. Leerink and J. M. van Ruitenbeek, *Phys. Rev. Lett.*, 2008, 100, 196804. 100
29 Lett., 2008, 100, 196804. 101
30 230.E. Scheer, P. Konrad, C. Bacca, A. Mayer-Gindner, H. von Lohneysen, M. Hafner and J. C. Cuevas, *Phys. Rev. B*, 2006, 74, 205430. 102
31 M. Hafner and J. C. Cuevas, *Phys. Rev. B*, 2006, 74, 205430. 103
32 231.J. G. Kushmerick, J. Lazoricik, C. H. Patterson, R. Shashidhar, S. Seferos and G. C. Bazan, *Nano Lett.*, 2004, 4, 639-642. 104
33 S. Seferos and G. C. Bazan, *Nano Lett.*, 2004, 4, 639-642. 105
34 232.W. Wang, T. Lee, I. Kretzschmar and M. A. Reed, *Nano Lett.*, 2004, 4, 643-646. 106
35 643-646. 107
36 233.J. Hihath, C. Bruot, H. Nakamura, Y. Asai, I. Diez-Pérez, Y. Lee, L. Li and N. Tao, *ACS Nano*, 2011, 5, 8331-8339. 108
37 and N. Tao, *ACS Nano*, 2011, 5, 8331-8339. 109
38 234.Y. Kim, T. J. Hellmuth, M. Bürkle, F. Pauly and E. Scheer, *ACS Nano*, 2011, 5, 4104-4111. 110
39 2011, 5, 4104-4111. 111
40 235.Y. Kim, A. Garcia-Lekue, D. Sysoiev, T. Frederiksen, U. Groth and E. Scheer, *Phys. Rev. Lett.*, 2012, 109, 226801. 112
41 Scheer, *Phys. Rev. Lett.*, 2012, 109, 226801. 113
42 236.A. Troisi and M. A. Ratner, *J. Chem. Phys.*, 2006, 125, 214709. 114
43 237.J. M. Beebe, H. J. Moore, T. R. Lee and J. G. Kushmerick, *Nano Lett.*, 2007, 7, 1364-1368. 115
44 2007, 7, 1364-1368. 116
45 238.S. R. Burema and M.-L. Bocquet, *J. Phys. Chem. Lett.*, 2012, 3, 3011. 117
46 3011. 118
47 239.S. J. v. d. Molen and P. Liljeroth, *Journal of Physics: Condensed Matter*, 2010, 22, 133001. 119
48 2010, 22, 133001. 120
49 240.S. Lara-Avila, A. Danilov, V. Geskin, S. Bouzakroui, S. Kubatkin, S. Cornil and T. Bjørnholm, *J. Phys. Chem. C*, 2010, 114, 20686-20695. 121
50 Cornil and T. Bjørnholm, *J. Phys. Chem. C*, 2010, 114, 20686-20695. 122
51 241.S. Lara-Avila, A. V. Danilov, S. E. Kubatkin, S. L. Broman, C. R. Palacios and M. B. Nielsen, *J. Phys. Chem. C*, 2011, 115, 18372-18377. 123
52 and M. B. Nielsen, *J. Phys. Chem. C*, 2011, 115, 18372-18377. 124
53 242.S. L. Broman, S. Lara-Avila, C. L. Thisted, A. D. Bond, S. Kubatkin, S. Danilov and M. B. Nielsen, *Adv. Funct. Mater.*, 2012, 22, 4249-4258. 125
54 Danilov and M. B. Nielsen, *Adv. Funct. Mater.*, 2012, 22, 4249-4258. 126
55 243.T. A. Fulton and G. J. Dolan, *Phys. Rev. Lett.*, 1987, 59, 109-112. 127
56 244.M. Kastner, *Rev Mod Phys*, 1992, 64, 849. 128
57 245.D. C. Ralph, C. T. Black and M. Tinkham, *Phys. Rev. Lett.*, 1997, 78, 4087-4090. 129
58 4087-4090. 130
59 246.D. L. Klein, R. Roth, A. K. L. Lim, A. P. Alivisatos and P. L. McEuen, *Nature*, 1997, 389, 699-701. 131
60 Nature, 1997, 389, 699-701. 132
61 247.S. J. Tans, M. H. Devoret, R. J. A. Groeneveld and C. Dekker, *Nature*, 1998, 394, 761-764. 133
62 1998, 394, 761-764. 134
63 248.R. Y. Wang, R. A. Segalman and A. Majumdar, *Appl. Phys. Lett.*, 2005, 89, 173113. 135
64 89, 173113. 136
65 249.P. Hedegård and T. Bjørnholm, *Chem. Phys.*, 2005, 319, 350-359. 137
66 250.K. Kaasbjerg and K. Flensberg, *Nano Lett.*, 2008, 8, 3809-3814. 138
67 251.K. Moth-Poulsen and T. Bjørnholm, *Nat. Nanotechnol.*, 2009, 4, 556. 139
68 556. 140
69 252.A. R. Champagne, A. N. Pasupathy and D. C. Ralph, *Nano Lett.*, 2005, 5, 305-308. 141
70 5, 305-308. 142
71 253.J. P. Bergfield, M. A. Solis and C. A. Stafford, *ACS Nano*, 2010, 4, 5314-5320. 143
72 5314-5320. 144
- 254.C. M. Finch, V. M. Garcia-Suarez and C. J. Lambert, *Phys. Rev. B*, 2009, 79, 033405.
255.P. Murphy, S. Mukerjee and J. Moore, *Phys. Rev. B*, 2008, 78, 161406.
256.P. Reddy, S.-Y. Jang, R. A. Segalman and A. Majumdar, *Science*, 2007, 315, 1568-1571.
257.C. J. Vineis, A. Shakouri, A. Majumdar and M. G. Kanatzidis, *Adv. Mater.*, 2010, 22, 3970-3980.
258.L. D. Hicks and M. S. Dresselhaus, *Phys. Rev. B*, 1993, 47, 12727-12731.
259.T. C. Harman, P. J. Taylor, M. P. Walsh and B. E. LaForge, *Science*, 2002, 297, 2229-2232.
260.V. M. Garcia-Suarez, R. Ferradas and J. Ferrer, *Phys. Rev. B*, 2013, 88, 235417.
261.S. Hershfield, K. A. Muttalib and B. J. Nartowt, *Phys. Rev. B*, 2013, 88, 085426.
262.W. Lee, K. Kim, W. Jeong, L. A. Zotti, F. Pauly, J. C. Cuevas and P. Reddy, *Nature*, 2013, 498, 209-212.
263.Y. Wang, J. Liu, J. Zhou and R. Yang, *J. Phys. Chem. C*, 2013, 117, 24716-24725.
264.Z.-H. Wu, H.-Q. Xie and Y.-B. Zhai, *Appl. Phys. Lett.*, 2013, 103, 243901.
265.S. K. Yee, J. A. Malen, A. Majumdar and R. A. Segalman, *Nano Lett.*, 2011, 11, 4089-4094.
266.G. Chen, *Phys. Rev. B*, 1998, 57, 14958-14973.
267.M. Tsutsui, T. Kawai and M. Taniguchi, *Sci. Rep.*, 2012, 2, 1-11.
268.J. A. Malen, P. Doak, K. Baheti, T. D. Tilley, R. A. Segalman and A. Majumdar, *Nano Lett.*, 2009, 9, 1164-1169.
269.J. A. Malen, P. Doak, K. Baheti, T. D. Tilley, A. Majumdar and R. A. Segalman, *Nano Lett.*, 2009, 9, 3406-3412.
270.Y. Asai, *J. Phys.: Condens. Matter*, 2013, 25, 155305.
271.Z. Golsanamlou, S. Izadi Vishkayi, M. Bagheri Tagani and H. Rahimpour Soleimani, *Chem. Phys. Lett.*, 2014, 594, 51-57.
272.O. Karlstrom, M. Strange and G. C. Solomon, *J. Chem. Phys.*, 2014, 140, 044315.
273.F. Pauly, J. K. Viljas and J. C. Cuevas, *Phys. Rev. B*, 2008, 78, 035315.
274.A. Tan, J. Balachandran, B. D. Dunietz, S.-Y. Jang, V. Gavini and P. Reddy, *Appl. Phys. Lett.*, 2012, 101, 243107.
275.A. Tan, J. Balachandran, S. Sadat, V. Gavini, B. D. Dunietz, S.-Y. Jang and P. Reddy, *J. Am. Chem. Soc.*, 2011, 133, 8838-8841.
276.J. R. Widawsky, W. Chen, H. Vazquez, T. Kim, R. Breslow, M. S. Hybertsen and L. Venkataraman, *Nano Lett.*, 2013, 13, 2889-2894.
277.S.-H. Ke, W. Yang, S. Curtarolo and H. U. Baranger, *Nano Lett.*, 2009, 9, 1011-1014.
278.W. Liang, A. I. Hochbaum, M. Fardy, O. Rabin, M. Zhang and P. Yang, *Nano Lett.*, 2009, 9, 1689-1693.
279.K. Baheti, J. A. Malen, P. Doak, P. Reddy, S.-Y. Jang, T. D. Tilley, A. Majumdar and R. A. Segalman, *Nano Lett.*, 2008, 8, 715-719.
280.S. Datta and B. Das, *Appl. Phys. Lett.*, 1990, 56, 665-667.
281.S. A. Wolf, D. D. Awschalom, R. A. Buhrman, J. M. Daughton, S. von Molnar, M. L. Roukes, A. Y. Chtchelkanova and D. M. Treger, *Science*, 2001, 294, 1488-1495.
282.L. Bogani and W. Wernsdorfer, *Nat. Mater.*, 2008, 7, 179-186.
283.J. Kondo, *Prog. Theor. Phys.*, 1964, 32, 37-49.
284.N. Roch, S. Florens, V. Bouchiat, W. Wernsdorfer and F. Balestro, *Nature*, 2008, 453, 633-637.
285.J. J. Parks, A. R. Champagne, T. A. Costi, W. W. Shum, A. N. Pasupathy, E. Neuscamman, S. Flores-Torres, P. S. Cornaglia, A. A. Aligia, C. A. Balseiro, G. K.-L. Chan, H. D. Abruña and D. C. Ralph, *Science*, 2010, 328, 1370-1373.
286.S. Wagner, F. Kisslinger, S. Ballmann, F. Schramm, R. Chandrasekar, T. Bodenstern, O. Fuhr, D. Secker, K. Fink, M. Ruben and H. B. Weber, *Nat. Nanotechnol.*, 2013, 8, 575-579.
287.A. A. Houck, J. Labaziewicz, E. K. Chan, J. A. Folk and I. L. Chuang, *Nano Lett.*, 2005, 5, 1685-1688.
288.V. Iancu, A. Deshpande and S.-W. Hla, *Nano Lett.*, 2006, 6, 820-823.
289.M. J. Calderón, B. Koiller and S. Das Sarma, *Phys. Rev. B*, 2007, 75, 125311.
290.K. J. Franke, G. Schulze and J. I. Pascual, *Science*, 2011, 332, 940-944.
291.K. Yoshida, I. Hamada, S. Sakata, A. Umeno, M. Tsukada and K. Hirakawa, *Nano Lett.*, 2013, 13, 481-485.
292.M. Urdampilleta, S. Klyatskaya, J. P. Cleuziou, M. Ruben and W. Wernsdorfer, *Nat. Mater.*, 2011, 10, 502-506.

- 1 293.S. Xu, G. Podoprygorina, V. Boehmer, Z. Ding, P. Rooney, C. Rang and
2 and S. Mittler, *Org. Biomol. Chem.*, 2007, 5, 558-568. 74
- 3 294.R. Vincent, S. Klyatskaya, M. Ruben, W. Wernsdorfer and F. Balestro
4 *Nature*, 2012, 488, 357-360. 75
- 5 295.S. Thiele, R. Vincent, M. Holzmann, S. Klyatskaya, M. Ruben,
6 Balestro and W. Wernsdorfer, *Phys. Rev. Lett.*, 2013, 111, 037203. 76
- 7 296.M. Ganzhorn, S. Klyatskaya, M. Ruben and W. Wernsdorfer, *Nano*
8 *Nanotechnol.*, 2013, 8, 165-169. 77
- 9 297.R. Baer and D. Neuhauser, *J. Am. Chem. Soc.*, 2002, 124, 4200-4201. 78
- 10 298.R. A. Webb, S. Washburn, C. P. Umbach and R. B. Laibowitz, *Phys.*
11 *Rev. Lett.*, 1985, 54, 2696. 79
- 12 299.K. Walczak, *Cent. Eur. J. Chem.*, 2004, 2, 524-533. 80
- 13 300.D. Walter, D. Neuhauser and R. Baer, *Chem. Phys.*, 2004, 299, 139-148. 81
- 14 301.S.-H. Ke, W. Yang and H. U. Baranger, *Nano Lett.*, 2008, 8, 3257-3267. 82
- 15 302.G. C. Solomon, D. Q. Andrews, T. Hansen, R. H. Goldsmith, M. A. Ratner,
16 Wasielewski, R. P. Van Duyne and M. A. Ratner, *J. Chem. Phys.*, 2008, 129,
17 054701. 83
- 18 303.J. Rincón, K. Hallberg, A. A. Aligia and S. Ramasesha, *Phys. Rev. Lett.*
19 2009, 103, 266807. 84
- 20 304.G. C. Solomon, C. Herrmann, T. Hansen, V. Mujica and M. A. Ratner, *Nat. Chem.*,
21 2010, 2, 223-228. 85
- 22 305.S. Ballmann, R. Haertle, P. B. Coto, M. Elbing, M. Mayor, M. R. Bryce,
23 M. Thoss and H. B. Weber, *Phys. Rev. Lett.*, 2012, 109, 056801. 86
- 24 306.R. Haertle, M. Butzin, O. Rubio-Pons and M. Thoss, *Phys. Rev. Lett.*
25 2011, 107, 046802. 87
- 26 307.S. V. Aradhya, J. S. Meisner, M. Krikorian, S. Ahn, R. Parameswaran,
27 M. L. Steigerwald, C. Nuckolls and L. Venkataraman, *Nano Lett.*, 2010,
28 12, 1643-1647. 88
- 29 308.C. R. Arroyo, S. Tarkuc, R. Frisenda, J. S. Seldenthuis, C. H. J. Busnel,
30 Woerde, R. Eelkema, F. C. Grozema and H. S. J. van der Zant, *Angew. Chem. Int. Ed.*,
31 2013, 52, 3152-3155. 89
- 32 309.C. R. Arroyo, R. Frisenda, K. Moth-Poulsen, J. S. Seldenthuis, S. Bjornholm and
33 d. Z. H. S. van, *Nanoscale Res. Lett.*, 2013, 8, 234. 90
- 34 310.C. Nef, P. L. T. M. Frederix, J. Brunner, C. Schonenberger and M. Calame, *Nanotechnology*,
35 2012, 23, 365201. 91
- 36 311.M. Irie, *Chem. Rev.*, 2000, 100, 1685-1716. 92
- 37 312.H. Duerr, H. Bouas-Laurent and Editors, *Studies in Organic Chemistry*,
38 40: Photochromism: Molecules and Systems, Elsevier, 1990. 93
- 39 313.B. L. Feringa and Editor, *Molecular Switches*, Wiley-VCH, 2001. 94
- 40 314.J. C. Crano, R. J. Guglielmetti and Editors, *Organic Photochromic and Thermochromic*
41 *Compounds, Volume 1: Main Photochromic Families*, Plenum, 1999. 95
- 42 315.N. Tanifuji, K. Matsuda and M. Irie, *Org. Lett.*, 2005, 7, 3777-3780. 96
- 43 316.P. Gutlich, Y. Garcia and T. Woike, *Coord. Chem. Rev.*, 2001, 219, 839-879. 97
- 44 317.M. Irie, T. Fukaminato, T. Sasaki, N. Tamai and T. Kawai, *Nature*, 2009, 460,
45 420, 759-760. 98
- 46 318.T. Fukaminato, T. Sasaki, T. Kawai, N. Tamai and M. Irie, *J. Am. Chem. Soc.*,
47 2004, 126, 14843-14849. 99
- 48 319.P. A. Liddell, G. Kodis, A. L. Moore, T. A. Moore and D. Gust, *J. Am. Chem. Soc.*,
49 2002, 124, 7668-7669. 100
- 50 320.K. Uchida, N. Izumi, S. Sukata, Y. Kojima, S. Nakamura and M. Irie, *Angew. Chem. Int. Ed.*,
51 2006, 45, 6470-6473. 101
- 52 321.T. B. Norsten and N. R. Branda, *J. Am. Chem. Soc.*, 2001, 123, 1187-1188. 102
- 53 322.M. Irie, S. Kobatake and M. Horichi, *Science*, 2001, 291, 1769-1772. 103
- 54 323.H. Cho and E. Kim, *Macromolecules*, 2002, 35, 8684-8687. 104
- 55 324.N. Tanifuji, M. Irie and K. Matsuda, *J. Am. Chem. Soc.*, 2005, 127, 13344-13353. 105
- 56 325.T. A. Golovkova, D. V. Kozlov and D. C. Neckers, *J. Org. Chem.*, 2005, 70, 5545-5549. 106
- 57 326.K. Matsuda and M. Irie, *Chem. Eur. J.*, 2001, 7, 3466-3473. 107
- 58 327.V. W.-W. Yam, C.-C. Ko and N. Zhu, *J. Am. Chem. Soc.*, 2004, 126, 12734-12735. 108
- 59 328.G. M. Tsvigoulis and J.-M. Lehn, *Angew. Chem. Int. Ed.*, 1995, 34, 1119-1122. 109
- 60 329.N. P. M. Huch and B. L. Feringa, *J. Chem. Soc., Chem. Commun.*, 1998, 1095-1096. 110
- 61 330.T. J. Wigglesworth, D. Sud, T. B. Norsten, V. S. Lekhi and N. R. Branda, *J. Am. Chem. Soc.*,
62 2005, 127, 7272-7273. 111
- 63 331.P. Dedecker, C. Flors, J.-i. Hotta, H. Uji-i and J. Hofkens, *Angew. Chem. Int. Ed.*,
64 2007, 46, 8330-8332. 112
- 65 332.T. Fukaminato, *J. Photochem. Photobiol., C*, 2011, 12, 177-208. 113
- 66 333.J. W. Shaevitz, *Nat. Methods*, 2008, 5, 471-472. 114
- 67 334.M. Sauer, *Proc. Natl. Acad. Sci. U. S. A.*, 2005, 102, 9433-9434. 115
- 68 335.C. Geisler, A. Schoenle, C. von Middendorff, H. Bock, C. Eggeling, A. Egner and S. W. Hell, *Appl. Phys. A: Mater. Sci. Process.*, 2007, 88, 223-226. 116
- 69 336.T. Yamaguchi, K. Uchida and M. Irie, *J. Am. Chem. Soc.*, 1997, 119, 6066-6071. 117
- 70 337.M. Heilemann, P. Dedecker, J. Hofkens and M. Sauer, *Laser Photonics Rev.*, 2009, 3, 180-202. 118
- 71 338.J. Vogelsang, C. Steinhauer, C. Forthmann, I. H. Stein, B. Person-Skegro, T. Cordes and P. Tinnefeld, *ChemPhysChem*, 2010, 11, 2475-2490. 119
- 72 339.T. Tsujioka and M. Irie, *J. Photochem. Photobiol., C*, 2010, 11, 1-14. 120
- 73 340.A. Bianchi, E. Delgado-Pinar, E. Garcia-Espana, C. Giorgi and F. Pina, *Coord. Chem. Rev.*, 2014, 260, 156-215. 121
- 341.J. Zhou, G. Du and J. Chen, *Curr. Opin. Biotechnol.*, 2014, 25, 17-23. 122
- 342.C. Yun, J. You, J. Kim, J. Huh and E. Kim, *J. Photochem. Photobiol., C*, 2009, 10, 111-129. 123
- 343.J. Hwang, M. Pototschnig, R. Lettow, G. Zumofen, A. Renn, S. Gotzinger and V. Sandoghdar, *Nature*, 2009, 460, 76-80. 124
- 344.H. Song, Y. Kim, Y. H. Jang, H. Jeong, M. A. Reed and T. Lee, *Nature*, 2009, 462, 1039-1043. 125
- 345.T. Fukaminato, *J. Photochem. Photobiol. C*, 2011, 12, 177-208. 126
- 346.C. Jia, J. Wang, C. Yao, Y. Cao, Y. Zhong, Z. Liu, Z. Liu and X. Guo, *Angew. Chem. Int. Ed.*, 2013, 52, 8666-8670. 127
- 347.Y. Kim, T. J. Hellmuth, D. Syssoiev, F. Pauly, T. Pietsch, J. Wolf, A. Erbe, T. Huhn, U. Groth, U. E. Steiner and E. Scheer, *Nano Lett.*, 2012, 12, 3736-3742. 128
- 348.P. Liljeroth, *Nat. Nanotechnol.*, 2012, 7, 5-6. 129
- 349.A. Perrier, F. Maurel and D. Jacquemin, *Acc. Chem. Res.*, 2012, 45, 1173-1182. 130
- 350.E. G. Petrov, V. O. Leonov and V. Snitsarev, *J. Chem. Phys.*, 2013, 138, 184709. 131
- 351.C. Sciascia, R. Castagna, M. Dekermenjian, R. Martel, A. R. Srimath Kandada, F. Di Fonzo, A. Bianco, C. Bertarelli, M. Meneghetti and G. Lanzani, *J. Phys. Chem. C*, 2012, 116, 19483-19489. 132
- 352.D. Kim, H. Jeong, H. Lee, W.-T. Hwang, J. Wolf, E. Scheer, T. Huhn, H. Jeong and T. Lee, *Adv. Mater.*, 2014, In press, DOI: 10.1002/adma.201306316. 133
- 353.T. Tsujioka, Y. Hamada, K. Shibata, A. Taniguchi and T. Fuyuki, *Appl. Phys. Lett.*, 2001, 78, 2282-2284. 134
- 354.T. Tsujioka and M. Irie, *J. Opt. Soc. Am. B*, 2002, 19, 297-303. 135
- 355.Y. Kim and E. Kim, *Macromol. Res.*, 2006, 14, 584-587. 136
- 356.P. Zacharias, M. C. Gather, A. Koehn, N. Rehm and K. Meerholz, *Angew. Chem. Int. Ed.*, 2009, 48, 4038-4041. 137
- 357.Z. Zhang, X. Liu, Z. Li, Z. Chen, F. Zhao, F. Zhang and C.-H. Tung, *Adv. Funct. Mater.*, 2008, 18, 302-307. 138
- 358.V. Ramamurthy, K. S. Schanze and Editors, *Optical sensors and switches. Mol. Supramol. Photochem.*, 2001; 7, Marcel Dekker, Inc., 2001. 139
- 359.N. Koumura, R. W. J. Zijlstra, R. A. van Delden, N. Harada and B. L. Feringa, *Nature*, 1999, 401, 152-155. 140
- 360.T. Hugel, N. B. Holland, A. Cattani, L. Moroder, M. Seitz and H. E. Gaub, *Science*, 2002, 296, 1103-1106. 141
- 361.T. Tsujioka and M. Irie, *J. Photochem. Photobiol. C*, 2010, 11, 1-14. 142
- 362.K. Matsuda and M. Irie, *Polyhedron*, 2005, 24, 2477-2483. 143
- 363.J. He, F. Chen, P. A. Liddell, J. Andreasson, S. D. Straight, D. Gust, T. A. Moore, A. L. Moore, J. Li, O. F. Sankey and S. M. Lindsay, *Nanotechnology*, 2005, 16, 695-702. 144
- 364.A. Aviram, M. Ratner and Editors, *Proceedings of a Conference on Molecular Electronics: Science and Technology*, held 14-18 December 1997, in Humacao, Puerto Rico. [In: *Ann. N. Y. Acad. Sci.*, 1998; 852], New York Academy of Sciences, 1998. 145
- 365.A. C. Whalley, M. L. Steigerwald, X. Guo and C. Nuckolls, *J. Am. Chem. Soc.*, 2007, 129, 12590-12591. 146
- 366.M. Taniguchi, Y. Nojima, K. Yokota, J. Terao, K. Sato, N. Kambe and T. Kawai, *J. Am. Chem. Soc.*, 2006, 128, 15062-15063. 147
- 367.A. Staykov, D. Nozaki and K. Yoshizawa, *J. Phys. Chem. C*, 2007, 111, 3517-3521. 148
- 368.J. Huang, Q. Li, H. Ren, H. Su, Q. W. Shi and J. Yang, *J. Chem. Phys.*, 2007, 127, 094705. 149
- 369.M. Kondo, T. Tada and K. Yoshizawa, *Chem. Phys. Lett.*, 2005, 412, 55-59. 150

- 1 370.N. Katsonis, T. Kudernac, M. Walko, S. J. van der Molen, B. J. van
2 Wees and B. L. Feringa, *Adv. Mater.*, 2006, 18, 1397-1400. 74
- 3 371.M. Ikeda, N. Tanifuji, H. Yamaguchi, M. Irie and K. Matsuda, *Chem*
4 *Commun.*, 2007, 1355-1357. 75
- 5 372.S. J. van der Molen, J. Liao, T. Kudernac, J. S. Agustsson, L. Berna
6 M. Calame, B. J. van Wees, B. L. Feringa and C. Schonenberger, *Nano*
7 *Let.*, 2009, 9, 76-80. 77
- 8 373.R. W. Taylor, R. J. Coulston, F. Biedermann, S. Mahajan, J. J. Baumbach
9 and O. A. Scherman, *Nano Let.*, 2013, 13, 5985-5990. 81
- 10 374.A. B. Petersen, E. Thyraug, T. Jain, K. Kilsaa, M. Bols, K. Moberg
11 Poulsen, N. Harrit and T. Bjørnholm, *J. Phys. Chem. B*, 2010, 114,
12 11771-11777. 84
- 13 375.C. W. Marquardt, S. Grunder, A. Blaszczyk, S. Dehm, F. Hennrich, H.
14 Lohneysen, M. Mayor and R. Krupke, *Nat. Nanotechnol.*, 2010, 5, 866-
15 867. 87
- 16 376.A. Peters and N. R. Branda, *J. Am. Chem. Soc.*, 2003, 125, 3404-3405. 88
- 17 377.T. Saika, M. Irie and T. Shimidzu, *J. Chem. Soc., Chem. Commun.*,
18 1994, 2123-2124. 90
- 19 378.A. Peters and N. R. Branda, *Chem. Commun.*, 2003, 954-955. 91
- 20 379.N. Darwish, I. Diez-Perez, P. Da Silva, N. Tao, J. J. Gooding and M.
21 Paddon-Row, *Angew. Chem. Int. Ed.*, 2012, 51, 3203-3206. 93
- 22 380.D. I. Gittins, D. Bethell, D. J. Schiffrin and R. J. Nichols, *Nature*, 2009,
23 408, 67-69. 95
- 24 381.Y.-Y. Sun, Z.-L. Peng, R. Hou, J.-H. Liang, J.-F. Zheng, X.-Y. Zhou,
25 S. Zhou, S. Jin, Z.-J. Niu and B.-W. Mao, *Phys Chem Chem Phys*, 2009,
26 16, 2260-2267. 98
- 27 382.D. L. Feldheim and C. D. Keating, *Chem. Soc. Rev.*, 1998, 27, 1-12. 99
- 28 383.N. J. Tao, *Phys. Rev. Lett.*, 1996, 76, 4066-4069. 100
- 29 384.W. Han, E. N. Durantini, T. A. Moore, A. L. Moore, D. Gust, P. Rezak
30 Leatherman, G. R. Seely, N. Tao and S. M. Lindsay, *J. Phys. Chem. B*,
31 1997, 101, 10719-10725. 102
- 32 385.N. J. Kay, S. J. Higgins, J. O. Jeppesen, E. Leary, J. Lycoops, J. Ulstrup
33 and R. J. Nichols, *J. Am. Chem. Soc.*, 2012, 134, 16817-16826. 104
- 34 386.C. Li, A. Mishchenko, Z. Li, I. Pobelov, T. Wandlowski, X. Q. Li,
35 W. Wurthner, A. Bagrets and F. Evers, *J. Phys.: Condens. Matter*, 2008, 20,
36 374122. 106
- 37 387.S. Tsoi, I. Griva, S. A. Trammell, A. S. Blum, J. M. Schnur and N.
38 Lebedev, *ACS Nano*, 2008, 2, 1289-1295. 108
- 39 388.E. Leary, S. J. Higgins, H. van Zalinge, W. Haiss, R. J. Nichols,
40 Nygaard, J. O. Jeppesen and J. Ulstrup, *J. Am. Chem. Soc.*, 2008, 130,
41 12204-12205. 111
- 42 389.F. Mohn, J. Repp, L. Gross, G. Meyer, M. S. Dyer and M. Persson, *Phys.*
43 *Rev. Lett.*, 2010, 105, 266102. 113
- 44 390.N. Darwish, I. Diez-Perez, S. Guo, N. Tao, J. J. Gooding and M.
45 Paddon-Row, *J. Phys. Chem. C*, 2012, 116, 21093-21097. 114
- 46 391.T. Avellini, H. Li, A. Coskun, G. Barin, A. Trabolsi, A. N. Basuray,
47 K. Dey, A. Credi, S. Silvi, J. F. Stoddart and M. Venturi, *Angew. Chem.*
48 *Int. Ed.*, 2012, 51, 1611-1615. 117
- 49 392.A. B. Gaspar, V. Ksenofontov, M. Seredyuk and P. Guetlich, *Coord.*
50 *Chem. Rev.*, 2005, 249, 2661-2676. 119
- 51 393.F. Meng, Y.-M. Hervault, Q. Shao, B. Hu, L. Norel, S. Rigaut and
52 Chen, *Nat. Commun.*, 2014, 5, 3023. 121
- 53 394.W. Zhai, C. Du and X. Li, *Chem. Comm.*, 2014, 50, 2093-2095. 122
- 54 395.X.-S. Zhou, L. Liu, P. Fortgang, A.-S. Lefevre, A. Serra-Muns, S.
55 Raouafi, C. Amatore, B.-W. Mao, E. Maisonhaute and B. Schöllhorn,
56 *Am. Chem. Soc.*, 2011, 133, 7509-7516. 124
- 57 396.J. Liao, J. S. Agustsson, S. Wu, C. Schönenberger, M. Calame,
58 Leroux, M. Mayor, O. Jeannin, Y.-F. Ran, S.-X. Liu and S. Decurtis,
59 *Nano Let.*, 2010, 10, 759-764. 126
- 60 397.J. S. Seldenthuis, F. Prins, J. M. Thijssen and H. S. J. van der Zant,
61 *Nano*, 2010, 4, 6681-6686. 129
- 62 398.M. Rief, M. Gautel, F. Oesterhelt, J. M. Fernandez and H. E. Gaub,
63 *Science*, 1997, 276, 1109-1112. 130
- 64 399.J. Liphardt, B. Onoa, S. B. Smith, I. Tinoco and C. Bustamante, *Science*,
65 2001, 292, 733-737. 132
- 66 400.A. F. Oberhauser, P. K. Hansma, M. Carrion-Vazquez and J. D.
67 Fernandez, *Proc. Natl. Acad. Sci. U. S. A.*, 2001, 98, 468-472. 134
- 68 401.C. Joachim, J. K. Gimzewski and A. Aviram, *Nature*, 2000, 408, 485-
69 548. 136
- 70 402.A. Nitzan and M. A. Ratner, *Science*, 2003, 300, 1384-1389. 137
- 71 403.C. Joachim and M. A. Ratner, *Proc. Natl. Acad. Sci. U. S. A.*, 2005, 102,
72 8801-8808. 138
- 404.M. Galperin, M. A. Ratner, A. Nitzan and A. Troisi, *Science*, 2008, 319,
1056-1060. 139
- 405.F. Chen and N. J. Tao, *Acc. Chem. Res.*, 2009, 42, 429-438.
- 406.L. Fabbrizzi, F. Gatti, P. Pallavicini and E. Zambarbieri, *Chem. Eur. J.*,
1999, 5, 682-690.
- 407.C. A. Martin, R. H. M. Smit, H. S. J. van der Zant and J. M. van
Ruitenbeek, *Nano Let.*, 2009, 9, 2940-2945.
- 408.M. Taniguchi, M. Tsutsui, K. Yokota and T. Kawai, *Chem. Sci.*, 2010, 1,
247-253.
- 409.T. Kawai, M. Poetschke, Y. Miyamoto, C. G. Rocha, S. Roche and G.
Cuniberti, *Phys. Rev. B*, 2011, 83, 241405.
- 410.M. Zemanová Diešková, I. Štich and P. Bokes, *Phys. Rev. B*, 2013, 87,
245418.
- 411.E. S. Tam, J. J. Parks, W. W. Shum, Y.-W. Zhong, M. E. B. Santiago-
Berrios, X. Zheng, W. Yang, G. K. L. Chan, H. D. Abruña and D. C.
Ralph, *ACS Nano*, 2011, 5, 5115-5123.
- 412.I. Franco, C. B. George, G. C. Solomon, G. C. Schatz and M. A. Ratner,
J. Am. Chem. Soc., 2011, 133, 2242-2249.
- 413.I. Diez-Perez, J. Hihath, T. Hines, Z.-S. Wang, G. Zhou, K. Mullen and
N. Tao, *Nat. Nanotechnol.*, 2011, 6, 226-231.
- 414.M. Manheller, S. Trellenkamp, R. Waser and S. Karthaeuser,
Nanotechnology, 2012, 23, 125302.
- 415.Y. Wu, W. Hong, T. Akiyama, S. Gautsch, V. Kolivoska, T.
Wandlowski and N. F. de Rooij, *Nanotechnology*, 2013, 24, 235302.

Dr. Lanlan Sun is a postdoctor in the Department of Chemical and Biological Engineering, Chalmers University of Technology. She received her ph. D degree in State Key Laboratory of Electroanalytical Chemistry, Changchun Institute of Applied Chemistry, China in 2009. Her current research interests are single molecule device fabricated by chemical assembly of gold nanoparticle dimers.



Yuri A. Diaz Fernandez (YDF) received his BSc and MSc degrees at the Nuclear Science Institute of Havana (Cuba), and his PhD degree from the University of Pavia (Italy). YDF has several years of experience on Nanotechnology, Surface Science, Chemistry of Materials, and Colloidal Chemistry. During his research career, YDF has gained expertise on the design and synthesis of supramolecular systems and self-assembled nanostructured materials for different applications, including antibacterial surfaces, chemical catalysis, and molecular sensing. Currently YDF is working as Science Innovator in the Open Innovation Hub for Antimicrobial Surfaces, at the Surface Science Center of University of Liverpool (UK)



Tina Gschneidner (TG) received her Dipl. NanoSc in 2011 from the University of Kassel in Germany. She was an exchange student in 2009 at the University of California at Berkeley (Prof. C. Chang) and is currently a doctoral student at Chalmers University of Technology with KMP. TG is working on synthetic organic chemistry, plasmonic and catalytic nano particles, and light-directed surface functionalization.



1
2

Fredrik Westerlund (FW) received his MSc (2001) and Phd (2006) from Chalmers University of Technology (Sweden). He was a postdoctoral fellow at the University of Copenhagen (2007-2009), with Profs. Bjørnholm and Laursen, and Gothenburg University (2009-2010), with Prof. Tegenfeldt. In 2010 FW was recruited to Chalmers University of Technology as an Assistant Professor. His research is focused

13 on single DNA molecule techniques

14

15



Samuel Lara-Avila graduated as Mechatronics Engineer in 2005 (ITESM, Mexico), received his MSc in 2007 (KU Leuven, Belgium and Chalmers University of Technology, Sweden) and PhD degree in 2012 from Chalmers University of Technology (Sweden). After completing his PhD studies, he joined the Quantum Device Physics Laboratory at Chalmers University of Technology as Assistant Professor. His research interests include electron transport

26 through low dimensional-systems such as single-molecules and
27 graphene, directed assembly of nanoparticles and light-matter
28 interactions.

29

20



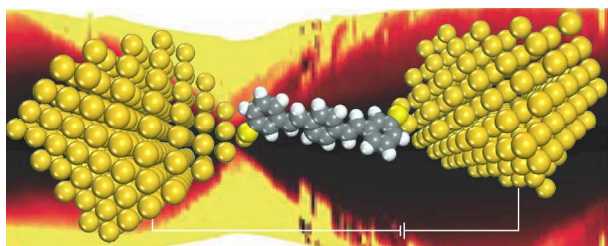
Kasper Moth-Poulsen (KMP) received his BSc (2000), Cand. Scient. (2003) and PhD (2007) degrees in Chemistry from University of Copenhagen (Denmark). He was a post doctoral fellow at the University of Copenhagen (2007-2009), with prof. Bjørnholm, and then at University of California at Berkeley (2009-2010) with prof.s Segalman and Vollhardt. In 2011 KMP was recruited to Chalmers University

40 of Technology (Sweden) as an assistant professor and since 2014 as
41 Associate professor. His research is focused on synthetic chemistry,
42 single molecule electronics, nanoparticle synthesis, energy storage
43 and self-assembly.

44

45 TOC Graphic

46



47

48

49